MYC INDEPENDENT ROLE OF MGA IN NEURAL CREST SPECIFICATION DURING ZEBRAFISH EARLY EMBRYONIC DEVELOPMENT

by

MUMINGJIANG MUNISHA

(Under the Direction of SCOTT T. DOUGAN)

ABSTRACT

One of the major questions in developmental biology is how cells take on different cell fates based on the molecular cues that are presented to them. During early embryonic development, cells gradually restrict their potential to become more differentiated and take on specific functions. One example that is implicated in this transition is a unique dual specificity transcription factor Max gene-associated protein (MGA). MGA is known to be a tumor suppressor for its ability to antagonize MYC dependent cell proliferation and promoting differentiation in cell culture. Mga plays a critical role in pluripotency maintenance in mouse epiblast. It is also required in the extraembryonic yolk syncytial layer for normal dorsoventral patterning in zebrafish development. Here we identified a novel role of MGA in neural crest specification during early zebrafish embryogenesis utilizing both knockdown and knockout approaches. Depletion of Mga from 1-cell stage embryos using morpholinos resulted in defects in various lineages of the neural crest cell population. This is due to decreased specification of

neural crest at the neural plate border. Mga depleted embryos show a decrease in Bmp signaling activity and an increase in Myc activity. Although increased cell death was seen at later stages in *mga* morphants possibly due to unopposed Myc, suppression of Myc is not able to rescue neural crest defect. This is the first demonstration that Mga acts as a Myc antagonist *in vivo*, and that the neural crest defect seen in Mga depleted embryos is due to altered Bmp signaling activity which is independent of Myc. We successfully generated *mga* mutant alleles using the CRISPR/Cas9 system. One of the potential null alleles failed to show a morphologically distinct phenotype when compared to wild type. However, further molecular analysis in *mga* mutants show similar but milder alterations that are seen in knockdown embryos. Furthermore, we identified *mga* paralog, *mgab* and confirmed its expression at various developmental stages. We propose that Mga promotes cell fate specification during neural crest development and may act as a molecular switch in pluripotent cells to transition to differentiation.

INDEX WORDS: Zebrafish, Embryonic Development, Neural Crest, Transcription Factor, Mga, CRISPR/Cas9, MYC, BMP

MYC INDEPENDENT ROLE OF MGA IN NEURAL CREST SPECIFICATION DURING ZEBRAFISH EARLY EMBRYONIC DEVELOPMENT

by

MUMINGJIANG MUNISHA

MD, Norman Bethune College of Medicine, Jilin University, China, 2013

A Dissertation Submitted to the Graduate Faculty of The University of Georgia in Partial Fulfillment of the Requirements for the Degree

DOCTOR OF PHILOSOPHY

ATHENS, GEORGIA

2020

MYC INDEPENDENT ROLE OF MGA IN NEURAL CREST SPECIFICATION DURING ZEBRAFISH EARLY EMBRYONIC DEVELOPMENT

by

MUMINGJIANG MUNSIHA

Major Professor:	Scott T. Dougan
Committee:	James D. Lauderdale
	Jonathan Eggenschwiler
	Douglas Menke

Electronic Version Approved:

Ron Walcott
Interim Dean of the Graduate School
The University of Georgia
May 2020

DEDICATION

I dedicate this work to my beloved parents for being the pillars of my life, for giving me the inspiration and freedom to follow my dreams, and for their unconditional love and support that kept me going on this journey.

ACKNOWLEDGEMENTS

There are so many people helped me during my graduate career that I would love to express my gratitude. First, I wish to express my deepest gratitude to my thesis advisor Scott Dougan for his tremendous support, guidance, and encouragement that made this work possible. Although there were numerous ups and downs during the completion of this project, he always encouraged me to think critically and creatively, motivated me to push my limits and become a better professional. I am grateful for his patience and for giving me the freedom during my preparation for the United States Medical Licensing Exams. Without his support and openness, I doubt there would be another chance to pass those exams to fulfill my dream of being a physician.

I am very grateful to have Jim Lauderdale, Jonathan Eggenschwiler and Doug Menke as my committee members. I am thankful for their mentorship and guidance during my Ph.D. career. They have always been available to answer my questions and guide me in the right direction when I felt lost. Special thanks to Jim Lauderdale and members of the Lauderdale lab for helping me pretty much with every difficulty that I encountered with fish work.

I would like to thank the past and current members of the Dougan lab. Special thanks to Wei-chia Tseng who taught me everything about Zebrafish and trained me in molecular biology. He always took his time out to discuss my experiments, and patiently helped me with troubleshooting when things didn't work. I would also like to thank Nurgul Kaya, Suga, and Aimee for being there and listening to my frustration even when they already have plenty in their hands. I had my best memories of hiking the North Georgia Mountains and Smokies with them.

Lastly, I would like to thank those who have helped me during these years outside of academia. My best friend Snow Han, without whom I wouldn't be able to go through the toughest years of my graduate career. I am also thankful for my friends that I met in Athens whose names are not mentioned but will never be forgotten. I would like to thank my family and friends back in Urumqi and scattered all around the world that I hope one day I will reunite.

TABLE OF CONTENTS

Page

LIST OF TABLES

Page

LIST OF FIGURES

Page

CHAPTER 1

INTRODUCTION AND LITERATURE REVIEW

1. Molecular Mechanisms of Maintenance of Pluripotency and Differentiation

One of the major questions in developmental biology is how and when cells take on various cell fates based on the molecular cues that are presented to them. During early embryogenesis, when a sperm fertilizes an egg, the zygote forms and has the potential to develop into all the structures in the adult organism, a characteristic known as the totipotency. The zygote undergoes several rounds of cell division and become blastocyst. At this stage in mammals, cells of the blastomere make their first cell fate decision to become either inner cell mass (ICM), which later gives rise to the embryo proper, or trophectoderm (TE) which not only provides structural support and nutrients for the growth of embryo proper but also involves in sending molecular cues to pattern ICM. The ICM contains cells that are transiently pluripotent as they can develop into any cell type in the body. As development continues, cells within the ICM receive instructions from different transcription factors and signaling pathways, further proliferate and gradually lose their pluripotency as they become epiblast (Epi) and primitive endoderm (PE). Even though transient, pluripotency has to be maintained in the developing blastocyst for proper embryogenesis to occur. Disruption of these molecular pathways that either maintain the pluripotency or instructs differentiation may result in developmental abnormalities or if severe embryonic death. Therefore, it's important that the expression of these molecular cues has to be

tightly regulated both spatially and temporally to generate fully functioning adult organisms. Many regulatory mechanisms, including transcription factors, signaling pathways as well as chromatin modifiers and cell cycle regulators, have been indicated in pluripotency maintenance and cell fate specification. Identification of these molecular cue were made possible with the help of *in vivo* and *in vitro* models such as Embryonic Stem Cells (ES Cells) that are derived from ICM or induced pluripotent stem cells (iPSCs) derived from reprogramming somatic cells. (Chen, Cheng, Yen, & Hsieh, 2017; Frum & Ralston, 2015; Paranjpe & Veenstra, 2015; Posfai, Tam, & Rossant, 2014; Sanges & Cosma, 2011; She, Wei, Kang, & Wang, 2017; Zhao & Jin, 2017)

Transcription factors in pluripotency and cell-fate specification

Transcription factors, for example, are important intermediates in translating environmental cues presented by cell-cell interaction and signaling pathways into cell-fate decision.(Stadhouders, Filion, & Graf, 2019) They bind to specific regions in the genome and activate or repress target genes, resulting in changes in gene expression landscape which helps define cell fates or maintain their original state. One of the well-known transcription factors that plays an important role in the earliest cell-fate determination, that is the specification of ICM and TE, is OCT4/POU5F1. (Marikawa & Alarcón, 2009; Rossant, 2018) Oct4 is strongly expressed in the ICM and loss of OCT4 results in differentiation of ICM into TE, indicating that Oct4 is required for the maintenance of the ICM fate. (Nichols et al., 1998; Niwa, Miyazaki, & Smith, 2000) Through ChIP-Seq and microarray experiments using mouse ESC as well as human ES cell lines, scientists have shown that OCT4 together with its binding partners NANOG and SOX2 transcriptionally activate genes that are also required for maintenance of pluripotency. (Niwa et al., 2000; Rossant, 2018) In addition, Oct4 maintains ICM fate by binding to the

promoter region of *Cdx2*, which encodes a transcription factor that specifies trophoblast fate, and repress its expression within the ICM. (Niwa et al., 2005; Rossant, 2018)

OCT4 dependent pluripotency maintenance is not only restricted to mammalian early embryogenesis. OCT4 homolog Pou5f1/3 is also broadly expressed in many non-mammalian vertebrates including frogs, teleost fish and chickens during early development. (Onichtchouk, 2016; Onichtchouk & Driever, 2016) Complementing mouse ESC that lack OCT4 with frog or axolotl Pou5f3 can rescue pluripotency, indicating that maintenance of pluripotency by OCT4 is an ancestral function common to both mammals and vertebrates. (Morrison & Brickman, 2006; Onichtchouk, 2016) In zebrafish, *pou5f3* mRNA is expressed both maternally and zygotically, and lack of maternal and zygotic Pou5f3 leads to premature activation of genes that promotes differentiation. (Onichtchouk, 2016; Onichtchouk & Driever, 2016; Onichtchouk et al., 2010) Although early lineage specification of vertebrates doesn't recapitulate mammalian early embryonic development, the zygotic genome activation (ZGA) during mid-blastula transition (MBT) in early zebrafish development is linked to pluripotent state. (M. T. Lee et al., 2013; Leichsenring, Maes, Mo̎ssner, Driever, & Onichtchouk, 2013) Combinatorial loss of mammalian pluripotency factors during zebrafish early development, including OCT4, Nanog and SoxB1, leads to developmental arrest before the initiation of gastrulation due to failed ZGA.

Communication of cells via signaling pathways

Signaling pathways play significant roles in cell-fate specification and maintaining pluripotency by mediating proper communication between adjacent cells or cells at a distance. For instance, ligands can be secreted from a cell and bind to their specific receptors on the surface of its own or other cells at a distance, such as BMP and FGF signaling pathways. On the other hand, ligands can be localized on the cell membrane and bind to its receptor localized on

the membrane of cell right next it, such as NOTCH. In either case, stimulation of a signaling pathway leads to activation of a cascade of downstream effector proteins. This results in changes in transcriptional regulation, cell adhesion and/or cell cycle regulation leading to cell-fate specification. In mammals, the second lineage specification occurs when the ICM differentiate into epiblast (Epi) and primitive endoderm (PE). While Epi contributes to the whole embryo proper and extraembryonic mesoderm, PE gives rise to the endodermal layer of the yolk sac. (Rossant, 2018) Several signaling pathways have been shown to specify and maintain Epi and PE. For example, perturbation of FGF signaling either by mutational analysis of FGF4 ligand as well as its receptor or by blocking FGF signaling via small molecules can result in abolishment of PE fate and all cells within ICM transform into Epi due to loss of PE specific transcription factor GATA6. (Feldman, Poueymirou, Papaioannou, DeChiara, & Goldfarb, 1995; Kang, Garg, & Hadjantonakis, 2017; Yamanaka, Lanner, & Rossant, 2010) Conversely, overexpression of exogenous FGF4 ligand is sufficient to induce all ICM to take on PE fate. (Frum & Ralston, 2015; Yamanaka et al., 2010) Differential expression of BMP signaling pathway components has been noted during mammalian pre-implantation embryos where *Bmp4* and *Bmp7* are expressed in cells of the ICM while *Bmpr2* in TE. (Graham et al., 2014; Guo et al., 2010) Inhibition of BMP signaling using drugs or siRNAs at 2-cell stage embryos results in decreased numbers of PE cells without affecting Epi, indicating that BMP signaling is involved in maintenance of PE fate rather than initial formation. (Graham et al., 2014)

In vitro models, such as ICM derived ESCs and Epiblast derived stem cells (EpiSCs) contributed significantly in our understating of pluripotency maintenance. (Posfai et al., 2014) For example, Leukemia Inhibitory Factor (LIF) maintain mouse ES cell pluripotency by positively regulating pluripotency factors SOX2 and NANOG, OCT4 through JAK/STAT and

PI3K pathways respectively. (Nakai-Futatsugi & Niwa, 2013; Posfai et al., 2014) Activation of FGF signaling, particularly FGF4, stimulates mouse ES cells to exit from self-renewal and commit to somatic lineages by activating Tcf15 expression. (Davies et al., 2013; Kunath et al., 2007) Expression of Tcf15, on the other hand, is inhibited by a basic Helix-Loop-Helix domain protein known as Id protein, which is upregulated by BMP signaling. (Davies et al., 2013; Kunath et al., 2007; Patel & Subramanian, 2006) On the contrary, BMPs induce differentiation to various cell types and inhibition of BMP signaling via FGF42 or by activation of Smad2/3 is necessary to maintain pluripotency in human ESCs. (Xu et al., 2005)

Cell cycle in pluripotency and differentiation

Another important phenomenon has to be taken into consideration in pluripotency maintenance and cell-fate specification is the differential regulation of cell-cycle during early embryonic development. In non-mammalian system, such as zebrafish, Xenopus and Drosophila, the early cleavage and blastula stages are characterized by very rapid cell-division consisting of only S- phase and M-phase, and gradual lengthening of the cell cycle as development proceeds towards gastrulation right after MBT. (Liu, Michowski, Kolodziejczyk, & Sicinski, 2019) Like non-mammals, peri-implantation mouse embryos spend very little time during G1 phase and sees a lengthening of the cell-cycle during gastrulation as cells spend more time in gap phases. (Liu et al., 2019; Soufi & Dalton, 2016) In contrast, reprograming of somatic cells (that is converting differentiated somatic cells into induced pluripotent stem cells, aka iPSCs) using OSKM factors (Oct4, Sox2, Klf4 and c-Myc) significantly shortens cell-cycle. (Liu et al., 2019) It is thought that increased G1 length may provide pluripotent cells with a unique window of opportunity to switch on lineage specific transcription factors. (Soufi and Dalton 2016) In agreement, Pauklin et al reported that the capacity of human ES cells differentiate into three germ layers is dependent

on the cell-cycle state, that is the pluripotent cells commit to mesoderm and endoderm during early G1 and ectoderm during late G1 phase. (Pauklin & Vallier, 2013; Soufi & Dalton, 2016) It is also proposed that the enhanced propensity of pluripotent stem cells to differentiate during G1 phase is be due to increased H3K4 trimethylation, which marks active chromatin, of the developmental genes, although the level of H3K27me3 repressive marks stays constant. (Hsiung et al., 2016) This co-occurrence of H3K4me3 and H3K27me3 in the chromatin during mammalian G1 phase, a.k.a bivalent chromatin, is also seen immediately after the MBT of and Zebrafish. (Vastenhouw et al., 2010) This suggests that although developmental genes are not active during G1 phase, they are primed for rapid activation and specifies pluripotent cells into various cell fates upon stimulation by molecular cues. (Dalton, 2015; Hsiung et al., 2016; Soufi & Dalton, 2016)

During tumorigenesis, a small population of cells have the ability to re-establish tumor in an ectopic region. (Kim & Orkin, 2011) These are termed cancer stem cells and behave very much like ES cells as they can divide rapidly and maintain in stem-like state without turning on differentiation signals. (Klimczak, 2015) It is proposed that the characteristics of cancer stem-cells to self-renew and maintain their pluripotency is governed by molecular mechanisms that are common in the ES cells. (Kim & Orkin, 2011; Klimczak, 2015) The genes that are normally expressed and enriched in ES cells are often overexpressed in poorly differentiated tumors, and may associate with poor clinical outcomes. (Ben-Porath et al., 2008) Therefore, understanding how cells maintain their pluripotency and how do the cells know when to switch from proliferation to differentiation and wise versa is of great importance in elucidating the pathogenesis of various cancers and developing anti-cancer therapies.

2. Max Transcriptional Network in Development and Cancer

Max interacting network of transcriptional factors are a group of proteins that bind to DNA in a sequence specific manner and carry out transcriptional regulation of target genes. (Grandori, Cowley, James, & Eisenman, 2000) These proteins contain basic-Helix-Loop-Helix (bHLH) domain and a leucine zipper (Zip) domain which directs protein-protein interaction with other bHLH proteins and sequence specific binding to E-box elements (CACGTG) in the target genes respectively. (Grandori et al., 2000) These proteins are involved in many cellular processes, including cell proliferation and survival, differentiation, cell cycle regulation as well as metabolism during embryonic development. Dysregulation of these proteins in adult tissues is commonly associated with cancer. (Carroll, Freie, Mathsyaraja, & Eisenman, 2018) Therefore, how these proteins interact in cells and regulate transcription is of great interest to study tumorigenesis.

The role of Myc during vertebrate development

One of the infamous members of Max network is the protooncogene *myc* (myelocytosis) which was initially discovered in the early 1980s. *v-myc* encodes a retroviral protein that is commonly associated with cancer in birds. (Enrietto, Payne, & Hayman, 1983) Subsequently, the human homologs of *v-myc* have been identified, including C-myc, N-myc and L-myc, and were known to be overexpressed in many human cancers. (Grandori et al., 2000; Peter J. Hurlin & Huang, 2006) Since its initial discovery, many efforts have been done to elucidate Myc's role in various cell behaviors during embryonic development and tumorigenesis. (Carroll et al., 2018) In general, Myc forms heterodimers with Max (Myc Associated Factor X) via its C-terminal bHLHZip domain and bind to E-box elements of target genes and activate their expression

through N-terminal transactivating domain. (Grandori et al., 2000; Peter J. Hurlin & Huang, 2006) c-Myc is one of the transcription factors that are required for induced pluripotency, and elimination of c-Myc results in decreased reprograming efficiency. (Takahashi & Yamanaka, 2006) This is mainly due to Myc's role in promoting cellular proliferation by lifting the inhibition of S-phase entry by p21. (Gallant & Steiger, 2009) Although an effort to identify cell type specific Myc target genes has been unsuccessful, it was shown that Myc regulates a core set of genes that are involved in ribosome synthesis and RNA processing in both human and mouse ESC as well as other cancer cell types. (Peter J. Hurlin, 2013; Ji et al., 2011) This may also explain the low reprogramming efficiency of somatic cells in that decreased biomass accumulation in the absence of Myc may results in defective cellular growth and cell division. (Ji et al., 2011; Lempiäinen & Shore, 2009)

In contrast to its requirement in induced pluripotency, c-Myc seems to be dispensable for early mammalian embryonic development. Although c-Myc null mouse embryos die around E10.5 due to defects in multi-organ development, conditional knockout of c-Myc from the epiblast has no impact in embryonic development, and that the embryonic lethality is due to abnormalities in definitive hematopoiesis within the placenta. (Davis, Wims, Spotts, Hann, & Bradley, 1993; Dubois et al., 2008) Mutations in MYCN, on the other hand, is associated with a human developmental disorder known as Feingold Syndrome, which is characterized by microcephaly, micrognathia, and multiple organ dysplasia.(Celli, van Bokhoven, & Brunner, 2003; Marcelis et al., 2008) Mouse embryos that are homozygous null for MYCN dies around E11.5. due to multiple organ hypoplasia. (Charron et al., 1992) However, tissue specific deletion of MYCN from various organs revealed that MYCN is required for heart and lung development. (Peter J. Hurlin, 2013) In zebrafish, *myc* homologous genes are differentially expressed during

embryonic development. (Torres, Chiu, & Depinho, 1993) Their role in vertebrate development will be discussed in detail in the later chapters.

MAX and its interacting proteins

It's been known that Max serves as an obligate co-factor for Myc to activate target gene expression. (Blackwood & Eisenman, 1991) Unlike Myc, Max is ubiquitously expressed in both embryonic and extraembryonic tissues at a constant level, and is stored maternally during mammalian development. (Shen-Li et al., 2000) Homozygous Max null embryos die shortly after implantation (E5.5 -6.5) due to massive cellular degeneration in embryonic and extraembryonic tissues. (Shen-Li et al., 2000) It is proposed that sufficient amount of maternal Max is required for proper functioning of Myc superfamily during early development. (Shen-Li et al., 2000)

Although Max can form homodimers, transcriptional activity of these homodimers is very low. (Blackwood & Eisenman, 1991) This led to the identification of other proteins in the Myc superfamily including Max dimerization protein families (MXD1-4), MNT and MGA. (Blackwood & Eisenman, 1991; Grandori et al., 2000; P J Hurlin, Steingrimsson, Copeland, Jenkins, & Eisenman, 1999; Peter J. Hurlin, 2013) These proteins also contains conserved bHLHZip domain, and compete with Myc for binding to Max and antagonize Myc dependent cell cycle progression and promote differentiation by repressing Myc target genes. (Blackwood & Eisenman, 1991; P J Hurlin et al., 1999) For example, overexpression of Mxd1 during mouse embryonic development leads to early embryonic lethality and dwarfism resulting from profound inhibition of cell cycle progression from G0 to S phase. (Quéva, McArthur, Ramos, & Eisenman, 1999) Similar phenomenon was observed in embryos overexpressing Mnt under the control of β-actin promoter. (Peter J. Hurlin, Quéva, & Eisenman, 1997) Furthermore, mouse embryonic fibroblasts (MEFs) lacking Mnt shows increased CyclinE1 and Cdk4 which are known to be

positively regulated by Myc. (Lafita-Navarro et al., 2020) Increased expression of these cell-cycle regulators is also seen in homozygous Mnt null embryos. (Toyo-oka et al., 2004) These experiments further validate the Myc antagonistic role of Max interacting family proteins in cell cycle progression and maintenance of the differentiated state. Loss of function of these Myc antagonists may be the underlying mechanism of increased cancer risk in certain cell types due to deregulation of Myc activity. (Bretones, Delgado, & León, 2015; Diolaiti, McFerrin, Carroll, & Eisenman, 2015; Nilsson & Cleveland, 2003) Indeed, Mxd2 null mouse embryos show increased susceptibility to squamous cell carcinoma and malignant lymphomas when treated with carcinogens.(Schreiber-Agus et al., 1998) Similarly, conditional disruption of Mnt in mouse mammary epithelium leads to adenocarcinoma *in vivo*. (Peter J Hurlin et al., 2003)

Max Gene Associated protein (MGA) is one of the least studied members of the Max interacting protein. Although mutations in MGA is found in many cancer types according to cancer genome atlas (TCGA) and mutation frequency in MGA is much higher than the other Max interacting network proteins (Table 1), not much attention has been given to elucidate its function during tumorigenesis not to mention in embryonic development. Unlike MXD proteins and MNT, MGA is a unique member of the Max interacting proteins due to the presence of another DNA binding domain, the T-box domain, in addition to the bHLHZip domain. The T-box domain is also transcriptionally active. (P J Hurlin et al., 1999) Together with Max, Mga exhibits dose dependent increase in the activation of reporter constructs that contains T-box element. (P J Hurlin et al., 1999) T-box domain is found in a group of evolutionary ancient transcription factors known as T-box proteins. (Naiche, Harrelson, Kelly, & Papaioannou, 2005) Some of these proteins play critical role in early embryonic development in vertebrates. For example, *Bruchyury/T* is involved in mesoderm formation in mouse, xenopus and zebrafish.

(Papaioannou, 2001) Loss of Eomesodermin (Eomes) results in early embryonic lethality due to defects in trophectoderm differentiation. (Russ et al., 2000) Involvement of T-box proteins in early embryogenesis suggests that MGA may also play important roles during early development. Indeed, Mga is expressed as early as E3.5 in mouse embryos and Mga is deposited maternally in zebrafish eggs. (Y. Sun, Tseng, Fan, Ball, & Dougan, 2014a; Washkowitz et al., 2015) Furthermore, mouse embryos that are lacking functional Mga die before implantation due to loss of pluripotent cells. (Washkowitz et al., 2015) It is proposed that Mga is required for pluripotency maintenance by positively regulating the expression of an enzyme, Ornithine Decarboxylase 1 (ODC1), in the polyamine synthesis pathway. (Washkowitz et al., 2015) However, the expression of Mga at later stage in mouse embryos is seen in developing heart, brain, limbs, kidneys and gonads. (Burn, Washkowitz, Gavrilov, & Papaioannou, 2018) In addition, mutations in MGA were found in many cancer types involving various organs (Figure 1.3). This warrants further investigations of Mga's role during cell-fate specification and differentiation during embryogenesis.

Due to early embryonic lethality of mouse embryos lacking Mga, ex utero developing zebrafish embryos can be great model for studying Mga's role in early embryonic development. With modern genome targeting technology, such as CRISPR/Cas9, and knockdown approaches being available in zebrafish, our studying of Mga function in zebrafish embryogenesis will expand our knowledge of how the pluripotency is maintained and/or how cells switch from active proliferation to differentiation. Most importantly, it will shed more lights on the pathogenesis of cancer.

3. TGF-β Signaling in Development

Transforming Growth Factor (TGF) beta superfamily is composed of a group of secreted factors including Nodal, Activin, Bone Morphogenic Proteins (BMPs) and Growth and Differentiation Factors (GDFs). These are evolutionary conserved proteins and play a wide variety of roles ranging from early embryonic development to adult tissue homeostasis. (Weiss & Attisano, 2013) Signaling via TGF-β superfamily work via binding of a secreted ligand to its specific receptors, which are serine-threonine kinase receptors, on the cell surface. There are two types of receptors, Type I and Type II receptors that form complexes upon ligand binding. This leads to phosphorylation of Smad proteins (R-Smads) by Type I receptors which phosphorylates different R-Smads based on the pathway that is been activated. BMP signaling pathway utilizes Smad1/5/8, while activation of Type I receptor by TGF-β/Nodal/Activin leads to phosphorylation of Smad2/3. Consequently, phosphorylated R-Smads form protein complexes with each other and with Smad4 (Co-Smad), which is a transcription factor and regulate target gene expression within the nucleus. (Wu & Hill, 2009)

TGF-β signaling in pluripotency and early lineage specification

Components of both Nodal and BMP signaling pathways are expressed during pre-implantation embryos and play important roles in lineage specification and pluripotency maintenance. (Pera & Tam, 2010) It's been shown that Nodal signaling is required to maintain epiblast pluripotency even before the patterning of germ layers. The evidence comes from analysis of pluripotency markers Oct4 and Foxd3 in Nodal mutant mouse embryos in which the expression of above markers are decreased. (Mesnard, Guzman-Ayala, & Constam, 2006) In addition, Epiblast cells that are lacking Nodal precociously differentiate into neuroepithelial

characteristics. (Camus, Perea-Gomez, Moreau, & Collignon, 2006) As mentioned in earlier section, BMP signaling is important for maintenance of pluripotency in mouse ESCs while promotes differentiation in human ESCs. It's been proposed that BMP mediated pluripotency maintenance in mouse ESCs is due to activation of JAK-STAT signaling via LIF, which is not active in human ESCs. (Cells, Tgf-, & Massagué, 2000) In addition, while active transcription of pluripotency factor *Nanog* in human ESC requires Smad2/3 via Nodal/Activin signaling, Nanog expression is repressed by Smad1/5 mediated by BMP signaling. (Vallier et al., 2009; Xu et al., 2008)

TGF-β in germ layer and axes formation

The induction of three different germ layers in the epiblast is carried out by a combined action of different signaling pathways, including BMP, Nodal, WNT and FGF signaling. (Kiecker, Bates, & Bell, 2016) Nodal is expressed throughout the epiblast and the overlying visceral endoderm. Nodal antagonistic signals from the anterior visceral endoderm (AVE), such as Lefty1, Cerl1 and Dkk1 that are also induced by Nodal, as well as positive regulatory circuit from the Extraembryonic Ectoderm (ExE), including BMP and Wnt signaling, further restricts Nodal expression to the future posterior region of the epiblast where primitive streak will form. (Conlon et al., 1994; Robertson, 2014) In mouse embryos that are lacking Nodal, the primitive streak fail to form and gastrulation doesn't occur.(Conlon et al., 1994) In addition, loss of Smad2, downstream effector of Nodal signaling, results in embryos that fail to acquire A-P axis. (Waldrip, Bikoff, Hoodless, Wrana, & Robertson, 1998) In addition to its role in axes formation, Nodal acts as a morphogen and pattern three germ layers depending on the concentration gradient. Patterning the germ layers utilizing Nodal gradient is evolutionary conserved among different species, including Mouse, Chicken, Xenopus, and Zebrafish. (Tseng, Munisha,

Gutierrez, & Dougan, 2017) Perturbation of Nodal gradient, either by overexpression or by loss-of-function analysis of components of Nodal signaling pathway or its antagonists leads to disruption of germ layer patterning. (Agius, Oelgeschlager, Wessely, Kemp, & De Robertis, 2000; Feldman et al., 1998; Meno et al., 2001; Piepenburg, Grimmer, Williams, & Smith, 2004; Thisse & Thisse, 1999) In zebrafish, loss of both *nodal* genes, *squint (sqt)* and *cyclops (cyc)*, results in loss of mesodermal structures in the head and trunk as well as endoderm. (Feldman et al., 1998) Consistently, embryos overexpressing Nodal antagonist Lefty2 abolishes mesodermal fate and develop well-patterned ectoderm, and overexpression of Activin in these embryos rescues mesoderm fate. (Thisse & Thisse, 1999) On the other hand, loss of Lefty2 in mouse embryos results in expansion of mesoderm. (Piepenburg et al., 2004)

Unlike Nodal/Activin, Bmp is a weak mesoderm inducer,(Koster et al., 1991) but plays important role in establishment of dorsoventral and anterior-posterior axis via acting as a morphogen. During mammalian early development, BMP4 is expressed in the trophoblast derived ExE and is required for the formation of Anterior Posterior Axis formation, a process which is important for normal gastrulation to happen. (Winnier, Blessing, Labosky, & Hogan, 1995) Loss of BMP4 during early development results in abnormal node formation and posterior morphology. (Fujiwara, Dehart, Sulik, & Hogan, 2002) The abnormalities in posterior morphology includes loss of allantois and primordial germ cells that both arise from the proximal epiblast. (Lawson et al., 1999) These data suggest that BMP signaling plays an important role in anterior posterior patterning in mammalian development.

In Zebrafish and Xenopus, Bmp ligands form gradient along the ventral to dorsal axis with high levels expressing in the ventral cells and low level in the dorsal cells. Loss of Bmp ligands in zebrafish embryos, *bmp2b* or *bmp7a*, or their receptors, *alk8*, leads to dorsalization of

the developing embryo. (Dick et al., 2000; Langdon & Mullins, 2011; Mintzer et al., 2001) The BMP gradient is established at multiple levels. First, transcription of Bmp ligands is differentially regulated in ventral and dorsal cell types. The zygotic BMPs, *bmp2b* and *bmp7a* is regulated by maternal transcription factors, such as Pou2/Oct4 and maternal BMP molecule Gdf6a/Radar. The dorsalization phenotype in both Pou2 and Radar mutant embryos can be rescued by overexpression of BMP receptor *alk8*. (Reim & Brand, 2006; Sidi, Goutel, Peyriéras, & Rosa, 2003) It's interesting to note that another maternally deposited protein Mga, from the Max transcription network family, can bind to the upstream regulatory element of *bmp2b* together with Max and Smad4 in the YSL and activate *bmp2b* expression. (Y. Sun et al., 2014a) Although the dorsalizing effect of Mga knockdown in the YSL is mild and recapitulate *mini-fin* (alk8) mutants, it indicates that the signal from the extraembryonic tissue may be involved in maintaining *bmp* levels during post-gastrula stage embryos for proper dorsoventral patterning. In addition to maternal control, expression of *bmp* is also controlled via autoregulatory mechanism. Loss of Smad5 in Zebrafish embryos leads to loss of both *bmp2b* and *bmp7a.* (Hild et al., 1999) On the other hand, expression of BMPs on the dorsal side is repressed by Bozozok, whose expression is activated by Wnt/β-catenin pathway but is repressed by *vox/vent* on the ventral side of the zebrafish emrbyos.(Leung et al., 2003) Secondly, extracellular secreted molecules play important roles in modulating Bmp signaling. Examples of such extracellular molecules include Chordin (Chd), Noggin1, Follistatin-like 2. (Langdon & Mullins, 2011) These proteins are expressed in the dorsal region of both Zebrafish and Xenopus blastula and early gastrula embryos, and bind to Bmp ligands and inhibit ligand receptor binding. (Miller-Bertoglio, Fisher, Sanchez, Mullins, & Halpern, 1997) While loss of *chordin* only mildly ventralizes zebrafish embryos, loss of all three Bmp antagonizers lead to strong ventralization. (Dal-Pra, Furthauer,

Van-Celst, Thisse, & Thisse, 2006) Some other extracellular proteins such as Tolloid and Twisted Gastrulation (Tsg) promotes ventral cell fate by promoting Bmp signaling. Tolloid is a metalloproteinase which cleaves Bmp antagonist Chd and patterns ventral tail tissues during postgastrula stage. (Blader P, Rastegar S, Fischer N, 1997) Tsg was shown to bind to Chd and Bmp complex and enhance Tolloid cleavage of Chd. (Scott et al., 2001)

4. Neural Crest Development

Neural crest cells (NCCs) a group of migratory multipotent stem cells that arise at the border of neural and non-neural ectoderm, usually known as the neural plate border. Progenitors of NCCs are specified at the neural plate border with the instructions of various signaling pathways. As neural tube closes, NCCs delaminate from the dorsal neural tube through a process known as epithelial to mesenchymal transition (EMT) and migrate to various destination in the developing embryo and give rise to a variety of adult tissues and organs ranging from craniofacial structures, melanocytes and peripheral nervous system.

Development of NCCs begins during early gastrulation with the combinatorial action of multiple signaling molecules that are released from the neural and non-neural ectoderm as well as the underlying mesoderm. (Betancur, Bronner-Fraser, & Sauka-Spengler, 2010) In response to these signals, cells at the neural plate border are induced to take on their fate as the presumptive neural crest. (Betancur et al., 2010) One example that is involved in the early induction of NCCs is the BMP signaling pathway. During gastrulation, Bmp is highly expressed in the ventral non-neural ectoderm and is repressed by its antagonists emanating from the involuting mesoderm dorsally. (Betancur et al., 2010) While high levels of Bmp promote epidermal fate, lower level is required for the specification of neural fate in the dorsal ectoderm. The intermediate level of

BMP signaling, on the other hand, corresponds to the position of neural plate border in frogs and chicks. (Wilson, Lagna, Suzuki, & Hemmati-Brivanlou, 1997) Consistent with this, Zebrafish embryos in which Bmp levels are abolished show loss of neural crest progenitors. On the other hand, reduced Bmp level but not complete loss leads to expansion of the neural plate border, suggesting that BMP gradient is essential for establishment or early induction of neural crest population. (Nguyen et al., 1998) However, Bmp gradient alone is not sufficient to induce early neural specifiers. (García-Castro, Marcelle, & Bronner-Fraser, 2002; LaBonne & Bronner-Fraser, 1998) Adding Wnt and members of the FGF signaling pathway to the culture medium in addition to low level of BMP can induce frog neural plate explants to take on neural crest cell fate. (LaBonne & Bronner-Fraser, 1998) Confirming its role in neural crest induction, inhibition of Wnt signaling during Zebrafish early neurulation using an inducible Wnt inhibitor results in loss of early neural crest markers. (Lewis et al., 2004) In addition, Wnt6 is known to be expressed in the ectoderm at the time of neural crest formation in chickens, and culturing naïve neural plate explants with Wnt6 induces the formation of neural crest. (García-Castro et al., 2002) Other signaling pathways, such as FGF and Notch/Delta, are also found to be involved in neural crest development. (Betancur et al., 2010)

Although species specific differences do exits, it's generally thought that the combinatorial action of above-mentioned signaling pathway play important role in subsequent activation of a cascade of transcription factors that specify neural crest population (Betancur et al., 2010) Among these transcription factors, Msx1/2, Dlx5, Pax3/7, Gbx2, and Zic proteins are the first to appear in the neural plate border. (Betancur et al., 2010) These transcription factors further induce expression of a set of other transcription factors, including Sox9/10, Snail1/2, FoxD3, AP2a, Id proteins, as well as Twist and c-Myc, that promote neural crest survival as well

as subsequent migration. (Betancur et al., 2010) As an example, Snail2 acts to negatively regulate genes that are involved in cell adhesion, such as *E-cadherin* and *Cad6b* and promote EMT during neural crest migration. (Cano et al., 2000; Taneyhill, Coles, & Bronner-Fraser, 2007) Mych, a c-Myc homolog in zebrafish, was shown to be important for pre-migratory neural crest cell survival. (Hong, Tsang, & Dawid, 2008a)

Expressions of these early neural crest specifiers were examined in human embryos at the time of early neural crest development.(Betters, Liu, Kjaeldgaard, Sundström, & García-Castro, 2010) Sox9/10, Pax3 as well as AP2a were all shown to be expressed in the dorsal neural tube as early as Carnegie Stage 12, marking the pre-migratory neural crest population. Mutations in Sox10 and Pax3 in humans leads to a developmental disorder known as Waardenburg Syndrome, which is characterized by the patchy loss of pigmentation in the skin and hair and hearing loss. (Pingault et al., 2010) Taken together, formation of neural crest cells and their derivatives is controlled by a complex and conserved mechanism governed by early induction via different signaling pathways and by specification of neural crest progenitors through an intricate gene regulatory network.

Reference:

Agius, E., Oelgeschlager, M., Wessely, O., Kemp, C., & De Robertis, E. M. (2000). Endodermal Nodal-related signals and mesoderm induction in Xenopus. *Development (Cambridge, England)*, *127*(6), 1173–1183.

Altschul, S. F., Madden, T. L., Schäffer, A. A., Zhang, J., Zhang, Z., Miller, W., & Lipman, D. J.

(1997). Gapped BLAST and PSI-BLAST: a new generation of protein database search programs. *Nucleic Acids Research*, *25*(17), 3389–3402. https://doi.org/10.1093/nar/25.17.3389

Bachmann, A. S., & Geerts, D. (2018). Polyamine synthesis as a target of MYC oncogenes. *The Journal of Biological Chemistry*, *293*(48), 18757–18769. https://doi.org/10.1074/jbc.TM118.003336

Bellmeyer, A., Krase, J., Lindgren, J., & LaBonne, C. (2003). The protooncogene c-myc is an essential regulator of neural crest formation in xenopus. *Developmental Cell*, *4*(6), 827–839.

Bello-Fernandez, C., Packham, G., & Cleveland, J. L. (1993). The ornithine decarboxylase gene is a transcriptional target of c-Myc. *Proceedings of the National Academy of Sciences of the United States of America*, *90*(16), 7804–7808. https://doi.org/10.1073/pnas.90.16.7804

Ben-Porath, I., Thomson, M. W., Carey, V. J., Ge, R., Bell, G. W., Regev, A., & Weinberg, R. A. (2008). An embryonic stem cell–like gene expression signature in poorly differentiated aggressive human tumors. *Nature Genetics*, *40*(5), 499–507. https://doi.org/10.1038/ng.127

Betancur, P., Bronner-Fraser, M., & Sauka-Spengler, T. (2010). Assembling Neural Crest Regulatory Circuits into a Gene Regulatory Network. *Annual Review of Cell and Developmental Biology*, *26*(1), 581–603. https://doi.org/10.1146/annurev.cellbio.042308.113245

Betters, E., Liu, Y., Kjaeldgaard, A., Sundström, E., & García-Castro, M. I. (2010). Analysis of early human neural crest development. *Developmental Biology*, *344*(2), 578–592. https://doi.org/10.1016/j.ydbio.2010.05.012

Blackwood, E. M., & Eisenman, R. N. (1991). Max: a helix-loop-helix zipper protein that forms a sequence-specific DNA-binding complex with Myc. *Science (New York, N.Y.)*, *251*(4998),

1211–1217. https://doi.org/10.1126/science.2006410

Blader P, Rastegar S, Fischer N, S. U. (1997). Cleavage of the BMP-4 antagonist chordin by zebrafish tolloid. *Science (New York, N.Y.)*, *278*.

Bretones, G., Delgado, M. D., & León, J. (2015). Myc and cell cycle control. *Biochimica et Biophysica Acta - Gene Regulatory Mechanisms*, *1849*(5), 506–516. https://doi.org/10.1016/j.bbagrm.2014.03.013

Buitrago-Delgado, E., Nordin, K., Rao, A., Geary, L., & LaBonne, C. (2015). Shared regulatory programs suggest retention of blastula-stage potential in neural crest cells. *Science*, *348*(6241), 1332–1335. https://doi.org/10.1126/science.aaa3655

Burn, S. F., Washkowitz, A. J., Gavrilov, S., & Papaioannou, V. E. (2018). Postimplantation Mga expression and embryonic lethality of two gene-trap alleles. *Gene Expression Patterns*, *27*(September 2017), 31–35. https://doi.org/10.1016/j.gep.2017.10.006

Camp, E., & Lardelli, M. (2001). Tyrosinase gene expression in zebrafish embryos. *Development Genes and Evolution*, *211*(3), 150–153. https://doi.org/10.1007/s004270000125

Camus, A., Perea-Gomez, A., Moreau, A., & Collignon, J. (2006). Absence of Nodal signaling promotes precocious neural differentiation in the mouse embryo. *Developmental Biology*, *295*(2), 743–755. https://doi.org/https://doi.org/10.1016/j.ydbio.2006.03.047

Cano, A., Perez-Moreno, M. A., Rodrigo, I., Locascio, A., Blanco, M. J., del Barrio, M. G., … Nieto, M. A. (2000). The transcription factor snail controls epithelial-mesenchymal transitions by repressing E-cadherin expression. *Nature Cell Biology*, *2*(2), 76–83. https://doi.org/10.1038/35000025

Carroll, P. A., Freie, B. W., Mathsyaraja, H., & Eisenman, R. N. (2018). The MYC transcription factor network: balancing metabolism, proliferation and oncogenesis. *Frontiers of*

Medicine, *12*(4), 412–425. https://doi.org/10.1007/s11684-018-0650-z

CB, K., WW, B., SR, K., B, U., & TF, S. (1995). Stages of embryonic development of the zebrafish. *Developmental Dynamics*, *203*(3), 253–310. Retrieved from https://www.mbl.edu/zebrafish/files/2013/03/Kimmel_stagingseries1.pdf%0Ahttp://www.researchgate.net/profile/Bonnie_Ullmann/publication/227763372_Stages_of_embryonic_development_of_the_zebrafish/links/55352d8b0cf268fd00156437.pdf

Celli, J., van Bokhoven, H., & Brunner, H. G. (2003). Feingold syndrome: Clinical review and genetic mapping. *American Journal of Medical Genetics Part A*, *122A*(4), 294–300. https://doi.org/doi:10.1002/ajmg.a.20471

Cells, H. O. W., Tgf-, R., & Massagué, J. (2000). REVIEWS, *1*(December).

Charron, J., Malynn, B. A., Fisher, P., Stewart, V., Jeannotte, L., Goff, S. P., … Alt, F. W. (1992). Embryonic lethality in mice homozygous for a targeted disruption of the N-myc gene. *Genes & Development*, *6*(12A), 2248–2257. https://doi.org/10.1101/gad.6.12a.2248

Chen, C. Y., Cheng, Y. Y., Yen, C. Y. T., & Hsieh, P. C. H. (2017). Mechanisms of pluripotency maintenance in mouse embryonic stem cells. *Cellular and Molecular Life Sciences*, *74*(10), 1805–1817. https://doi.org/10.1007/s00018-016-2438-0

Comprehensive molecular profiling of lung adenocarcinoma. (2014). *Nature*, *511*(7511), 543–550. https://doi.org/10.1038/nature13385

Conlon, F. L., Lyons, K. M., Takaesu, N., Barth, K. S., Kispert, A., Herrmann, B., & Robertson, E. J. (1994). A primary requirement for nodal in the formation and maintenance of the primitive streak in the mouse. *Development (Cambridge, England)*, *120*(7), 1919–1928.

Dal-Pra, S., Furthauer, M., Van-Celst, J., Thisse, B., & Thisse, C. (2006). Noggin1 and Follistatin-like2 function redundantly to Chordin to antagonize BMP activity.

Developmental Biology, *298*(2), 514–526. https://doi.org/10.1016/j.ydbio.2006.07.002

Dalton, S. (2015). Linking the Cell Cycle to Cell Fate Decisions. *Trends in Cell Biology*, *25*(10), 592–600. https://doi.org/10.1016/j.tcb.2015.07.007

Davies, O. R., Lin, C. Y., Radzisheuskaya, A., Zhou, X., Taube, J., Blin, G., … Lowell, S. (2013). Tcf15 Primes Pluripotent Cells for Differentiation. *Cell Reports*, *3*(2), 472–484. https://doi.org/10.1016/j.celrep.2013.01.017

Davis, A. C., Wims, M., Spotts, G. D., Hann, S. R., & Bradley, A. (1993). A null c-myc mutation causes lethality before 10.5 days of gestation in homozygotes and reduced fertility in heterozygous female mice. *Genes and Development*, *7*(4), 671–682. https://doi.org/10.1101/gad.7.4.671

de Paoli, L., Cerri, M., Monti, S., Rasi, S., Spina, V., Bruscaggin, A., … Rossi, D. (2012). MGA, a suppressor of MYC, is recurrently inactivated in high risk chronic lymphocytic leukemia. *Leukemia & Lymphoma*, *54*(May 2012), 1087–1090. https://doi.org/10.3109/10428194.2012.723706

De Paoli, L., Cerri, M., Monti, S., Rasi, S., Spina, V., Bruscaggin, A., … Rossi, D. (2013, May). MGA, a suppressor of MYC, is recurrently inactivated in high risk chronic lymphocytic leukemia. *Leukemia & Lymphoma*. United States. https://doi.org/10.3109/10428194.2012.723706

Dick, A., Hild, M., Bauer, H., Imai, Y., Maifeld, H., Schier, A. F., … Hammerschmidt, M. (2000). Essential role of Bmp7 (snailhouse) and its prodomain in dorsoventral patterning of the zebrafish embryo. *Development (Cambridge, England)*, *127*(2), 343–354.

Diolaiti, D., McFerrin, L., Carroll, P. A., & Eisenman, R. N. (2015). Functional interactions among members of the MAX and MLX transcriptional network during oncogenesis.

Biochimica et Biophysica Acta - Gene Regulatory Mechanisms, *1849*(5), 484–500. https://doi.org/10.1016/j.bbagrm.2014.05.016

Dubois, N. C., Adolphe, C., Ehninger, A., Wang, R. A., Robertson, E. J., & Trumpp, A. (2008). Placental rescue reveals a sole requirement for c-Myc in embryonic erythroblast survival and hematopoietic stem cell function. *Development*, *135*(14), 2455 LP – 2465. https://doi.org/10.1242/dev.022707

El-Brolosy, M. A., Kontarakis, Z., Rossi, A., Kuenne, C., Günther, S., Fukuda, N., … Stainier, D. Y. R. (2019). Genetic compensation triggered by mutant mRNA degradation. *Nature*, *568*(7751), 193–197. https://doi.org/10.1038/s41586-019-1064-z

El-Brolosy, M. A., & Stainier, D. Y. R. (2017). Genetic compensation: A phenomenon in search of mechanisms. *PLOS Genetics*, *13*(7), e1006780. Retrieved from https://doi.org/10.1371/journal.pgen.1006780

Enrietto, P. J., Payne, L. N., & Hayman, M. J. (1983). A recovered avian myelocytomatosis virus that induces lymphomas in chickens: pathogenic properties and their molecular basis. *Cell*, *35*(2 PART 1), 369–379. https://doi.org/10.1016/0092-8674(83)90170-8

Eve, A. M. J., Place, E. S., & Smith, J. C. (2017). Comparison of Zebrafish tmem88a mutant and morpholino knockdown phenotypes. *PloS One*, *12*(2), e0172227. https://doi.org/10.1371/journal.pone.0172227

Feldman, B., Gates, M. A., Egan, E. S., Dougan, S. T., Rennebeck, G., Sirotkin, H. I., … Talbot, W. S. (1998). Zebrafish organizer development and germ-layer formation require nodal-related signals. *Nature*, *395*(6698), 181–185. https://doi.org/10.1038/26013

Feldman, B., Poueymirou, W., Papaioannou, V. E., DeChiara, T. M., & Goldfarb, M. (1995). Requirement of FGF-4 for postimplantation mouse development. *Science (New York, N.Y.)*,

267(5195), 246–249.

Frum, T., & Ralston, A. (2015). Cell signaling and transcription factors regulating cell fate during formation of the mouse blastocyst. *Trends in Genetics*, *31*(7), 402–410. https://doi.org/10.1016/j.tig.2015.04.002

Fuentes, R., Letelier, J., Tajer, B., Valdivia, L. E., & Mullins, M. C. (2018). Fishing forward and reverse: Advances in zebrafish phenomics. *Mechanisms of Development*, *154*(August), 296–308. https://doi.org/10.1016/j.mod.2018.08.007

Fujiwara, T., Dehart, D. B., Sulik, K. K., & Hogan, B. L. M. (2002). Distinct requirements for extra-embryonic and embryonic bone morphogenetic protein 4 in the formation of the node and primitive streak and coordination of left-right asymmetry in the mouse. *Development*, *129*(20), 4685–4696.

Gallant, P., & Steiger, D. (2009). Myc's secret life without Max. *Cell Cycle*, *8*(23), 3848–3853. https://doi.org/10.4161/cc.8.23.10088

García-Castro, M. I., Marcelle, C., & Bronner-Fraser, M. (2002). Ectodermal Wnt Function as a Neural Crest Inducer. *Science*, *297*(5582), 848 LP – 851. https://doi.org/10.1126/science.1070824

Ghosh, T. K., Brook, J. D., & Wilsdon, A. (2017). T-Box Genes in Human Development and Disease. *Current Topics in Developmental Biology*, *122*, 383–415. https://doi.org/10.1016/bs.ctdb.2016.08.006

Graham, S. J. L., Wicher, K. B., Jedrusik, A., Guo, G., Herath, W., Robson, P., & Zernicka-Goetz, M. (2014). BMP signalling regulates the pre-implantation development of extra-embryonic cell lineages in the mouse embryo. *Nature Communications*, *5*(May). https://doi.org/10.1038/ncomms6667

Grandori, C., Cowley, S. M., James, L. P., & Eisenman, R. N. (2000). T He M Yc / M Ax / M Ad N Etwork and the. *Cancer Research*.

Guo, G., Huss, M., Tong, G. Q., Wang, C., Li Sun, L., Clarke, N. D., & Robson, P. (2010). Resolution of Cell Fate Decisions Revealed by Single-Cell Gene Expression Analysis from Zygote to Blastocyst. *Developmental Cell*, *18*(4), 675–685. https://doi.org/10.1016/j.devcel.2010.02.012

Hendzel, M. J., Wei, Y., Mancini, M. A., Van Hooser, A., Ranalli, T., Brinkley, B. R., … Allis, C. D. (1997). Mitosis-specific phosphorylation of histone H3 initiates primarily within pericentromeric heterochromatin during G2 and spreads in an ordered fashion coincident with mitotic chromosome condensation. *Chromosoma*, *106*(6), 348–360. https://doi.org/10.1007/s004120050256

Hild, M., Dick, A., Rauch, G. J., Meier, A., Bouwmeester, T., Haffter, P., & Hammerschmidt, M. (1999). The smad5 mutation somitabun blocks Bmp2b signaling during early dorsoventral patterning of the zebrafish embryo. *Development*, *126*(10), 2149 LP – 2159. Retrieved from http://dev.biologists.org/content/126/10/2149.abstract

Hong, S.-K., Tsang, M., & Dawid, I. B. (2008a). The mych gene is required for neural crest survival during zebrafish development. *PloS One*, *3*(4), e2029. https://doi.org/10.1371/journal.pone.0002029

Hong, S.-K., Tsang, M., & Dawid, I. B. (2008b). The Mych Gene Is Required for Neural Crest Survival during Zebrafish Development. *PLOS ONE*, *3*(4), e2029. Retrieved from https://doi.org/10.1371/journal.pone.0002029

Hsiung, C. C. S., Bartman, C. R., Huang, P., Ginart, P., Stonestrom, A. J., Keller, C. A., … Blobel, G. A. (2016). A hyperactive transcriptional state marks genome reactivation at the

mitosis-G1 transition. *Genes and Development*, *30*(12), 1423–1439. https://doi.org/10.1101/gad.280859.116

Hurlin, P J, Steingrimsson, E., Copeland, N. G., Jenkins, N. A., & Eisenman, R. N. (1999). Mga, a dual-specificity transcription factor that interacts with Max and contains a T-domain DNA-binding motif. *The EMBO Journal*, *18*(24), 7019–7028. https://doi.org/10.1093/emboj/18.24.7019

Hurlin, Peter J. (2013). Control of vertebrate development by MYC. *Cold Spring Harbor Perspectives in Medicine*, *3*(9). https://doi.org/10.1101/cshperspect.a014332

Hurlin, Peter J., & Huang, J. (2006). The MAX-interacting transcription factor network. *Seminars in Cancer Biology*, *16*(4), 265–274. https://doi.org/10.1016/j.semcancer.2006.07.009

Hurlin, Peter J., Quéva, C., & Eisenman, R. N. (1997). Mnt, a novel Max-interacting protein is coexpressed with Myc in proliferating cells and mediates repression at Myc binding sites. *Genes and Development*, *11*(1), 44–58. https://doi.org/10.1101/gad.11.1.44

Hurlin, Peter J, Zhou, Z.-Q., Toyo-oka, K., Ota, S., Walker, W. L., Hirotsune, S., & Wynshaw-Boris, A. (2003). Deletion of Mnt leads to disrupted cell cycle control and tumorigenesis. *The EMBO Journal*, *22*(18), 4584–4596. https://doi.org/10.1093/emboj/cdg442

Hwang, W. Y., Fu, Y., Reyon, D., Maeder, M. L., Tsai, S. Q., Sander, J. D., … Joung, J. K. (2013). Efficient genome editing in zebrafish using a CRISPR-Cas system. *Nature Biotechnology*, *31*(3), 227–229. https://doi.org/10.1038/nbt.2501

Jao, L.-E., Wente, S. R., & Chen, W. (2013). Efficient multiplex biallelic zebrafish genome editing using a CRISPR nuclease system. *Proceedings of the National Academy of Sciences of the United States of America*, *110*(34), 13904–13909.

https://doi.org/10.1073/pnas.1308335110

Ji, H., Wu, G., Zhan, X., Nolan, A., Koh, C., de Marzo, A., … Zeller, K. I. (2011). Cell-type independent MYC target genes reveal a primordial signature involved in biomass accumulation. *PLoS ONE*, *6*(10). https://doi.org/10.1371/journal.pone.0026057

Jo, Y. S., Kim, M. S., Yoo, N. J., & Lee, S. H. (2016a). Somatic mutation of a candidate tumour suppressor MGA gene and its mutational heterogeneity in colorectal cancers. *Pathology*, *48*(5), 525–527. https://doi.org/10.1016/j.pathol.2016.04.010

Jo, Y. S., Kim, M. S., Yoo, N. J., & Lee, S. H. (2016b, August). Somatic mutation of a candidate tumour suppressor MGA gene and its mutational heterogeneity in colorectal cancers. *Pathology*. England. https://doi.org/10.1016/j.pathol.2016.04.010

Juin, P., Hueber, A. O., Littlewood, T., & Evan, G. (1999). c-Myc-induced sensitization to apoptosis is mediated through cytochrome c release. *Genes and Development*, *13*(11), 1367–1381. https://doi.org/10.1101/gad.13.11.1367

Kang, M., Garg, V., & Hadjantonakis, A.-K. (2017). Lineage Establishment and Progression within the Inner Cell Mass of the Mouse Blastocyst Requires FGFR1 and FGFR2. *Developmental Cell*, *41*(5), 496-510.e5. https://doi.org/10.1016/j.devcel.2017.05.003

Kara, N., Wei, C., Commanday, A. C., & Patton, J. G. (2017). miR-27 regulates chondrogenesis by suppressing focal adhesion kinase during pharyngeal arch development. *Developmental Biology*, *429*(1), 321–334. https://doi.org/https://doi.org/10.1016/j.ydbio.2017.06.013

Kelsh, R. N., Harris, M. L., Colanesi, S., & Erickson, C. A. (2009). Stripes and belly-spots-A review of pigment cell morphogenesis in vertebrates. *Seminars in Cell and Developmental Biology*, *20*(1), 90–104. https://doi.org/10.1016/j.semcdb.2008.10.001

Kerosuo, L., & Bronner, M. E. (2016). cMyc Regulates the Size of the Premigratory Neural

Crest Stem Cell Pool. *Cell Reports*, *17*(10), 2648–2659. https://doi.org/10.1016/j.celrep.2016.11.025

Kiecker, C., Bates, T., & Bell, E. (2016). Molecular specification of germ layers in vertebrate embryos. *Cellular and Molecular Life Sciences*, *73*(5), 923–947. https://doi.org/10.1007/s00018-015-2092-y

Kim, J., & Orkin, S. H. (2011). Embryonic stem cell-specific signatures in cancer: Insights into genomic regulatory networks and implications for medicine. *Genome Medicine*, *3*(11). https://doi.org/10.1186/gm291

Klimczak, M. (2015). Oncogenesis and induced pluripotency-Commonalities of signalling pathways. *Wspolczesna Onkologia*, *1A*, A16–A21. https://doi.org/10.5114/wo.2014.47133

Kok, F. O., Shin, M., Ni, C.-W., Gupta, A., Grosse, A. S., van Impel, A., … Lawson, N. D. (2015). Reverse Genetic Screening Reveals Poor Correlation between Morpholino-Induced and Mutant Phenotypes in Zebrafish. *Developmental Cell*, *32*(1), 97–108. https://doi.org/https://doi.org/10.1016/j.devcel.2014.11.018

Koster, M., Plessow, S., Clement, J. H., Lorenz, A., Tiedemann, H., & Knochel, W. (1991). Bone morphogenetic protein 4 (BMP-4), a member of the TGF-beta family, in early embryos of Xenopus laevis: analysis of mesoderm inducing activity. *Mechanisms of Development*, *33*(3), 191–199. https://doi.org/10.1016/0925-4773(91)90027-4

Kunath, T., Saba-El-Leil, M. K., Almousailleakh, M., Wray, J., Meloche, S., & Smith, A. (2007). FGF stimulation of the Erk1/2 signalling cascade triggers transition of pluripotent embryonic stem cells from self-renewal to lineage commitment. *Development*, *134*(16), 2895 LP – 2902. https://doi.org/10.1242/dev.02880

LaBonne, C., & Bronner-Fraser, M. (1998). Neural crest induction in Xenopus: evidence for a

two-signal model. *Development*, *125*(13), 2403 LP – 2414. Retrieved from http://dev.biologists.org/content/125/13/2403.abstract

Lafita-Navarro, M. C., Liaño-Pons, J., Quintanilla, A., Varela, I., Blanco, R., Ourique, F., … León, J. (2020). The MNT transcription factor autoregulates its expression and supports proliferation in MYC-associated factor X (MAX)-deficient cells. *The Journal of Biological Chemistry*, *295*(7), 2001–2017. https://doi.org/10.1074/jbc.RA119.010389

Lai, J. K. H., Gagalova, K. K., Kuenne, C., El-Brolosy, M. A., & Stainier, D. Y. R. (2019). Induction of interferon-stimulated genes and cellular stress pathways by morpholinos in zebrafish. *Developmental Biology*, *454*(1), 21–28. https://doi.org/10.1016/j.ydbio.2019.06.008

Langdon, Y. G., & Mullins, M. C. (2011). Maternal and Zygotic Control of Zebrafish Dorsoventral Axial Patterning. *Annual Review of Genetics*, *45*(1), 357–377. https://doi.org/10.1146/annurev-genet-110410-132517

Lawson, K. A., Dunn, N. R., Roelen, B. A. J., Zeinstra, L. M., Davis, A. M., Wright, C. V. E., … Hogan, B. L. M. (1999). Bmp4 is required for the generation of primordial germ cells in the mouse embryo. *Genes and Development*, *13*(4), 424–436. https://doi.org/10.1101/gad.13.4.424

Lee, M. T., Bonneau, A. R., Takacs, C. M., Bazzini, A. A., Divito, K. R., Fleming, E. S., & Giraldez, A. J. (2013). Nanog, Pou5f1 and SoxB1 activate zygotic gene expression during the maternal-to-zygotic transition. *Nature*, *503*(7476), 360–364. https://doi.org/10.1038/nature12632

Lee, S. G., Huang, M., Obholzer, N. D., Sun, S., Li, W., Petrillo, M., … Chen, Z.-Y. (2016). Myc and Fgf Are Required for Zebrafish Neuromast Hair Cell Regeneration. *PLOS ONE*,

11(6), e0157768. Retrieved from https://doi.org/10.1371/journal.pone.0157768

Leichsenring, M., Maes, J., Mo̎ssner, R., Driever, W., & Onichtchouk, D. (2013). Pou5f1 transcription factor controls zygotic gene activation in vertebrates. *Science*, *341*(6149), 1005–1009. https://doi.org/10.1126/science.1242527

Lempiäinen, H., & Shore, D. (2009). Growth control and ribosome biogenesis. *Current Opinion in Cell Biology*, *21*(6), 855–863. https://doi.org/10.1016/j.ceb.2009.09.002

Leung, T., Bischof, J., Soll, I., Niessing, D., Zhang, D., Ma, J., … Driever, W. (2003). bozozok directly represses bmp2b transcription and mediates the earliest dorsoventral asymmetry of bmp2b expression in zebrafish. *Development (Cambridge, England)*, *130*(16), 3639–3649. https://doi.org/10.1242/dev.00558

Lewis, J. L., Bonner, J., Modrell, M., Ragland, J. W., Moon, R. T., Dorsky, R. I., & Raible, D. W. (2004). Reiterated Wnt signaling during zebrafish neural crest development. *Development*, *131*(6), 1299 LP – 1308. https://doi.org/10.1242/dev.01007

Liu, L., Michowski, W., Kolodziejczyk, A., & Sicinski, P. (2019). The cell cycle in stem cell proliferation, pluripotency and differentiation. *Nature Cell Biology*, *21*(9), 1060–1067. https://doi.org/10.1038/s41556-019-0384-4

Llabata, P., Mitsuishi, Y., Choi, P. S., Cai, D., Francis, J. M., Torres-Diz, M., … Zhang, X. (2019). Multi-Omics Analysis Identifies MGA as a Negative Regulator of the MYC Pathway in Lung Adenocarcinoma. *Molecular Cancer Research : MCR*. https://doi.org/10.1158/1541-7786.MCR-19-0657

Ma, Z., Zhu, P., Shi, H., Guo, L., Zhang, Q., Chen, Y., … Chen, J. (2019). PTC-bearing mRNA elicits a genetic compensation response via Upf3a and COMPASS components. *Nature*, *568*(7751), 259–263. https://doi.org/10.1038/s41586-019-1057-y

Marcelis, C. L. M., Hol, F. A., Graham, G. E., Rieu, P. N. M. A., Kellermayer, R., Meijer, R. P. P., … de Brouwer, A. P. M. (2008). Genotype–phenotype correlations in MYCN-related Feingold syndrome. *Human Mutation*, *29*(9), 1125–1132. https://doi.org/doi:10.1002/humu.20750

Marikawa, Y., & Alarcón, V. B. (2009). Establishment of trophectoderm and inner cell mass lineages in the mouse embryo. *Molecular Reproduction and Development*, *76*(11), 1019–1032. https://doi.org/10.1002/mrd.21057

Mashal, R. D., Koontz, J., & Sklar, J. (1995). Detection of mutations by cleavage of DNA heteroduplexes with bacteriophage resolvases. *Nature Genetics*, *9*(2), 177–183. https://doi.org/10.1038/ng0295-177

McMahon, S. B. (2014). MYC and the control of apoptosis. *Cold Spring Harbor Perspectives in Medicine*, *4*(7), 1–10. https://doi.org/10.1101/cshperspect.a014407

Mendieta-Serrano, M. A., Schnabel, D., Lomelí, H., & Salas-Vidal, E. (2013). Cell Proliferation Patterns in Early Zebrafish Development. *Anatomical Record*, *296*(5), 759–773. https://doi.org/10.1002/ar.22692

Menescal, L. A., Schmidt, C., Liedtke, D., & Schartl, M. (2012). Liver hyperplasia after tamoxifen induction of Myc in a transgenic medaka model. *Disease Models & Mechanisms*, *5*(4), 492–502. https://doi.org/10.1242/dmm.008730

Meno, C., Takeuchi, J., Sakuma, R., Koshiba-Takeuchi, K., Ohishi, S., Saijoh, Y., … Hamada, H. (2001). Diffusion of nodal signaling activity in the absence of the feedback inhibitor Lefty2. *Developmental Cell*, *1*(1), 127–138. https://doi.org/10.1016/s1534-5807(01)00006-5

Mesnard, D., Guzman-Ayala, M., & Constam, D. B. (2006). Nodal specifies embryonic visceral endoderm and sustains pluripotent cells in the epiblast before overt axial patterning.

Development, *133*(13), 2497 LP – 2505. https://doi.org/10.1242/dev.02413

Miller-Bertoglio, V. E., Fisher, S., Sanchez, A., Mullins, M. C., & Halpern, M. E. (1997). Differential regulation of chordin expression domains in mutant zebrafish. *Developmental Biology*, *192*(2), 537–550. https://doi.org/10.1006/dbio.1997.8788

Mintzer, K. A., Lee, M. A., Runke, G., Trout, J., Whitman, M., & Mullins, M. C. (2001). Lost-a-fin encodes a type I BMP receptor, Alk8, acting maternally and zygotically in dorsoventral pattern formation. *Development (Cambridge, England)*, *128*(6), 859–869.

Morrison, G. M., & Brickman, J. M. (2006). Conserved roles for Oct4 homologues in maintaining multipotency during early vertebrate development. *Development*, *133*(10), 2011–2022. https://doi.org/10.1242/dev.02362

Naiche, L. a, Harrelson, Z., Kelly, R. G., & Papaioannou, V. E. (2005). T-box genes in vertebrate development. *Annual Review of Genetics*, *39*, 219–239. https://doi.org/10.1146/annurev.genet.39.073003.105925

Nakai-Futatsugi, Y., & Niwa, H. (2013). Transcription factor network in embryonic stem cells: Heterogeneity under the stringency. *Biological and Pharmaceutical Bulletin*, *36*(2), 166–170. https://doi.org/10.1248/bpb.b12-00958

Nguyen, V. H., Schmid, B., Trout, J., Connors, S. A., Ekker, M., & Mullins, M. C. (1998). Ventral and Lateral Regions of the Zebrafish Gastrula, Including the Neural Crest Progenitors, Are Established by abmp2b/swirlPathway of Genes. *Developmental Biology*, *199*(1), 93–110. https://doi.org/https://doi.org/10.1006/dbio.1998.8927

Nichols, J., Zevnik, B., Anastassiadis, K., Niwa, H., Klewe-Nebenius, D., Chambers, I., … Smith, A. (1998). Formation of pluripotent stem cells in the mammalian embryo depends on the POU transcription factor Oct4. *Cell*, *95*(3), 379–391. https://doi.org/10.1016/S0092-

8674(00)81769-9

Nilsson, J. A., & Cleveland, J. L. (2003). Myc pathways provoking cell suicide and cancer. *Oncogene*, *22*(56 REV. ISS. 8), 9007–9021. https://doi.org/10.1038/sj.onc.1207261

Niwa, H., Miyazaki, J., & Smith, A. G. (2000). Quantitative expression of Oct-3/4 defines differentiation, dedifferentiation or self-renewal of ES cells. *Nature Genetics*, *24*(4), 372–376. https://doi.org/10.1038/74199

Niwa, H., Toyooka, Y., Shimosato, D., Strumpf, D., Takahashi, K., Yagi, R., & Rossant, J. (2005). Interaction between Oct3/4 and Cdx2 Determines Trophectoderm Differentiation. *Cell*, *123*(5), 917–929. https://doi.org/10.1016/j.cell.2005.08.040

Novodvorsky, P., Watson, O., Gray, C., Wilkinson, R. N., Reeve, S., Smythe, C., … Chico, T. J. A. (2015). klf2ash317 Mutant Zebrafish Do Not Recapitulate Morpholino-Induced Vascular and Haematopoietic Phenotypes. *PLOS ONE*, *10*(10), e0141611. Retrieved from https://doi.org/10.1371/journal.pone.0141611

Ogawa, H., Ishiguro, K. I., Gaubatz, S., Livingston, D. M., & Nakatani, Y. (2002). A complex with chromatin modifiers that occupies E2f- and Myc-responsive genes in G0 cells. *Science*, *296*(5570), 1132–1136. https://doi.org/10.1126/science.1069861

Onichtchouk, D. (2016). Evolution and functions of Oct4 homologs in non-mammalian vertebrates. *Biochimica et Biophysica Acta - Gene Regulatory Mechanisms*, *1859*(6), 770–779. https://doi.org/10.1016/j.bbagrm.2016.03.013

Onichtchouk, D., & Driever, W. (2016). *Zygotic Genome Activators, Developmental Timing, and Pluripotency*. *Current Topics in Developmental Biology* (1st ed., Vol. 116). Elsevier Inc. https://doi.org/10.1016/bs.ctdb.2015.12.004

Onichtchouk, D., Geier, F., Polok, B., Messerschmidt, D. M., Mössner, R., Wendik, B., …

Driever, W. (2010). Zebrafish Pou5f1-dependent transcriptional networks in temporal control of early development. *Molecular Systems Biology*, *6*(354). https://doi.org/10.1038/msb.2010.9

Papaioannou, V. E. B. T.-I. R. of C. (2001). T-box genes in development: From hydra to humans. In *A Survey of Cell Biology* (Vol. 207, pp. 1–70). Academic Press. https://doi.org/https://doi.org/10.1016/S0074-7696(01)07002-4

Paranjpe, S. S., & Veenstra, G. J. C. (2015). Establishing pluripotency in early development. *Biochimica et Biophysica Acta - Gene Regulatory Mechanisms*, *1849*(6), 626–636. https://doi.org/10.1016/j.bbagrm.2015.03.006

Patel, M., & Subramanian, R. B. (2006). Effect of a chelating agent on lead uptake by Spinacia oleracea. *Pollution Research*, *25*(1), 77–79.

Pauklin, S., & Vallier, L. (2013). XThe cell-cycle state of stem cells determines cell fate propensity. *Cell*, *155*(1), 135. https://doi.org/10.1016/j.cell.2013.08.031

Pendeville, H., Carpino, N., Marine, J.-C., Takahashi, Y., Muller, M., Martial, J. A., & Cleveland, J. L. (2001). The Ornithine Decarboxylase Gene Is Essential for Cell Survival during Early Murine Development. *Molecular and Cellular Biology*, *21*(19), 6549 LP – 6558. https://doi.org/10.1128/MCB.21.19.6549-6558.2001

Pera, M. F., & Tam, P. P. L. (2010). Extrinsic regulation of pluripotent stem cells. *Nature*, *465*(7299), 713–720. https://doi.org/10.1038/nature09228

Piepenburg, O., Grimmer, D., Williams, P. H., & Smith, J. C. (2004). Activin redux: specification of mesodermal pattern in Xenopus by graded concentrations of endogenous activin B. *Development (Cambridge, England)*, *131*(20), 4977–4986. https://doi.org/10.1242/dev.01323

Pingault, V., Ente, D., Dastot-Le Moal, F., Goossens, M., Marlin, S., & Bondurand, N. (2010). Review and update of mutations causing Waardenburg syndrome. *Human Mutation*, *31*(4), 391–406. https://doi.org/10.1002/humu.21211

Place, E. S., & Smith, J. C. (2017). Zebrafish atoh8 mutants do not recapitulate morpholino phenotypes. *PLoS ONE*, *12*(2), 1–12. https://doi.org/10.1371/journal.pone.0171143

Plouhinec, J.-L., Roche, D. D., Pegoraro, C., Figueiredo, A. L., Maczkowiak, F., Brunet, L. J., … Monsoro-Burq, A. H. (2014). Pax3 and Zic1 trigger the early neural crest gene regulatory network by the direct activation of multiple key neural crest specifiers. *Developmental Biology*, *386*(2), 461–472. https://doi.org/https://doi.org/10.1016/j.ydbio.2013.12.010

Popp, M. W.-L., & Maquat, L. E. (2013). Organizing Principles of Mammalian Nonsense-Mediated mRNA Decay. *Annual Review of Genetics*, *47*(1), 139–165. https://doi.org/10.1146/annurev-genet-111212-133424

Posfai, E., Tam, O. H., & Rossant, J. (2014). *Mechanisms of Pluripotency In Vivo and In Vitro*. *Current Topics in Developmental Biology* (1st ed., Vol. 107). Elsevier Inc. https://doi.org/10.1016/B978-0-12-416022-4.00001-9

Quéva, C., McArthur, G. A., Ramos, L. S., & Eisenman, R. N. (1999). Dwarfism and dysregulated proliferation in mice overexpressing the MYC antagonist MAD1. *Cell Growth & Differentiation : The Molecular Biology Journal of the American Association for Cancer Research*, *10*(12), 785—796. Retrieved from http://intl-cgd.aacrjournals.org/cgi/content/full/10/12/785

Reichert, S., Randall, R. A., & Hill, C. S. (2013). A BMP regulatory network controls ectodermal cell fate decisions at the neural plate border. *Development*, *140*(21), 4435 LP – 4444. https://doi.org/10.1242/dev.098707

Reim, G., & Brand, M. (2006). Maternal control of vertebrate dorsoventral axis formation and epiboly by the POU domain protein Spg/Pou2/Oct4. *Development (Cambridge, England)*, *133*(14), 2757–2770. https://doi.org/10.1242/dev.02391

Rikin, A., & Evans, T. (2010). The tbx/bHLH transcription factor mga regulates gata4 and organogenesis. *Developmental Dynamics*, *239*(2), 535–547. https://doi.org/10.1002/dvdy.22197

Robertson, E. J. (2014). Dose-dependent Nodal/Smad signals pattern the early mouse embryo. *Seminars in Cell & Developmental Biology*, *32*, 73–79. https://doi.org/https://doi.org/10.1016/j.semcdb.2014.03.028

Robu, M. E., Larson, J. D., Nasevicius, A., Beiraghi, S., Brenner, C., Farber, S. A., & Ekker, S. C. (2007). p53 Activation by Knockdown Technologies. *PLOS Genetics*, *3*(5), e78. Retrieved from https://doi.org/10.1371/journal.pgen.0030078

Rocha, M., Singh, N., Ahsan, K., Beiriger, A., & Prince, V. E. (2020). Neural crest development: insights from the zebrafish. *Developmental Dynamics*, *249*(1), 88–111. https://doi.org/10.1002/dvdy.122

Rossant, J. (2018). Genetic Control of Early Cell Lineages in the Mammalian Embryo. *Annual Review of Genetics*, *52*(1), 185–201. https://doi.org/10.1146/annurev-genet-120116-024544

Rossi, A., Kontarakis, Z., Gerri, C., Nolte, H., Hölper, S., Krüger, M., & Stainier, D. Y. R. (2015). Genetic compensation induced by deleterious mutations but not gene knockdowns. *Nature*, *524*, 230. Retrieved from https://doi.org/10.1038/nature14580

Russ, A. P., Wattler, S., Colledge, W. H., Aparicio, S. A. J. R., Carlton, M. B. L., Pearce, J. J., … Evans, M. J. (2000). Eomesodermin is required for mouse trophoblast development and mesoderm formation. *Nature*, *404*(6773), 95–99. https://doi.org/10.1038/35003601

Salmerón, C. (2018). Adipogenesis in fish. *The Journal of Experimental Biology*, *221*(Pt Suppl 1). https://doi.org/10.1242/jeb.161588

Sander, J. D., Maeder, M. L., Reyon, D., Voytas, D. F., Joung, J. K., & Dobbs, D. (2010). ZiFiT (Zinc Finger Targeter): an updated zinc finger engineering tool. *Nucleic Acids Research*, *38*(suppl_2), W462–W468. https://doi.org/10.1093/nar/gkq319

Sander, J. D., Zaback, P., Joung, J. K., Voytas, D. F., & Dobbs, D. (2007). Zinc Finger Targeter (ZiFiT): an engineered zinc finger/target site design tool. *Nucleic Acids Research*, *35*(Web Server issue), W599–W605. https://doi.org/10.1093/nar/gkm349

Sanges, D., & Cosma, M. P. (2011). Reprogramming cell fate to pluripotency: The decision-making signalling pathways. *International Journal of Developmental Biology*, *54*(11–12), 1575–1587. https://doi.org/10.1387/ijdb.103190ds

Schreiber-Agus, N., Meng, Y., Hoang, T., Hou, H., Chen, K., Greenberg, R., … DePinho, R. A. (1998). Role of Mxi1 in ageing organ systems and the regulation of normal and neoplastic growth. *Nature*, *393*(6684), 483–487. https://doi.org/10.1038/31008

Schumacher, J. A., Hashiguchi, M., Nguyen, V. H., & Mullins, M. C. (2011). An Intermediate Level of BMP Signaling Directly Specifies Cranial Neural Crest Progenitor Cells in Zebrafish. *PLOS ONE*, *6*(11), e27403. Retrieved from https://doi.org/10.1371/journal.pone.0027403

Scott, I. C., Blitz, I. L., Pappano, W. N., Maas, S. A., Cho, K. W., & Greenspan, D. S. (2001). Homologues of Twisted gastrulation are extracellular cofactors in antagonism of BMP signalling. *Nature*, *410*(6827), 475–478. https://doi.org/10.1038/35068572

She, S., Wei, Q., Kang, B., & Wang, Y. J. (2017). Cell cycle and pluripotency: Convergence on octamer-binding transcription factor 4 (Review). *Molecular Medicine Reports*, *16*(5), 6459–

6466. https://doi.org/10.3892/mmr.2017.7489

Shen-Li, H., O'Hagan, R. C., Hou, H., Horner, J. W., Lee, H. W., & DePinho, R. A. (2000). Essential role for Max in early embryonic growth and development. *Genes and Development*, *14*(1), 17–22. https://doi.org/10.1101/gad.14.1.17

Sidi, S., Goutel, C., Peyriéras, N., & Rosa, F. M. (2003). Maternal induction of ventral fate by zebrafish radar *Proceedings of the National Academy of Sciences*, *100*(6), 3315 LP – 3320. https://doi.org/10.1073/pnas.0530115100

Simoes-Costa, M., & Bronner, M. E. (2015). Establishing neural crest identity: a gene regulatory recipe. *Development*, *142*(2), 242–257. https://doi.org/10.1242/dev.105445

Simões-Costa, M., & Bronner, M. E. (2015). Establishing neural crest identity: a gene regulatory recipe. *Development (Cambridge, England)*, *142*(2), 242–257. https://doi.org/10.1242/dev.105445

Soufi, A., & Dalton, S. (2016). Cycling through developmental decisions: How cell cycle dynamics control pluripotency, differentiation and reprogramming. *Development (Cambridge)*, *143*(23), 4301–4311. https://doi.org/10.1242/dev.142075

Stadhouders, R., Filion, G. J., & Graf, T. (2019). Transcription factors and 3D genome conformation in cell-fate decisions. *Nature*, *569*(7756), 345–354. https://doi.org/10.1038/s41586-019-1182-7

Sun, X., Chen, J., Zhang, Y., Munisha, M., Dougan, S., & Sun, Y. (2018). Mga modulates Bmpr1a activity by antagonizing Bs69 in zebrafish. *Frontiers in Cell and Developmental Biology*, *6*(SEP), 1–14. https://doi.org/10.3389/fcell.2018.00126

Sun, Y., Tseng, W. C., Fan, X., Ball, R., & Dougan, S. T. (2014a). Extraembryonic Signals under the Control of MGA, Max, and Smad4 Are Required for Dorsoventral Patterning.

Developmental Cell, *28*(3), 322–334. https://doi.org/10.1016/j.devcel.2014.01.003

Sun, Y., Tseng, W. C., Fan, X., Ball, R., & Dougan, S. T. (2014b). Extraembryonic Signals under the Control of MGA, Max, and Smad4 Are Required for Dorsoventral Patterning. *Developmental Cell*, *28*(3), 322–334. https://doi.org/10.1016/j.devcel.2014.01.003

Takahashi, K., & Yamanaka, S. (2006). Induction of Pluripotent Stem Cells from Mouse Embryonic and Adult Fibroblast Cultures by Defined Factors. *Cell*, *126*(4), 663–676. https://doi.org/10.1016/j.cell.2006.07.024

Taneyhill, L. A., Coles, E. G., & Bronner-Fraser, M. (2007). Snail2 directly represses cadherin6B during epithelial-to-mesenchymal transitions of the neural crest. *Development (Cambridge, England)*, *134*(8), 1481–1490. https://doi.org/10.1242/dev.02834

Thisse, C., & Thisse, B. (1999). Antivin, a novel and divergent member of the TGFbeta superfamily, negatively regulates mesoderm induction. *Development (Cambridge, England)*, *126*(2), 229–240.

Torres, R., Chiu, F., & Depinho, R. A. (1993). I-, *13*(5), 2765–2775.

Toyo-oka, K., Hirotsune, S., Gambello, M. J., Zhou, Z.-Q., Olson, L., Rosenfeld, M. G., … Wynshaw-Boris, A. (2004). Loss of the Max-interacting protein Mnt in mice results in decreased viability, defective embryonic growth and craniofacial defects: relevance to Miller–Dieker syndrome. *Human Molecular Genetics*, *13*(10), 1057–1067. https://doi.org/10.1093/hmg/ddh116

Tríbulo, C., Aybar, M. J., Nguyen, V. H., Mullins, M. C., & Mayor, R. (2003). Regulation of Msx genes by a Bmp gradient is essential for neural crest specification. *Development*, *130*(26), 6441 LP – 6452. https://doi.org/10.1242/dev.00878

Tseng, W.-C., Munisha, M., Gutierrez, J. B., & Dougan, S. T. (2017). Establishment of the

Vertebrate Germ Layers. *Advances in Experimental Medicine and Biology*, *953*, 307–381. https://doi.org/10.1007/978-3-319-46095-6_7

Vallier, L., Mendjan, S., Brown, S., Ching, Z., Teo, A., Smithers, L. E., … Pedersen, R. A. (2009). Activin/Nodal signalling maintains pluripotency by controlling Nanog expression. *Development*, *136*(8), 1339–1349. https://doi.org/10.1242/dev.033951

van den Berg, D. L. C., Snoek, T., Mullin, N. P., Yates, A., Bezstarosti, K., Demmers, J., … Poot, R. A. (2010). An Oct4-Centered Protein Interaction Network in Embryonic Stem Cells. *Cell Stem Cell*, *6*(4), 369–381. https://doi.org/10.1016/j.stem.2010.02.014

Vastenhouw, N. L., Zhang, Y., Woods, I. G., Imam, F., Regev, A., Liu, X. S., … Schier, A. F. (2010). Chromatin signature of embryonic pluripotency is established during genome activation. *Nature*, *464*(7290), 922–926. https://doi.org/10.1038/nature08866

Vickaryous, M. K., & Mclean, K. E. (2011). *Vertebrate Embryogenesis*. *Reptile Embryology* (Vol. 770). https://doi.org/10.1007/978-1-61779-210-6

Waldrip, W. R., Bikoff, E. K., Hoodless, P. A., Wrana, J. L., & Robertson, E. J. (1998). Smad2 Signaling in Extraembryonic Tissues Determines Anterior-Posterior Polarity of the Early Mouse Embryo. *Cell*, *92*(6), 797–808. https://doi.org/10.1016/S0092-8674(00)81407-5

Washkowitz, A. J., Schall, C., Zhang, K., Wurst, W., Floss, T., Mager, J., & Papaioannou, V. E. (2015). Mga is essential for the survival of pluripotent cells during peri-implantation development. *Development*, *142*(1), 31–40. https://doi.org/10.1242/dev.111104

Wei, K., Chen, J., Akrami, K., Galbraith, G. C., Lopez, I. A., & Chen, F. (2007). Neural crest cell deficiency of c-myc causes skull and hearing defects. *Genesis (New York, N.Y. : 2000)*, *45*(6), 382–390. https://doi.org/10.1002/dvg.20304

Weiss, A., & Attisano, L. (2013). The TGFbeta superfamily signaling pathway. *Wiley*

Interdisciplinary Reviews: Developmental Biology, *2*(1), 47–63. https://doi.org/10.1002/wdev.86

Wilkinson, M. F. (2019, April). Genetic paradox explained by nonsense. *Nature*. England. https://doi.org/10.1038/d41586-019-00823-5

Wilson, P. A., Lagna, G., Suzuki, A., & Hemmati-Brivanlou, A. (1997). Dear Dr. Alfandari, First of all, thank you so much for inviting me to have campus visit at UMass. I really appreciate the opportunity. However, due to the current COVID19 outbreak within the US, I was wondering if there's a possibility to postpone my vis. *Development*, *124*(16), 3177 LP – 3184. Retrieved from http://dev.biologists.org/content/124/16/3177.abstract

Winnier, G., Blessing, M., Labosky, P. A., & Hogan, B. L. (1995). Bone morphogenetic protein-4 is required for mesoderm formation and patterning in the mouse. *Genes & Development*, *9*(17), 2105–2116. https://doi.org/10.1101/gad.9.17.2105

Wu, M. Y., & Hill, C. S. (2009). TGF-β Superfamily Signaling in Embryonic Development and Homeostasis. *Developmental Cell*, *16*(3), 329–343. https://doi.org/10.1016/j.devcel.2009.02.012

Xu, R.-H., Peck, R. M., Li, D. S., Feng, X., Ludwig, T., & Thomson, J. A. (2005). Basic FGF and suppression of BMP signaling sustain undifferentiated proliferation of human ES cells. *Nature Methods*, *2*(3), 185–190. https://doi.org/10.1038/nmeth744

Xu, R.-H., Sampsell-Barron, T. L., Gu, F., Root, S., Peck, R. M., Pan, G., … Thomson, J. A. (2008). NANOG is a direct target of TGFbeta/activin-mediated SMAD signaling in human ESCs. *Cell Stem Cell*, *3*(2), 196–206. https://doi.org/10.1016/j.stem.2008.07.001

Yamanaka, Y., Lanner, F., & Rossant, J. (2010). FGF signal-dependent segregation of primitive endoderm and epiblast in the mouse blastocyst. *Development (Cambridge, England)*,

137(5), 715–724. https://doi.org/10.1242/dev.043471

Zhao, H., & Jin, Y. (2017). Signaling networks in the control of pluripotency. *Current Opinion in Genetics and Development*, *46*, 141–148. https://doi.org/10.1016/j.gde.2017.07.013

Tables and Table Descriptions

Table 1. Mutations in MAX interacting proteins are found in various cancers. Data is generated from the Genomic Data Commons (GDC) data portal from the National Cancer Institute. Among 10202 total cases available on GDC, a total of 4178 cases carry Simple Somatic Mutations (SSM) affecting MGA, MAX, c-MYC, MXD1, MNT, MLX, MXI1/MXD2 and MXD4. Among these 4178 cases, a total of 539 cases were tested positive for mutations in MGA, representing the highest percentage of affected cases in Max interacting network of transcription factors. In addition, a total of 4487 cases were analyzed for Copy Number Variation (CNV) events, and the loss of MGA is found in 16% of cases analyzed, representing the highest CNV loss events affecting MAX interacting proteins and supporting MGA's role as a tumor suppressor. It's important to note that mutations in c-MYC were only found in less than 4% of cases, but CNV gain event is found in as high as 36%. This data is consistent with the fact that dysregulation of MYC in the majority of cancer is not due to mutations in DNA sequence but rather is related to amplification of MYC activity.

Symbol	Name	# SSM Affected Cases in Cohort	# SSM Affected Cases Across the GDC	# CNV Gain	# CNV Loss
MGA	MGA, MAX dimerization protein	539 / 4,178 (12.90%)	539 / 10,202	130 / 4,487 (2.90%)	743 / 4,487 (16.56%)
MAX	MYC associated factor X	150 / 4,178 (3.59%)	150 / 10,202	198 / 4,487 (4.41%)	457 / 4,487 (10.18%)
c-MYC	v-myc avian myelocytomatosis viral oncogene homolog	140 / 4,178 (3.35%)	140 / 10,202	1595 / 4,487 (35.55%)	102 / 4,487 (2.27%)
MXD1	MAX dimerization protein 1	121 / 4,178 (2.90%)	121 / 10,202	303 / 4,487 (6.75%)	146 / 4,487 (3.25%)
MNT	MAX network transcriptional repressor	110 / 4,178 (2.63%)	110 / 10,202	237 / 4,487 (5.28%)	316 / 4,487 (7.04%)
MLX	MLX, MAX dimerization protein	89 / 4,178 (2.13%)	89 / 10,202	273 / 4,487 (6.08%)	370 / 4,487 (8.25%)
MXI1	MAX interactor 1, dimerization protein	82 / 4,178 (1.96%)	82 / 10,202	263 / 4,487 (5.86%)	539 / 4,487 (12.01%)
MXD4	MAX dimerization protein 4	40 / 4,178 (0.96%)	40 / 10,202	408 / 4,487 (9.09%)	239 / 4,487 (5.33%)

CHAPTER 2

MYC INDEPENDENT ROLE OF MGA IN NEURAL CREST SPECIFICATION DURING ZEBRAFISH EARLY EMBRYONIC DEVELOPMENT[1]

[1] Munisha, M., Tseng, WC., Aston, A., Dougan, ST. To be submitted to Developmental Dynamics

ABSTRACT

During early embryogenesis, cells gradually transition from a rapidly proliferating pluripotent state into a non-dividing, differentiated state. A large number of transcription factors and signaling pathways are involved in mediating this process, but the key triggers are still unknown. Max's giant associated protein (Mga) promotes pluripotency in mouse embryos and mouse embryonic stem cells (ESCs). Here we identify a novel role of Mga in promoting cell fate specification during zebrafish early embryonic development. Depletion of Mga from 1-cell stage embryos using antisense morpholinos results in defects in various lineages of the neural crest derivatives. This appears to be due to reduced neural crest specification at the neural plate border. Suppression of Mga results in increased Myc activity and consequently increased expression of Myc target genes *in vivo*. This is consistent with Mga's role as a Myc antagonist in cell culture. However, reduced specification of neural crest cells in Mga depleted embryos is not due elevated Myc as suppression of Myc activity is not sufficient to rescue neural crest defects. We found that Bmp signaling is decreased in *mga* morphants during gastrulation. These results suggest that Mga promote neural crest specification by regulating Bmp signaling. Therefore, we propose that Mga acts as a molecular switch in the naïve ectoderm to promote neural crest fate rather than survival of neural crest population in zebrafish.

INTRODUCTION

In vertebrates, embryonic development is characterized by rapid proliferation of pluripotent cells during blastula stage and gradual restriction of potency during gastrulation through which ectoderm, mesoderm and endoderm are specified. As development continues,

cells further restrict their lineages and potencies to take on specific functions. However, even in terminally differentiated adult tissues, some cells remain to be multipotent, which render them the ability to self-renew and in the meantime differentiate into cells in their own lineage. Understanding the underlying mechanism of how pluripotency or multipotency is maintained and how cells switch from more pluripotent to less potent or differentiated state in the developing embryos will not only contribute substantially to our knowledge in embryonic development but also shed more lights on the pathogenesis of cancer. (Kim & Orkin, 2011; Klimczak, 2015)

Neural crest cells are unique population of multipotent stem cells that arise in the ectodermal germ layer, more specifically at the neural plate border between neural and non-neural ectoderm, during late gastrulation. Although transient, neural crest cells have the ability to differentiate into a wide variety of cell types of ectodermal and mesodermal origin, including neurons and glia of the peripheral nervous system, chromaffin cells in the adrenal medulla, craniofacial cartilages and bones, adipocytes, cardiac muscles, melanocytes as well as connective tissues. (Simões-Costa & Bronner, 2015) The potential of neural crest cells to take on cross-lineage cell fates raises the question of how these population of cells acquire their fate from naïve ectoderm. The classic model of neural crest formation states that the initial induction event through combinatorial action of key developmental signaling pathways emanating from the surrounding tissues, such as BMP, WNT and FGF signaling pathways, results in the establishment of neural plate border between neural and non-neural ectoderm.(Betancur, Bronner-Fraser, & Sauka-Spengler, 2010) The combined action of these signaling pathways leads to a cascade of transcriptional activation of gene regulatory network (GRN) that specify

neural crest cell fate. (Betancur et al., 2010) However, the exact mechanism of how and when the initial signaling induction events specify neural crest at the neural plate border is still unknown.

Here we identified a novel role of pluripotency factor Max Gene Associated protein (MGA) in early neural crest specification. MGA is a transcription factor in the family of MAX interacting network of transcription factors. Proteins in this network contain a conserved C-terminally located bHLHZip domain that directs sequence specific binding to the E-box elements of target genes. (Peter J. Hurlin & Huang, 2006) MGA is a unique member of the MAX interacting network in that it contains another DNA binding motif, T-box domain, in addition to the bHLHZip domain. (P J Hurlin, Steingrimsson, Copeland, Jenkins, & Eisenman, 1999) MGA is initially identified for its ability to bind to MAX (MYC Associated Factor X) and inhibit MYC dependent cell-cycle progression and promote exit from the cell-cycle and differentiation. (P J Hurlin et al., 1999) Consistent with its role as a MYC antagonist, loss of MGA has been found in many human cancers including colorectal cancer and the malignant transformation of chronic lymphocytic leukemia known as the Richter Transformation. (De Paoli et al., 2013; Jo, Kim, Yoo, & Lee, 2016) Given its involvement in tumorigenesis, MGA remains to be the least studied member of the MAX interacting network compared to the other proteins in the family.

In contrast to promoting differentiation, Mga is also shown to be essential for pluripotency maintenance both *in vivo* and *in vitro*. (Hu et al., 2009; Washkowitz et al., 2015) Knocking down Mga from mouse embryonic stem cells (ESCs) leads to decreased expression of pluripotency factors such as Oct4 and Nanog. (Hu et al., 2009) Mga also interacts with core pluripotency factor Oct4 in mouse ESCs. (van den Berg et al., 2010) Mouse embryos lacking functional Mga die before implantation due to failure of the ICM to maintain pluripotency. (Washkowitz et al., 2015) The authors proposed that the decreased expression of a rate limiting

enzyme, Ornithine Decarboxylase 1(Odc1) in the polyamine synthesis pathway contributed to the loss of pluripotent cells in *Mga* mutants. (Washkowitz et al., 2015) Given the fact that putrescine, downstream product of Odc1, partially rescued cell survival in ICM, it's possible that Mga may regulate pluripotency maintenance through other mechanisms that are currently unknown. Furthermore, it's unclear how Mga can promote differentiation in certain cells and maintain pluripotency in a different type of cells.

Due to early embryonic lethality in mouse, and with an aim to address the above questions, we used zebrafish embryos to study Mga function during early embryonic development. Using gene knockdown and knockout methods, we found that Mga is essential for early embryonic development. Knocking down Mga from 1-cell stage embryos with a high dose morpholinos resulted in early embryonic lethality. With a lower dose, we were able to generate highly reproducible phenotype involving defects in the neural crest derivatives, including melanocytes, craniofacial cartilages and peripheral and enteric nervous system. We were also able to generate *mga* null alleles using CRISPR/Cas9 system. Although our mutants fail to show phenotypes present in the morphants, we found similar molecular changes in *mga* mutants to a lesser degree. We believe that the lack of severity in *mga* mutants is possibly due to genetic compensation as previously proposed. (El-Brolosy et al., 2019; Kok et al., 2015; Ma et al., 2019)

Nonetheless, we found that neural crest defects seen in Mga depleted embryos were due to reduced specification of neural crest progenitors resulting from decreased Bmp signaling. This is consistent with our previous finding where Mga positively regulates *bmp2b* expression in the extraembryonic yolk syncytial layer. (Y. Sun, Tseng, Fan, Ball, & Dougan, 2014a) Consistent with Mga's function as a Myc antagonist, we also found that Myc activity is elevated upon suppression of Mga. While both Myc and Bmp signaling is involved in early neural crest

development, we found that suppression of Myc activity is not sufficient to rescue neural crest defects. Our data suggest that Mga promotes specification of early neural crest cells by positively regulating Bmp signaling which is independent of Myc activity. In addition, our study provides an evidence for Mga acting as a molecular switch between pluripotency maintenance and differentiation in cells at the neural plate border and promoting neural crest fate by regulating Bmp signaling.

MATERIAL AND METHODS

Zebrafish care

Both wild type (WIK) and mutant fish lines are maintained at 28.5°C in the fish facility according to Animal Use Protocol (AUP) approved by the University of Georgia IACUC committee (A2017 08-020-Y3-A0). Embryos were collected using single or multiple pair mating and were kept at 28.5°C in egg water (60µg/ml Instant Ocean Sea Salt Mix, 0.3µg/ml Methylene Blue). Embryos were staged as previously described. (CB, WW, SR, B, & TF, 1995)

Generation of mga mutants

For the generation of *mga* mutants, target site (5'-GGAAGGTGGAGTGGTTGT-3') was identified using online gRNA designing web tool ZiFiT target finder. (Sander et al., 2010; Sander, Zaback, Joung, Voytas, & Dobbs, 2007) Two DNA oligos (Forward: 5'-TAGGAAGGTGGAGTGGTTGT-3'; Reverse: 5'- AAACACAACCACTCCACCTT

-3') containing the target site were used to clone into pT7-gRNA plasmid. Single gRNAs were then transcribed using MEGAshortscript T7 transcription kit (Thermo Fisher Scientific, Cat# AM1354) according to manufacturer's protocol. sgRNA were purified using ethanol precipitation and dissolved in nuclease free water. Capped *cas9* mRNA is transcribed using mMessage mMachine SP6 transcription kit (Invitrogen™ AM1340) using pCS2+-nls-zCas9-nls plasmid which is linearized with NotI and phenol-chloroform purified prior to in vitro transcription. 100pg of single gRNAs and 150pg of *cas9* mRNA together with 0.1% phenol red and 0.2M KCl were injected directly into the single cell of 1-cell stage embryos. Embryos were then raised to adulthood and genotyped for possible indel mutations. $mga^{ga121-/-}$ was genotyped by analyzing PCR products generated from primer pairs mgaT100F (5'-CATTAGATTAGCCTTGTCATT -3') and mgaT100R (5'- CATGAAGAGGGCGTGACTG -3') on a 15% PAGE gel.

Morpholino injections

Two translation blocking morpholinos (*mgaTL1MO*: 5'-ACCCTGTTTCTCTGTATCGGCC-3' and *mgaTL3MO*: 5'-TCTGGATAGCTTCTGACCCTCTCAC-3'-Lissamine) were used to knockdown Mga. A total amount of 1.6ng of *mgaTL1MO* and *mgaTL3MO* together with 2.4ng of *p53MO* (5'-GCGCCATTGCTTTGCAAGAATTG-3') were injected into 1-cell stage embryos. For control, 1.6ng of mismatch morpholinos (*mgaTL1misMO*: 5'- ACgCTcTTTgTCTcTATCGcCC-3'; *mgaTL3misMO*: 5'- TCaGcATAGgTTCTcACgCTCTCAC-3') were injected with 2.4ng of *p53MO.* Microinjections were carried out as previously described. (Vickaryous & Mclean, 2011) Injected embryos were kept at 28.5°C until desired stage for further analysis.

In vitro transcription

Zebrafish *mxd3* full-length cDNA (GE Lifesciences) was cloned into BamHI and XbaI sites of pCS2+ expression vector using In-Fusion® HD Cloning Plus Kit (Clontech) following the manufacturer's protocol. Primers used for cloning *mxd3* are Mxd3 IF_F: 5'-TCTTTTTGCAGGATCCAAACATCTTATTATTCGAAAATGGAG -3'; Mxd3 IF_R: 5'-TCACTATAGTTCTAGATCATAACCAGGCGTGATCCGA -3'. Mouse full-length *mga* cDNA was cloned into pCS2+ vector. For microinjection controls, pCS2+-*nβ-gal* construct is used to make full-length *β-galactosidase* (*β-gal*) mRNA. All plasmids are linearized with NotI and were used as a template for *in vitro* transcription. For transcribing capped mRNA, mMessage mMachine SP6 transcription kit (Invitrogen™ AM1340) was used according to manufacturer's protocol. Transcribed mRNAs were purified using LiCl and dissolved in nuclease free water and stored in -80°C for future injections. For rescue experiments, 100pg of mouse *mga* mRNA or same amount of *β-gal* mRNA were injected into 1- to 2 - cell stage embryos along with MOs as described earlier. For suppressing Myc activity, 200pg of Zebrafish *mxd3* mRNA or same amount of *β-gal* mRNA were injected into 1- to 2 - cell stage embryos along with MOs as described. Microinjections were carried out as previously described. (Vickaryous & Mclean, 2011) Injected embryos were kept at 28.5°C until desired stage for further analysis.

RT-PCR and qRT-PCR

Total RNA was extracted at desired stages using TRIzol™ Reagent (Invitrogen™, Cat #: 15596026) For each experimental and control group, total number of 10 to 20 embryos were used based on the developmental stage. Total RNA was dissolved in nuclease free water, quantified using NanoDrop 2000 (Thermo Scientific™) and stored at -80°C until use. Extracted

total RNA was treated with DNaseI (Roche, Cat #: 04716728001) at 37°C for 15 minutes. cDNA was synthesized using RevertAid First Strand cDNA Synthesis Kit (Thermo Scientific™ Cat #: K1622) following manufacturer's protocol. For subsequence PCR analysis, 1µl of 10X diluted cDNA in nuclease free water was used as template. Primers used for evaluating *mga* transcripts in $mga^{ga121-/-}$: MgaEx14F: 5'-CAGCCCGGTCCCCATTGG-3'; MgaEx14R: 5'-CCAGAGGCAGGCTGGGTGAC-3'; zGAPDH-Long F1: 5'- CGTCTGGTGACCCGTGCTGC-3'; zGAPDH-Long R1 5'-TGGGGGTGGGGACACGGAAG-3'. PCR conditions for RT-PCR: 94°C for 2min, 94°C for 30sec, 63°C for 30sec, 72°C for 45sec, 35 cycles, 72°C for 5min. PCR products were visualized using 1.5% agarose gel. For analyzing Myc target gene expression levels: qPCR was performed with Applied Biosystems™ 7500 Real-Time PCR System using PowerUp™ SYBR™ Green Master Mix (Applied Biosystems™, Cat #: A25742) following manufacturer's protocol. Primers used for qPCR: id2RTF: 5'-CGTGATGAAACCTTGTGAACTCT-3'; id2RTR: 5'-TCTCAGCATACAGCATAACACTTTG-3'; cdc25bRTF: 5'-AGTGGAGAGGCTGTTTGTTATCG -3'; cdc25bRTR: 5'-GGGCAGTCAGGGAGAATAGGA-3'; odc1RTF: 5'- TACACACTGGCGGTCAACATCA-3'; odc1RTR: 5'- TCGGTCATTGGACACATCCTCT-3'; ccnd1RTF: 5'-CCAGAACCTCACCAACTTCCTC-3'; ccnd1RTR: 5'- GACTCGATCTGTTCCTGACACG-3'; cebpaRTF: 5'- CGAGTTCCTGGCTGACTTATTCC-3'; cebpaRTR: 5'-TTCTTGCTTGGCTGTCGTAGATG-3'. Np63F: 5'- AATGGTGCCTTCATCCCACTGC - 3'; Np63R: 5'- CCTCAACAGGAAACTGGAAATGC -3'.

TUNEL Assay

Programmed cell death in embryos were analyzed using DeadEnd™ Fluorometric TUNEL System (Promega, Cat#: G3250). Embryos are fixed at desired stage with 4% PFA at 4°C overnight. Fixed embryos were then dechorionated, rinsed twice with 1X PBS, gradually dehydrated with serial dilution of Methanol (25%, 50%, 75%) in PBST (1X PBS with 0.5% Tween-20), and stored in 100% Methanol at -20°C until use. For TUNEL assay, embryos were rehydrated with serial dilution of Methanol in PBST and rinsed twice with 1X PBS. 20µg/ml Proteinase K (in 1X PBS) was added to permeabilize embryos and were incubated at room temperature for 10 minutes. Permeabilized embryos were fixed again in 4%PFA for 20min at room temperature to quench Proteinase K activity. Embryos were then incubated with Equilibrium Buffer at room temperature for 10 minutes. Cell death was detected using the mixture of fluorescein-12-dUTP and Terminal Deoxynucleotidyl Transferase (TdT). Embryos were counterstained with DAPI (Invitrogen™, Cat#: D1306) to visualize the nuclei.

Phospho-Histone 3 Staining

Wild type and *mga*$^{ga121-/-}$ embryos were fixed at 24hpf with 4% PFA at 4°C overnight. Fixed embryos were dehydrated in 100% Methanol and stored at -20°C until use. Embryos were then gradually rehydrated using serial dilution of Methanol (75%, 50%, 25%) in PBST (1XPBS and 0.1% Tween-20). After permeabilization with acetone at -20°C for 7 minutes, embryos were washed with water once and twice with 0.5%TritonX-100 in 1XPBS at room temperature. Embryos were then incubated with Antibody Blocking Solution (2% BSA, 0.5% normal goat serum, 1% DMSO, 0.5% Triton X-100 in PBS) at room temperature for 2 hours. Proliferating cells were detected using p-Histone H3 Antibody (Ser 10) (diluted to 1:200 in antibody blocking

solution; Santa Cruz Biotechnology; sc-8656-R) at 4°C overnight. After washing three times with 0.5% Triton X-100 in PBS, samples were then incubated with secondary antibody goat anti-rabbit IgG (H+L) conjugated to Alexa Fluor 488 (1:300 in antibody blocking solution, Thermo Fisher Scientific, catalog # A-11008) at room temperature for 2 hours. After the incubation, embryos were rinsed three times with 0.5% Triton X-100 in PBS. Embryos were counterstained with DAPI (Invitrogen™, Cat#: D1306) to visualize the nuclei.

Luciferase Assay

Both pT2-Luci-4XEbox (from Dickmeis Lab, Karlsruhe Institute of Technology, Germany) and pRL-TK were prepared using QIAGEN midi-prep kit prior to injection. 25pg of each luciferase vectors were injected along with *mgaMOs* or *misMOs* into WIK embryos at 1-cell stage. Injected embryos were collected for subsequent analysis at desired stages. Luciferase activity was measured using Dual-Luciferase® Reporter Assay System (Promega, Cat #: E1910) according to manufacturer's protocol with slight adjustments. Briefly, embryos injected with luciferase constructs were dechorionated at desired stages and placed into 96-well plates with approximately 10 embryos in each well. Embryos in each well were incubated with 20µl of passive lysis buffer for 15-20 minutes at room temperature. Firefly and Renilla luciferase activity were then measured using Synergy H4 Hybrid Multi-Mode Microplate Reader (BioTek Instruments, Inc.). For measuring firefly luciferase activity, 100µl of Luciferase Assay Reagent II was added to the embryo lysates. After measuring firefly luminescence, 100µl of Stop & Glo® Reagent was added to each well for measuring Renilla luminescence. Luciferase assay was performed in three biological replicates with three technical replicates for each experiment.

Whole Mount in situ Hybridization (WISH)

Antisense RNA probes used in this study are *tfap2a*, *mitfa*, *islet1* (from Schilling Lab, UCI, CA, USA), *hand2*, *snai1b* (from Yelon Lab, UCSD, CA, USA), *phox2bb* (from Shepherd Lab, Emory University, GA, USA), *ifabp*, *tfa* (from Gong Lab, NUS, Singapore), *sox10*, *foxd3*, *chordin* and *tbx6*. DIG-labeled antisense RNA probes were synthesized using DIG RNA Labeling Kit (SP6/T7) (Roche, Cat #: 11175025910) following manufacturer's protocol. WISH was performed as previously described. (Vickaryous & Mclean, 2011) Probed embryos were incubated with 1:3000 dilution of Anti-Digoxigenin-AP, Fab fragments (Roche, Cat #: 11093274910) in antibody blocking solution at 4°C overnight. Embryos were kept in the dark in NTMT solution (100mM Tris-HCl, pH9.5, 50mM MgCl2, 100mM NaCl, 0.1% Tween-20) with BCIP/NBT (Roche, Cat #: 11383221001/11383213001,) for 1 to 4 hours at room temperature for color development.

Alcian Blue Staining (Wei-Chia)

Zebrafish larvae were collected at 120hpf. For maintaining optical clarity, 0.003% 1-phenyl 2-thiouracil (PTU) was added into the egg water at 22hpf to inhibit skin pigmentation. After collection, larvae were fixed with 4% paraformaldehyde in 1X PBS overnight at 4°C. Fixed larvae were stained overnight at room temperature with 0.1% Alcian Blue 8GX (A3157, Sigma-Aldrich, St Louis, MO) in acid alcohol. Stained larvae were differentiated in acid alcohol and rinsed with distilled water until background was clear. For whole mount imaging, stained larvae were cleared with glycerol in 1% KOH solution and mounted in 80% glycerol. For cartilage dissection, stained larvae were rehydrated and rinsed with saturated sodium tetraborate solution. Larvae were digested in trypsin solution at room temperature until tissues turned loose.

Craniofacial cartilage dissection was carried out by gently removing surrounding tissues with fine forceps.

L-DOPA Staining (Wei-chia)

22hpf embryos were dechorinated and fixed with 4% paraformaldehyde in 1X PBS at room temperature for 2 hours. Fixed embryos were rinsed 5 times with 1X PBS. Embryos were then incubated with 0.1% 3,4-Dihydroxy-L-phenylalanine (L-DOPA) (D9628, Sigma-Aldrich, St. Louis, MO) in 1X PBS at 37°C for 1.5 to 2.5 hours. The reaction was stopped by rinsing embryos 3 times with 1X PBS when the staining reached desired intensity. Finally, embryos were stored in 80% glycerol for photography.

Western Blot (Wei-chia)

Total embryonic lysates were prepared from 8hpf embryos. 100µl RIPA Buffer (R0278, Sigma-Aldrich, St. Louis, MO) was added to 200 deyolked embryos for the protein extraction. BCA Assay Kit (23227, Thermo Scientific, Rockford, IL) was used to determine the concentration of each lysate. SDS-PAGE was carried out on a 4%-20% precast gel (456-1094, Bio-Rad Laboratories, Hercules, CA), with 20µg total protein loaded in each lane. After transferring to Hybond-P PVDF membranes (RPN303f, GE Healthcare, Piscataway, NJ), the membranes were incubated with either polyclonal rabbit anti-Mga antibody (1:500, AbMart, Shanghai, China) or 12G10 mouse monoclonal anti- α-tubulin antibody (1:500) at 4°C overnight. Either HRP-conjugated goat-anti rabbit IgG (1:3,000, SC-2004, Santa Cruz Biotechnology, Dallas, TX) or HRP-conjugated goat-anti mouse IgG (1:3,000, A5278, Sigma-Aldrich, St. Louis, MO) was used as secondary antibodies. After antibody incubation, bands were developed and

detected with the Western Blot ECL Substrate (170-5060, Bio-Rad Laboratories, Hercules, CA) and X- OMAT LS films (864-6770, Carestream, Rochester, NY).

Imaging

For fluorescent imaging, embryos were mounted in 80% glycerol on raised coverslip microscope slides. Fluorescent images were taken using Zeiss AXIO Imager D2 compound fluorescence microscope with Colibri.2 LED light source and AxioCam HR CCD camera (Carl Zeiss, Jena, Germany). For live imaging, embryos were mounted in 3% Methyl Cellulose in microscope slides with single concave. Pictures were taken using Leica MZ FLIII stereomicroscope (Leica Microsystems, Germany) and Moticam 5 (CMOS) 5.0MP camera (Motic Asia, Hong Kong). WISH signals were photographed using Zeiss Axioplan 2 compound microscope (Carl Zeiss, Germany) and RETIGA EX CCD camera (QImaging, Canada).

RESULTS

1. Generation of *mga* mutants using CRISPR/Cas9 system

To study Mga function during early embryonic development, we generated mutants that are null for *mga* using sgRNA targeting the coding region of the T-box domain. (Figure 2.1A) We successfully identified four different alleles with indel mutations. (Figure 2.1B) Among these four alleles, two of them, $mga^{ga121-/-}$ and $mga^{ga1921-/-}$, are potentially null. $mga^{ga121-/-}$ allele is a 5bp deletion resulting in a frameshift mutation and multiple stop codons leading to a truncated protein without functional T-box domain. Zygotic $mga^{ga121-/-}$ embryos are indistinguishable from

the wild type. (Data not shown) Mga is expressed both maternally and zygotically in Zebrafish embryos. (Y. Sun et al., 2014a) To prevent the maternal contribution of Mga in early embryonic development, we in-crossed Z*mga*$^{ga121-/-}$ adults to obtain maternal zygotic *mga* null embryos. Surprisingly, Maternal zygotic *mga*$^{ga121-/-}$ (*MZmga*$^{ga121-/-}$) embryos develop normally just as their wild type counterparts except for developmental delay (Figure 2.1C-F). Developmental delay could be resulted from reduced proliferation or increased apoptosis. We first analyzed cell proliferation profile using anti-phospho-Histone H3 (pH3) antibodies. We found that there is no significant difference in the number of proliferating cells in *MZmga*$^{ga121-/-}$ and in the wild type embryos at 24hpf. (Figure 2.2 C, D) To test for increased cell death, we performed TUNEL assay in both wild-type and *MZmga*$^{ga121-/-}$ embryos at 24hpf. *MZmga*$^{ga121-/-}$ showed increased TUNEL positive apoptotic cells when compared to the wild type. (Figure 2.2 A, B) These data indicate that the developmental delay in *mga* mutants is due to increased cell death as opposed to reduced proliferation.

We reasoned that the lack of severity in our mutants may be due to genetic compensation. Multiple reports have shown that mutants generated by CRISPR/Cas9 system did not recapitulate or showed less severe phenotypes than those in knockdown assays in Zebrafish. (Kok et al., 2015; Place & Smith, 2017; Rossi et al., 2015) This is due to genetic compensation mechanism triggered by non-sense mediated decay (NMD) of mutant mRNAs which consequently upregulates the expression of homologous and/or downstream genes. (El-Brolosy et al., 2019) We analyzed *mga* transcript level by RT-PCR in wild type and *MZmga*$^{ga121-/-}$ at different developmental stages. In wild type embryos, *mga* transcripts were seen at blastula stage confirming maternal expression. (Figure 2.2E) *mga* expression seems to be increased during gastrulation as well as at later stages. (Figure 2.2E) In *MZmga*$^{ga121-/-}$ on the other hand, *mga*

expression is consistently low when compared to wild type siblings at all stages. (Figure 2.2F) This suggest the possibility of NMD in *mga* mutants, and that compensation by genes that are similar to *mga* may explain the lack of severe phenotype in our mutants. However, further identification of *mga* homologous genes or evaluation of its downstream targets is needed to confirm that genetic compensation is present in *mga* mutants. Therefore, we used translation blocking morpholinos to knockdown Mga protein for subsequent analysis of Mga function in Zebrafish development.

2. Mga is required for normal pigmentation in Zebrafish

To suppress Mga expression, we used two translation blocking morpholinos (*mgaTL1MO* and *mgaTL3MO*) as previously described. (Y. Sun et al., 2014a) Majority of the embryos co-injected with both morpholinos at an amount of 3.2ng or 2.8ng along with 2.4ng *p53MO* die before 24hpf. In contrast, control embryos injected with the same amount of mismatch morpholinos (misMOs) development normally. (Figure 2.3A) An amount of 1.6ng of *mgaMOs* showed less toxicity and viable embryos showing highly reproducible phenotypes described below. Embryos injected with *mgaMOs* developed slowly in the first 24 hours with an approximately 1-2 hours delay compared to *misMOs* injected embryos. (Tseng, 2015) However, developmental delay was not so evident after 24hpf. At 32hpf, embryos injected with *mgaMOs* developed severely reduced pigmentation while control embryos develop normal pigments. (Figure 2.3B, C) In addition, pigmentation is affected early during melanoblast development. At 22hpf, there's decreased tyrosinase positive melanoblasts. (Figure S2.1A, B) Expression of the early melanoblast marker, *mitfa*, is also reduced in *mgaMOs* injected embryos at 22hpf. (Figure S2.1C, D) To assess if reduced pigmentation is specifically due to loss of Mga function, we co-

injected *mgaMOs* with 100pg of mouse *mga* mRNA or 100pg of β-galactosidase (*β-gal*) mRNA into 1-cell stage embryos. Loss of pigmentation was significantly rescued by mouse *mga* mRNA in Mga depleted zebrafish embryos (Figure 2.3E) while injection of *β-gal* mRNA cannot (Figure 2.3D, F). Furthermore, Mga protein level is reduced almost by half relative to the control. (Figure 2.3G, H) Taken together, low dose *mgaMOs* that we used are able to knock down Mga expression in zebrafish embryos.

3. Mga depletion also results in defects in other neural crest derivatives

Decreased early melanoblast population in *mga* morphants raises the possibility of early neural crest migration or specification defects due to loss of Mga function. Neural crest cells arise at the border of neural plate. As neural tube closes, cells at the neural plate border undergo epithelial to mesenchymal transition (EMT). This transition allows them to delaminate from the dorsal neural tube, migrate to various destination in the embryo and give rise to a diverse population of cells including melanocytes, craniofacial cartilages, neurons of the peripheral nervous system (PNS) as well as the enteric nervous system (ENS). We next examined whether other lineages of neural crest cells are affected by the loss of Mga. We visualized craniofacial cartilages using Alcian blue staining of 5dpf embryos injected with either *mgaMOs* or *misMOs*. Embryos depleted from Mga showed craniofacial cartilages that were severely disorganized and decreased in size compared to control. (Figure 2.4A-F) More specifically, the size of Meckel's, palatoquadrate, hyosymplectic, and ceratohyal cartilages were greatly reduced. Ceratobrachial 1-5, basihyal, and basibrachial cartilages were missing. (Figure 2.4C-F) Craniofacial cartilages develop from pharyngeal arches which is populated by migrating cranial neural crest cells. (Kara, Wei, Commanday, & Patton, 2017) Expression of two craniofacial cartilage precursor

markers, *dlx2a* and *hand2*, can be seen in the pharyngeal arches in control embryos at 36hpf. (Figure S2.2A, C) However, *dlx2a* and *hand2* expression is greatly reduced and is limited to the pharyngeal arches 1 and 2 in *mga* morphants at the same developmental stage in the control. (Figure S2.1B, D)

In addition to craniofacial cartilage defects, we found that the expression of *islet1* and *phox2bb*, which are markers for PNS and ENS respectively, is decreased in *mga* morphants compared to the control. (Figure 2.4G-J) This suggests that development of PNS and ENS are also affected in *mga* morphants. Taken together, loss of Mga function resulted in defects in the development of at least four different lineages of neural crest derivatives.

4. Mga antagonizes Myc activity in zebrafish embryos

In cell culture, Mga antagonizes Myc activity by binding to Max and preventing Max from forming a transcriptional activator complex with Myc. (Blackwood & Eisenman, 1991; P J Hurlin et al., 1999) As Myc family proteins are also involved in neural crest development in Zebrafish, Xenopus and Chicks, we hypothesize that neural crest defect in *mga* morphants is due to dysregulation of Myc. (Bellmeyer, Krase, Lindgren, & LaBonne, 2003; Hong, Tsang, & Dawid, 2008; Kerosuo & Bronner, 2016) To test this hypothesis, we co-injected Firefly reporter construct containing Myc response elements (Figure 2.5C) with either *mgaMOs* or *misMOs* into 1-cell stage embryos. The Firefly and Renilla luminescence were measured at 8hpf, 24hpf, and 31hpf. Firefly/Renilla ratio is increased by 2-fold and 1.7-fold at 24hpf and 31hpf respectively in *mgaMOs* injected embryos compared to the control. No significant difference is observed at 8hpf. (Figure 2.5D) This shows that Myc activity is increased in *mga* morphants. To see if increased Myc activity has any functional consequence, we analyzed the expression of Myc

target genes at 24hpf using qRT-PCR. Consistent with the increased Myc activity, four out of the five Myc target genes, *id2*, *cdc25b*, *odc1* and *cyclind1*, showed significantly increased expression when Mga function is suppressed. (Figure 2.5E)

We asked how an increased Myc activity contributes to defects in the developing neural crest population. As overexpression of Myc results in increased programmed cell death, we hypothesize that increased apoptosis may account for the loss of neural crest progenitors in *mga* morphants. To investigate cell death, TUNEL assay was performed in *mga* morphants as well as in control embryos at 22hpf. *mgaMOs* injected embryos showed increased apoptosis in the cranial and dorsal regions corresponding to the regions where pre-migratory and migratory neural crest cells are located. (Figure 2.5B) Control embryos injected with *misMOs*, on the other hand, showed very few apoptotic cells in the same regions. (Figure 2.5A) It's possible that defects in neural crest derivatives are resulted from decreased survival of early neural crest progenitors. However, this doesn't rule out Mga's involvement in the specification of early neural crest progenitors.

5. Mga acts early during neural crest development

Neural crest cells arise at the neural plate border which is specified as early as late gastrulation. Mga is broadly expressed at this stage. (Rikin & Evans, 2010; Y. Sun et al., 2014a) To investigate whether loss of Mga function affects early neural crest progenitors, we visualized the expression pattern of early neural crest markers using in situ hybridization at 3-somite stage. Embryos that are depleted from Mga showed decreased expression of *foxd3* (Figure 2.6A, B), *tfap2α* (Figure 2.6C, D), *snai1b* (Figure S2.4C, D) as well as *sox10* (Figure S2.4A, B) in the neural plate border at 3-somite stage compared to those in control. Reduced expressions of these

markers were persisted at 8-somite stage. (Figure S2.5) Interestingly, expression levels of *foxd3* (Figure 2.6F) and *tfap2a* (Figure 2.6H) at 3-somite stage were slightly reduced in *MZmga*$^{ga121-/-}$ compared to the wild type (Figure 2.6E, G). Lack of neural crest phenotype in the mutants may suggest that they somehow recover at later stages. Nonetheless, these data collectively support Mga function during early neural crest specification at the neural plate border.

6. Depletion of Mga leads to disruption of Bmp signaling activity

It's been shown that Bmp signaling play an important role in the early induction of presumptive neural crest during late gastrulation. (Betancur et al., 2010; Simoes-Costa & Bronner, 2015) Previous study showed Mga positively regulates *bmp2b* expression through the formation of transcriptional complex with Smad4 and Max. (Y. Sun, Tseng, Fan, Ball, & Dougan, 2014b) Therefore, we hypothesize that abnormal neural crest specification in *mga* morphants is due to altered Bmp signaling. To investigate whether Bmp signaling is affected by loss of Mga, we analyzed the expression of Bmp antagonist, *chordin*, at 8hpf using in situ hybridization. We found that *chordin* expression is expanded slightly to the ventrolateral side in *mgaMOs* injected embryos at 75% epiboly when compared to the control embryos. (Figure 2.7A, B; Figure S2.4A, B) In addition, expression of *tbx6*, a Bmp target gene, is decreased in *mga* morphants at 75% epiboly. (Figure 2.7C, D; Figure S2.4C, D) Furthermore, expression of *Δnp63*, another direct Bmp downstream target, is significantly decreased by 70% in *mga* morphants relative to the control at 75% epiboly. (Figure 2.7E) These data indicate that depletion of Mga from 1-cell stage embryos led to a decreased Bmp activity which may further perturb early induction events during neural crest development.

7. Suppression of Myc activity is not sufficient to rescue neural crest phenotype

We have shown that suppression of Mga function results in decreased Bmp activity during mid-gastrulation, which may contribute to defective neural plate border specification. However, depletion of Mga may also affect survival of neural crest progenitors due to increased apoptosis mediated by unopposed Myc activity. To resolve the underlying mechanism of how Mga function during neural crest development, whether by negatively regulating Myc or by positively controlling Bmp signaling, we overexpressed another known Myc antagonist, *mxd3*, in *mga* morphants. Mxd3 is one of the members of the Max interacting transcription factor family, and is shown to antagonize Myc by competitively binding to Max. (Peter J. Hurlin & Huang, 2006) We co-injected either 200pg of *mxd3* mRNA or equal amount of *β-gal* mRNA with *mgaMOs* into 1-cell stage embryos, and monitored embryos for possible neural crest phenotype. At 32hpf, *mga* morphants injected with *mxd3* mRNA still lacked pigmentation just as embryos injected with *β-gal* mRNA or as embryos injected with *mgaMOs* alone. (Figure 2.8A-D) To confirm that the failure of *mxd3* to rescue pigmentation defect is not due to shorter half-life or to other technical issuea, we analyzed the expression level Myc target genes in *mxd3* overexpressed *mga* morphants. At 24hpf, *mxd3* is able to suppress not all but some of the increased Myc targets, such as *odc1* and *cyclind1*. (Figure 2.8E) Furthermore, *mxd3* overexpressed embryos showed less TUNEL positive apoptotic cells compared to *β-gal* injected *mga* morphants or emrbyos injected with *mgaMOs* alone. (Figure 2.8F-I) These data indicate that suppression of Myc activity is not sufficient to rescue neural crest defect in Mga depleted embryos. It's highly likely that Mga function during early neural crest specification by regulating Bmp signaling, and that Mga involvement in neural crest is independent of its role as a Myc antagonist.

DISCUSSION

Neural crest cells are a group of unique migratory multipotent stem-cells that develop from the neural plate border in all vertebrates. Molecular mechanism of early neural crest induction, specification, migration and differentiation has been extensively studied in different model organisms. (Simões-Costa & Bronner, 2015) Here we report a novel regulator of neural crest development during zebrafish early embryogenesis. Knocking down Mga from 1-cell stage embryos resulted in defects in the development of neural crest derivatives, including loss of skin pigmentation, abnormal craniofacial cartilages as well as abnormalities in the PNS and ENS as shown by the decreased expression of precursor markers, *islet1* and *phox2bb*. Given that these defects can be rescued by overexpressing mouse *mga* mRNA, we conclude that neural crest abnormalities seen in *mgaMOs* injected embryos are specifically due to loss of Mga function.

Although loss of skin pigmentation was reported in a previous study, the underlying mechanism has never been explored. (Rikin & Evans, 2010) We found that this is due to defects in the early specification of neural crest cells. Expression of neural crest markers, such as *foxd3*, *sox10*, *tfap2a*, and *snai1b* is decreased at the neural plate border in *mga* morphants at 3-somite stage. (Figure 2.6A-D, Figure S2.3A-D) Although mild, expression of *foxd3* and *tfap2a* is also decreased in *MZmga*$^{ga121-/-}$ embryos. (Figure 2.6E-H) Slight reduction in neural crest specifiers in the mutants may not be enough to drive morphological changes. Decreased *mga* transcript levels may suggest the possibility of genetic compensation. Therefore, it's likely that increased expression of other genes that are similar to Mga or downstream of Mga may be compensating for the loss of Mga function. (El-Brolosy et al., 2019)

In zebrafish, Mga regulates *bmp2b* expression in the extraembryonic yolk syncytial layer by forming transcriptional complex with Smad4 and Max. (Y. Sun et al., 2014a) In the

cytoplasm, Mga also binds to Bs69 preventing it from binding to BMP type I receptor (Bmpr1a) and lifting the inhibitory effect of Bs69 on Bmp signal transduction. (X. Sun et al., 2018) We found that depletion of Mga from 1-cell stage embryos resulted in reduced Bmp levels as shown by slightly expanded *chordin* expression domain as well as reduced Bmp target genes, *tbx6* and *Δnp63,* during gastrulation. (Figure 2.7) These data are consistent with Mga's role as a positive regulator of Bmp signaling. In terms of neural crest development, Bmp signaling, especially the intermediate levels of Bmp is critical for patterning of the neural plate border by directly activating neural plate border specifiers such as *pax3* and *zic* genes in zebrafish. (Plouhinec et al., 2014; Reichert, Randall, & Hill, 2013; Schumacher, Hashiguchi, Nguyen, & Mullins, 2011; Tríbulo, Aybar, Nguyen, Mullins, & Mayor, 2003) These genes in turn promote cells at the neural plate border to take on neural crest cell fate by inducing the expression of neural crest markers such as *foxd3*. (Betancur et al., 2010) Therefore, decreased Bmp signaling due to suppression of Mga may result in perturbation of Bmp gradient at the neural plate border. As a consequence, early induction of neural crest fate can be affected. It's important to note that, although Bmp activity is slightly decreased during gastrulation, dorsoventral patterning is not affected in our knockdown study. One possibility is that the amount of morpholinos used in this study is much lower than we previously described. (Y. Sun et al., 2014a) Mga protein level is reduced but not completely abolished with the injection of low dose morpholinos. (Figure 2.3G-H) It's possible that residual Mga proteins are sufficient to maintain *bmp2b* levels for proper dorsoventral patterning, and that neural crest cells may be more sensitive to changes in Bmp levels.

In addition to decreased Bmp signaling, suppression of Mga also resulted in increased Myc activity *in vivo*. (Figure 2.5D) This is consistent with Mga's role as a Myc antagonist. (P J

Hurlin et al., 1999) Suppression of Mga expression may increase the availability of Max which consequently increases transcriptional activation of target genes by Myc. (Blackwood & Eisenman, 1991; P J Hurlin et al., 1999) Indeed, we found that some of the Myc target genes were significantly elevated in *mga* morphants. (Figure 2.5E) Among these target genes, *odc1* which encodes rate limiting enzyme Ornithine Decarboxylase 1 in the polyamine synthesis pathway, is likely to be direct target of Mga and is shown to be downregulated in mouse embryos that are lacking Mga. (Washkowitz et al., 2015) Our results do not exclude the fact that *odc1* is direct target gene of Mga as residual Mga protein is still present in our morphants. (Figure 2.3G-H) We also noted an increased expression of Id2. Id genes are directly regulated by c-Myc and are important for survival and maintenance of neural crest progenitors. (Bellmeyer et al., 2003; Hong et al., 2008; Kee & Bronner-Fraser, 2005; Kerosuo & Bronner, 2016; Martinsen, Bronner-fraser, Martinsen, & Bronner-fraser, 2020) Loss of Id proteins or Myc has been linked to decreased neural crest progenitors. (Hong et al., 2008; Kee & Bronner-Fraser, 2005; Kerosuo & Bronner, 2016; Martinsen et al., 2020) Overexpression of Id2/3 has been shown to promote proliferation and expansion of neural crest progenitors in frogs. (Kee & Bronner-Fraser, 2005) On the contrary, zebrafish embryos depleted from Mga showed decreased neural crest cells despite elevated Myc activity. (Figure 2.5A, B) This suggests that Mga act early during neural crest specification before neural crest cell fate and the multipotency is established. Further confirming our hypothesis, suppressing Myc activity by overexpressing *mxd3* is able to suppress cell death but is not able to rescue neural crest phenotype. Therefore, Mga's role during early neural crest development is independent of Myc.

In mouse embryos, Mga is required for the maintenance of pluripotency in the ICM by regulating the expression of ODC1, a rate limiting enzyme of the polyamine synthesis pathway.

(Washkowitz et al., 2015) Furthermore, Mga interacts with core pluripotency factor Oct4 in mouse ESCs and its inhibition using siRNA in ESCs leads to decreased expression of pluripotency markers. (Hu et al., 2009; van den Berg et al., 2010) As our study supports Mga's role as a promoter of differentiation, it raises the question of how and when Mga take part in pluripotency maintenance and when to promote cell fate specification. Previous studies have shown that Mga together with Max can form transcriptional repressor complex with E2F-6 and recruit Polycomb group proteins to suppress target genes containing E-box and T-box elements. (Ogawa, Ishiguro, Gaubatz, Livingston, & Nakatani, 2002) Therefore, depending on the presence of binding partners, Mga may activate or repress target genes that are either responsible for pluripotency or differentiation. Although further experiments are needed to elucidate Mga function in cell survival in zebrafish, we propose that Mga may act as a molecular switch at the neural plate and promote naïve ectoderm to take on multipotent neural crest cell fate by positively regulating Bmp signaling.

REFERENCES

Bellmeyer, A., Krase, J., Lindgren, J., & LaBonne, C. (2003). The protooncogene c-myc is an essential regulator of neural crest formation in xenopus. *Developmental Cell*, *4*(6), 827–839.

Betancur, P., Bronner-Fraser, M., & Sauka-Spengler, T. (2010). Assembling Neural Crest Regulatory Circuits into a Gene Regulatory Network. *Annual Review of Cell and Developmental Biology*, *26*(1), 581–603. https://doi.org/10.1146/annurev.cellbio.042308.113245

Blackwood, E. M., & Eisenman, R. N. (1991). Max: a helix-loop-helix zipper protein that forms a sequence-specific DNA-binding complex with Myc. *Science (New York, N.Y.)*, *251*(4998), 1211–1217. https://doi.org/10.1126/science.2006410

CB, K., WW, B., SR, K., B, U., & TF, S. (1995). Stages of embryonic development of the zebrafish. *Developmental Dynamics*, *203*(3), 253–310. Retrieved from https://www.mbl.edu/zebrafish/files/2013/03/Kimmel_stagingseries1.pdf%0Ahttp://www.researchgate.net/profile/Bonnie_Ullmann/publication/227763372_Stages_of_embryonic_development_of_the_zebrafish/links/55352d8b0cf268fd00156437.pdf

De Paoli, L., Cerri, M., Monti, S., Rasi, S., Spina, V., Bruscaggin, A., … Rossi, D. (2013, May). MGA, a suppressor of MYC, is recurrently inactivated in high risk chronic lymphocytic leukemia. *Leukemia & Lymphoma*. United States. https://doi.org/10.3109/10428194.2012.723706

El-Brolosy, M. A., Kontarakis, Z., Rossi, A., Kuenne, C., Günther, S., Fukuda, N., … Stainier, D. Y. R. (2019). Genetic compensation triggered by mutant mRNA degradation. *Nature*, *568*(7751), 193–197. https://doi.org/10.1038/s41586-019-1064-z

Hong, S.-K., Tsang, M., & Dawid, I. B. (2008). The Mych Gene Is Required for Neural Crest Survival during Zebrafish Development. *PLOS ONE*, *3*(4), e2029. Retrieved from https://doi.org/10.1371/journal.pone.0002029

Hu, G., Kim, J., Xu, Q., Leng, Y., Orkin, S. H., & Elledge, S. J. (2009). A genome-wide RNAi screen identifies a new transcriptional module required for self-renewal. *Genes and Development*, *23*(7), 837–848. https://doi.org/10.1101/gad.1769609

Hurlin, P J, Steingrimsson, E., Copeland, N. G., Jenkins, N. A., & Eisenman, R. N. (1999). Mga, a dual-specificity transcription factor that interacts with Max and contains a T-domain

DNA-binding motif. *The EMBO Journal*, *18*(24), 7019–7028. https://doi.org/10.1093/emboj/18.24.7019

Hurlin, Peter J., & Huang, J. (2006). The MAX-interacting transcription factor network. *Seminars in Cancer Biology*, *16*(4), 265–274. https://doi.org/10.1016/j.semcancer.2006.07.009

Jo, Y. S., Kim, M. S., Yoo, N. J., & Lee, S. H. (2016). Somatic mutation of a candidate tumour suppressor MGA gene and its mutational heterogeneity in colorectal cancers. *Pathology*, *48*(5), 525–527. https://doi.org/10.1016/j.pathol.2016.04.010

Kara, N., Wei, C., Commanday, A. C., & Patton, J. G. (2017). miR-27 regulates chondrogenesis by suppressing focal adhesion kinase during pharyngeal arch development. *Developmental Biology*, *429*(1), 321–334. https://doi.org/https://doi.org/10.1016/j.ydbio.2017.06.013

Kee, Y., & Bronner-Fraser, M. (2005). To proliferate or to die: Role of Id3 in cell cycle progression and survival of neural crest progenitors. *Genes and Development*, *19*(6), 744–755. https://doi.org/10.1101/gad.1257405

Kerosuo, L., & Bronner, M. E. (2016). cMyc Regulates the Size of the Premigratory Neural Crest Stem Cell Pool. *Cell Reports*, *17*(10), 2648–2659. https://doi.org/10.1016/j.celrep.2016.11.025

Kim, J., & Orkin, S. H. (2011). Embryonic stem cell-specific signatures in cancer: Insights into genomic regulatory networks and implications for medicine. *Genome Medicine*, *3*(11). https://doi.org/10.1186/gm291

Klimczak, M. (2015). Oncogenesis and induced pluripotency-Commonalities of signalling pathways. *Wspolczesna Onkologia*, *1A*, A16–A21. https://doi.org/10.5114/wo.2014.47133

Kok, F. O., Shin, M., Ni, C.-W., Gupta, A., Grosse, A. S., van Impel, A., … Lawson, N. D.

(2015). Reverse Genetic Screening Reveals Poor Correlation between Morpholino-Induced and Mutant Phenotypes in Zebrafish. *Developmental Cell*, *32*(1), 97–108. https://doi.org/https://doi.org/10.1016/j.devcel.2014.11.018

Ma, Z., Zhu, P., Shi, H., Guo, L., Zhang, Q., Chen, Y., … Chen, J. (2019). PTC-bearing mRNA elicits a genetic compensation response via Upf3a and COMPASS components. *Nature*, *568*(7751), 259–263. https://doi.org/10.1038/s41586-019-1057-y

Martinsen, B. J., Bronner-fraser, M., Martinsen, B. J., & Bronner-fraser, M. (2020). Neural Crest Specification Regulated by the Helix-Loop-Helix Repressor Id2 Published by : American Association for the Advancement of Science Stable URL : https://www.jstor.org/stable/2896124 REFERENCES Linked references are available on JSTOR for this article : digitize , preserve and extend access to Science Neurat Crest Specification Regulated by the Helix-Loop-Helix Repressor 1d2, *281*(5379), 988–991.

Ogawa, H., Ishiguro, K. I., Gaubatz, S., Livingston, D. M., & Nakatani, Y. (2002). A complex with chromatin modifiers that occupies E2f- and Myc-responsive genes in G0 cells. *Science*, *296*(5570), 1132–1136. https://doi.org/10.1126/science.1069861

Place, E. S., & Smith, J. C. (2017). Zebrafish atoh8 mutants do not recapitulate morpholino phenotypes. *PLoS ONE*, *12*(2), 1–12. https://doi.org/10.1371/journal.pone.0171143

Plouhinec, J.-L., Roche, D. D., Pegoraro, C., Figueiredo, A. L., Maczkowiak, F., Brunet, L. J., … Monsoro-Burq, A. H. (2014). Pax3 and Zic1 trigger the early neural crest gene regulatory network by the direct activation of multiple key neural crest specifiers. *Developmental Biology*, *386*(2), 461–472. https://doi.org/https://doi.org/10.1016/j.ydbio.2013.12.010

Reichert, S., Randall, R. A., & Hill, C. S. (2013). A BMP regulatory network controls ectodermal cell fate decisions at the neural plate border. *Development*, *140*(21), 4435 LP –

4444. https://doi.org/10.1242/dev.098707

Rikin, A., & Evans, T. (2010). The tbx/bHLH transcription factor mga regulates gata4 and organogenesis. *Developmental Dynamics*, *239*(2), 535–547. https://doi.org/10.1002/dvdy.22197

Rossi, A., Kontarakis, Z., Gerri, C., Nolte, H., Hölper, S., Krüger, M., & Stainier, D. Y. R. (2015). Genetic compensation induced by deleterious mutations but not gene knockdowns. *Nature*, *524*, 230. Retrieved from https://doi.org/10.1038/nature14580

Sander, J. D., Maeder, M. L., Reyon, D., Voytas, D. F., Joung, J. K., & Dobbs, D. (2010). ZiFiT (Zinc Finger Targeter): an updated zinc finger engineering tool. *Nucleic Acids Research*, *38*(suppl_2), W462–W468. https://doi.org/10.1093/nar/gkq319

Sander, J. D., Zaback, P., Joung, J. K., Voytas, D. F., & Dobbs, D. (2007). Zinc Finger Targeter (ZiFiT): an engineered zinc finger/target site design tool. *Nucleic Acids Research*, *35*(Web Server issue), W599–W605. https://doi.org/10.1093/nar/gkm349

Schumacher, J. A., Hashiguchi, M., Nguyen, V. H., & Mullins, M. C. (2011). An Intermediate Level of BMP Signaling Directly Specifies Cranial Neural Crest Progenitor Cells in Zebrafish. *PLOS ONE*, *6*(11), e27403. Retrieved from https://doi.org/10.1371/journal.pone.0027403

Simoes-Costa, M., & Bronner, M. E. (2015). Establishing neural crest identity: a gene regulatory recipe. *Development*, *142*(2), 242–257. https://doi.org/10.1242/dev.105445

Simões-Costa, M., & Bronner, M. E. (2015). Establishing neural crest identity: a gene regulatory recipe. *Development (Cambridge, England)*, *142*(2), 242–257. https://doi.org/10.1242/dev.105445

Sun, X., Chen, J., Zhang, Y., Munisha, M., Dougan, S., & Sun, Y. (2018). Mga modulates

Bmpr1a activity by antagonizing Bs69 in zebrafish. *Frontiers in Cell and Developmental Biology*, *6*(SEP), 1–14. https://doi.org/10.3389/fcell.2018.00126

Sun, Y., Tseng, W. C., Fan, X., Ball, R., & Dougan, S. T. (2014a). Extraembryonic Signals under the Control of MGA, Max, and Smad4 Are Required for Dorsoventral Patterning. *Developmental Cell*, *28*(3), 322–334. https://doi.org/10.1016/j.devcel.2014.01.003

Sun, Y., Tseng, W. C., Fan, X., Ball, R., & Dougan, S. T. (2014b). Extraembryonic Signals under the Control of MGA, Max, and Smad4 Are Required for Dorsoventral Patterning. *Developmental Cell*, *28*(3), 322–334. https://doi.org/10.1016/j.devcel.2014.01.003

Tríbulo, C., Aybar, M. J., Nguyen, V. H., Mullins, M. C., & Mayor, R. (2003). Regulation of Msx genes by a Bmp gradient is essential for neural crest specification. *Development*, *130*(26), 6441 LP – 6452. https://doi.org/10.1242/dev.00878

Tseng, W.-C. (2015). *NEURAL CREST SPECIFICATION BY MAX'S GIANT ASSOCIATED PROTEIN AND REGULATION OF MICROTUBULE'S FUNCTION BY ALPHA-TUBULIN ACETYLTRANSFERASE 1 IN ZEBRAFISH*. University of Georgia. Retrieved from http://dbs.galib.uga.edu/cgi-bin/write_stats.cgi?stattype=fulltext&dbscode=getd&format=pdf&redirect=http://getd.libs.uga.edu/pdfs/tseng_wei-chia_201505_phd.pdf

van den Berg, D. L. C., Snoek, T., Mullin, N. P., Yates, A., Bezstarosti, K., Demmers, J., … Poot, R. A. (2010). An Oct4-Centered Protein Interaction Network in Embryonic Stem Cells. *Cell Stem Cell*, *6*(4), 369–381. https://doi.org/10.1016/j.stem.2010.02.014

Vickaryous, M. K., & Mclean, K. E. (2011). *Vertebrate Embryogenesis*. *Reptile Embryology* (Vol. 770). https://doi.org/10.1007/978-1-61779-210-6

Washkowitz, A. J., Schall, C., Zhang, K., Wurst, W., Floss, T., Mager, J., & Papaioannou, V. E.

(2015). Mga is essential for the survival of pluripotent cells during peri-implantation development. *Development*, *142*(1), 31–40. https://doi.org/10.1242/dev.111104

Figures and Figure Legends

Figure 2.1. Generation of *mga* mutants using CRISPR/Cas9 system. [A]. Schematic representation of *mga* exons, and position of T-box domain and bHLHZip domain coding regions. A sgRNA (shown as black arrow) is designed to target the coding region of the T-box domain of Mga. [B]: Four different *mga* mutant alleles, mga^{ga121}, mga^{ga162}, mga^{ga194}, mga^{ga242}, were identified in F1 adults. Among these four alleles, mga^{ga121} and mga^{ga242} were hypothetically null. Blue letters represent target sequence; PAM was shown in green; yellow dashed lines represent deletions; Red lowercase letters represent inserted nucleotides. [C-F]: Live images of MZ$mga^{ga121-/-}$ embryos taken when their wild type siblings were at 9.5hpf and 28hpf. MZ$mga^{ga121-/-}$ embryos showed one to two hours of developmental delay (E, F) compared to the wild type (C, D), without showing any morphological abnormalities.

A

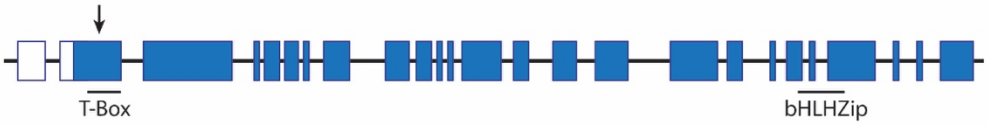

B

Target Site PAM

mga^{WT} : 5′ - AAATGGAAGGTGGAGTGGTTGTGGGAGGTG - 3′

mga^{ga121}: 5′ - AAATGGAAGGTGGAGTGGT - - - - - GAGGTG - 3′

mga^{ga162}: 5′ - AAATGGAAGGTGGAGTGGT - - - - - - AGGTG - 3′

mga^{ga192}: 5′ - AAATGGAAGGTGGAGTGGgagtggtgtggctcaataagtggTGTGGGAGGTG - 3′

mga^{ga242}: 5′ - AAATGGAAGGTGGAGTGGTTtcagTcTGGGAGGTG - 3′

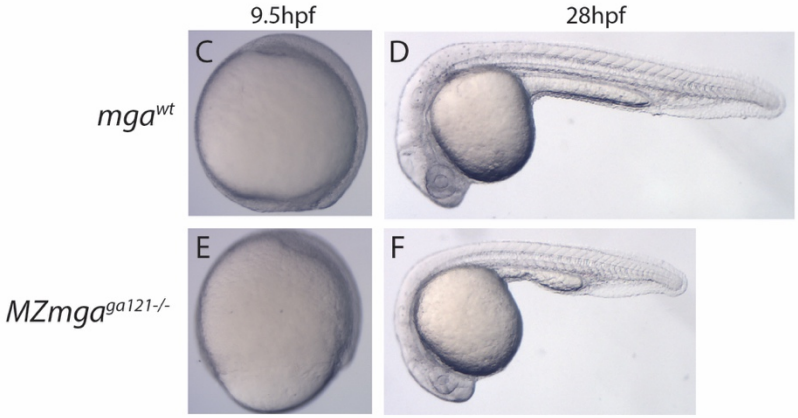

Figure 2.2. MZ*mga*$^{ga121-/-}$ have increased cell death. [A-B]: Programmed cell death was analyzed using TUNEL assay. There is a slightly increased apoptotic cells in the ventral trunk regions in MZ*mga*$^{ga121-/-}$ (B) compared to the wild type (A) [C-D]: Cell proliferation was analyzed using antibodies against phosphor-histone 3 (pH3). There is no significant difference in proliferation in MZ*mga*$^{ga121-/-}$ (D) when compared to the wild-type (C). For both TUNEL and pH3 staining, anterior:left; posterior: right. *Scale bar: 100μm*.[E-F]: Expression of *mga* transcript was analyzed using RT-PCR using total RNA extracts from both wild-type (E) and MZ*mga*$^{ga121-/-}$ (F) at various developmental time points.

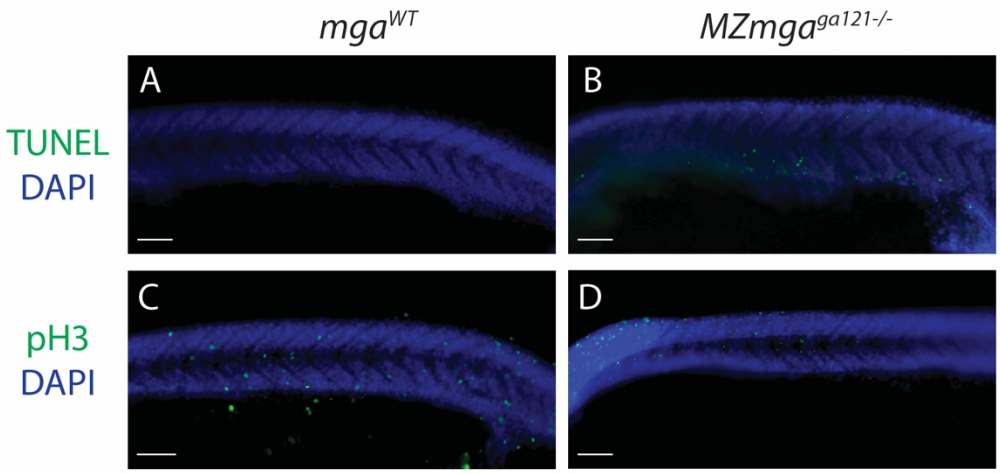
mga^WT
MZmga^ga121-/-
A
B
TUNEL
DAPI
C
D
pH3
DAPI

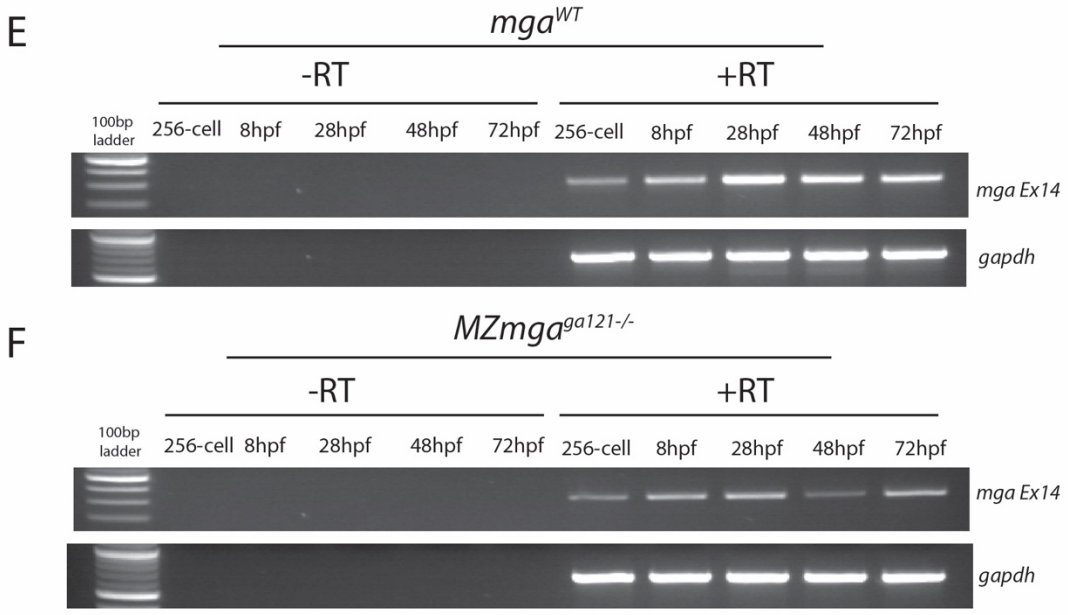
E
mga^WT
-RT
+RT
100bp ladder
256-cell
8hpf
28hpf
48hpf
72hpf
256-cell
8hpf
28hpf
48hpf
72hpf
mga Ex14
gapdh
F
MZmga^ga121-/-
-RT
+RT
100bp ladder
256-cell
8hpf
28hpf
48hpf
72hpf
256-cell
8hpf
28hpf
48hpf
72hpf
mga Ex14
gapdh

Figure 2.3. Mga depletion results in developmental defects in zebrafish. [A]: Titration of *mgaMOs* concentration. Majority of the embryos injected with higher amount of *mgaMOs* die before 24hpf. [B-C]: Live images of zebrafish embryos injected with *mgaMOs* and *misMOs* at 32hpf. Mga depleted embryos (C) show decreased pigmentation compared to the control (B). [D-F]: Live images of embryos injected with *mgaMOs* and either *β-gal* mRNA or mouse *mga* mRNA at 32hpf. Injection of mouse *mga* mRNA significantly rescues the pigmentation defect in *mga* morphants (E) compared to those injected with *β-gal* mRNA (D). [G-H]: Western blot analysis of Mga protein level in *mga* morphants and control embryos at 75% epiboly. Injection of 1.6ng of *mgaMOs* decreases Mga protein level to 57% of the controls. (n=2; Error bar: SEM)

A

	Dead at 24hpf/Total injected (percent lethality)	
	mgaMOs	*misMOs*
3.2ng	27/28 (96%)	3/30 (10%)
2.8ng	21/29 (72%)	2/19 (10%)
2.2ng	14/59 (23%)	2/54 (3%)

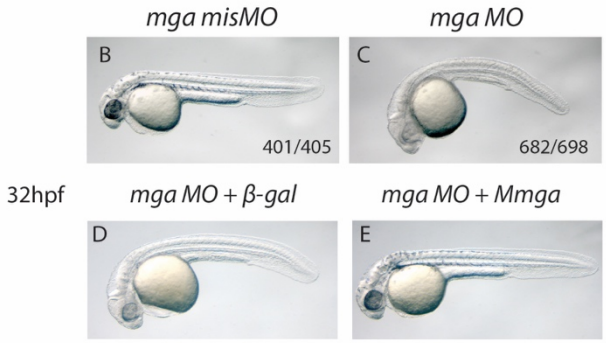

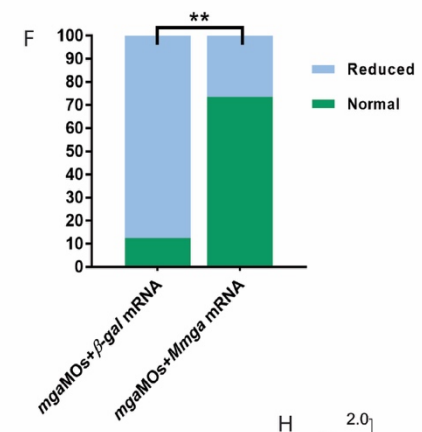

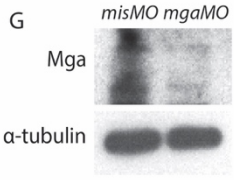

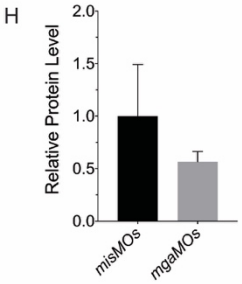

Figure 2.4. Depletion of Mga affects multiple lineages of neural crest derivatives. [A-F]: Alcian Blue staining of *mga* morphants and control embryos at 5dpf. Craniofacial cartilages are greatly reduced in size and some of the cartilages are missing in *mga* morphants (B, D, F) compared to the control (A, C, E). [G-J]: Expression of ENS and PNS markers, *phox2bb* (G, H) and *islet1* (I, J) are reduced in the *mga* morphants (H, J) compared to the control (G, I). Insets show specific areas of marker gene expression showed by the red arrows and arrowheads. T: Trabeculae; M: Meckel's; P: Palatoquadrate; HS: Hyosymplectic; CH: Ceratohyal. Scale bar=100μm.

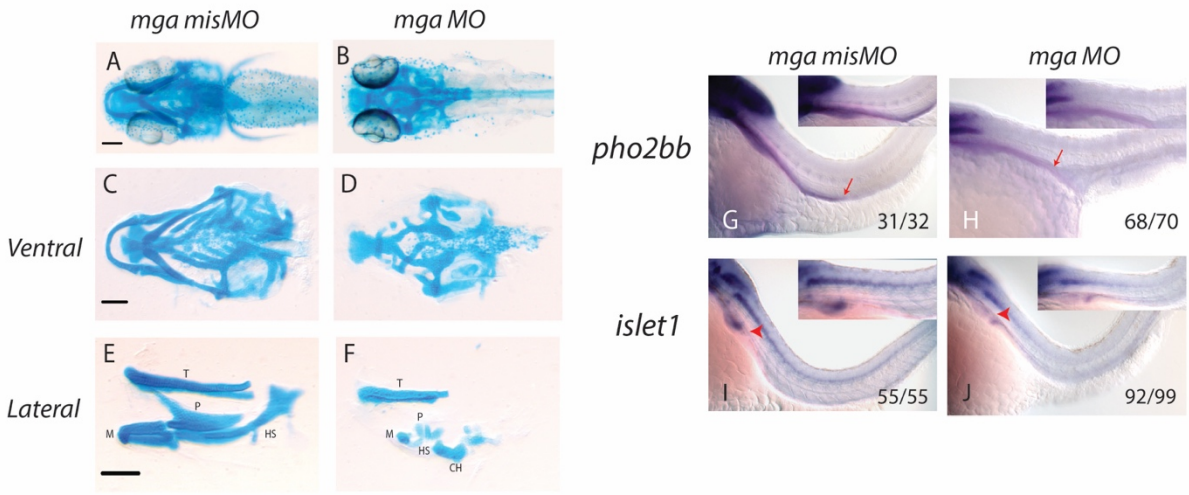
mga misMO
mga MO
A
B
C
D
E
F
Ventral
Lateral
T
P
M
HS
CH
pho2bb
islet1
G
H
I
J
31/32
68/70
55/55
92/99

Figure 2.5. Mga antagonize Myc activity *in vivo*. [A-B]: Programmed cell death is analyzed using TUNEL assay in *mga* morphants (B) and *misMOs* injected control embryos (A) at 24hpf. Increased cell death is seen in Mga depleted embryos (B) compared to the control (A). [C]: Luciferase assay is performed in *mga* morphants and control embryos at 8hpf, 24hpf and 31hpf. Depletion of Mga leads to increased Myc activity compared to the control. (*: $p = 0.005$; student's t-test, n=3; Error bar: SEM.) D: Expression of Myc target genes, *id2*, *cdc25b*, *odc1*, *cebpa* and *cyclind1* are increased in *mga* morphants. qRT-PCR was performed using total RNA extracts from *mgaMOs* and *misMOs* injected embryos at 24hpf. Relative gene expression is calculated using $2^{-\Delta\Delta Ct}$ method from five biological replicates, with three technical replicates for each experiment. (*: $p < 0.05$; **: $p < 0.005$. n=5; Error bars: SEM)

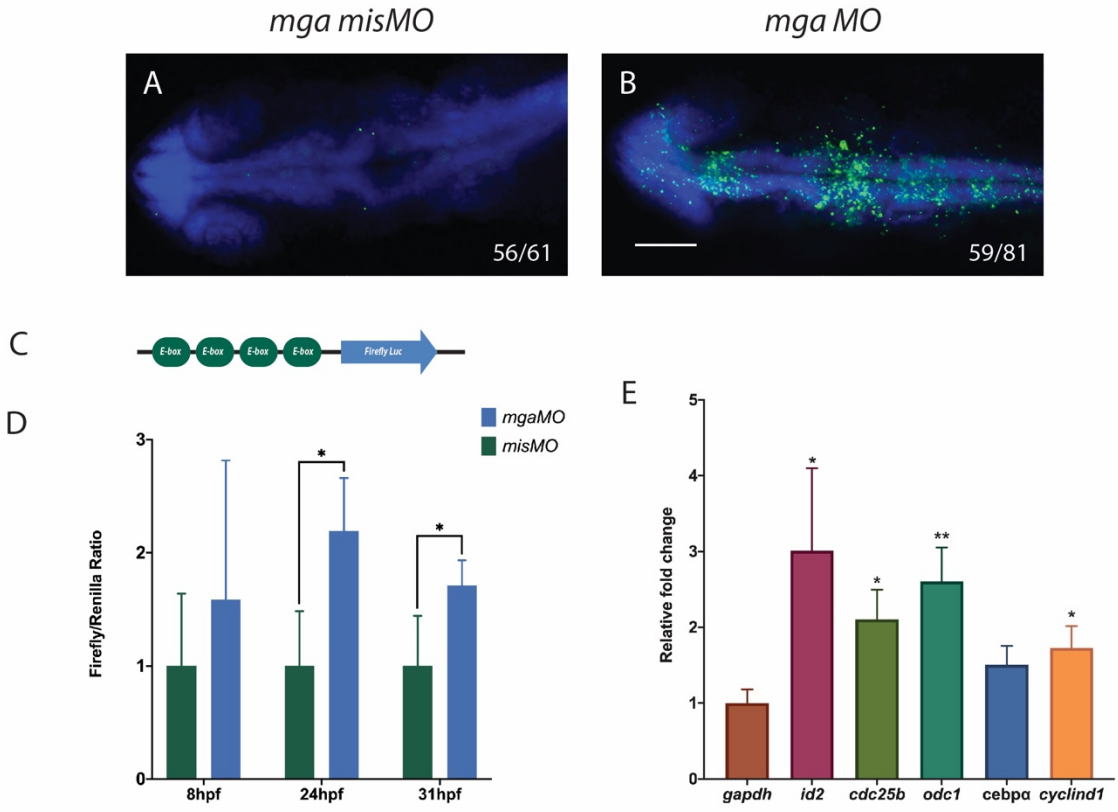
mga misMO
mga MO
A
B
56/61
59/81
C
E-box
E-box
E-box
E-box
Firefly Luc
D
mgaMO
misMO
Firefly/Renilla Ratio
8hpf
24hpf
31hpf
E
Relative fold change
gapdh
id2
cdc25b
odc1
cebpα
cyclind1

Figure 2.6. Depletion of Mga affects early neural crest specification. [A-D]: Expression of the early neural crest markers, *foxd3* (A, B) and *tfap2a* (C, D) are decreased in *mga* morphants (B, D) at 3-somite stage compared to the control (A, C). [E-H]: Expression of *foxd3* (E, F) and *tfap2a* (G, H) were analyzed in $MZmga^{ga121-/-}$ and mga^{WT} embryos at 3-somite stage. Both markers show decreased expression in $MZmga^{ga121-/-}$ (F, H) compared to control (E, G).

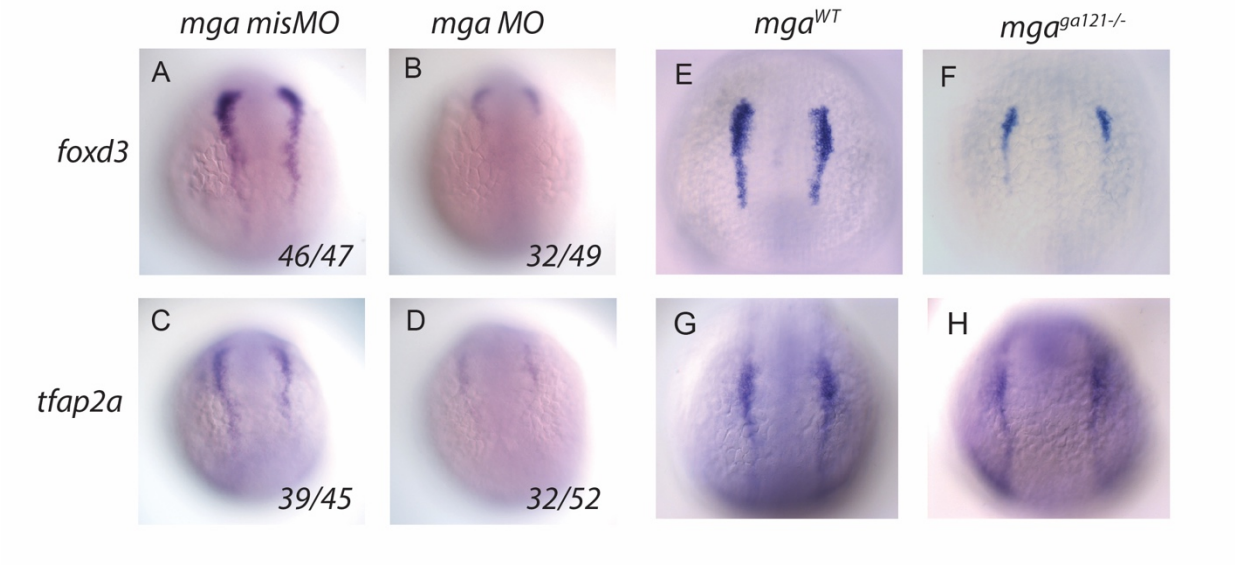
mga misMO
mga MO
mga^WT
mga^ga121-/-
foxd3
tfap2a
A
B
C
D
E
F
G
H
46/47
32/49
39/45
32/52

Figure 2.7. Bmp signaling pathway activity is decreased in *mga* morphants. [A-B]: *in situ* hybridization of Bmp antagonist, *chordin*, shows ventrally expanded chordin domain *mga* morphants (B) compared to the control (A) at 8hpf. [C-D]: expression of Bmp target gene *tbx6* is reduced in *mga* morphants (D) compared to the control (C) at 8hpf. For both *in situ* hybridization, dorsal view is shown. [E]: mRNA level of *Δnp63* is reduced significantly in *mga* morphants at 8hpf compared to the control. qRT-PCR was performed using total RNA extracts from *mgaMOs* and *misMOs* injected embryos at 8hpf. Relative fold change is calculated using $2^{-\Delta\Delta Ct}$ method from three biological replicates, with three technical replicates for each experiment. (*: $p < 0.05$. n=3; Error bars: SEM)

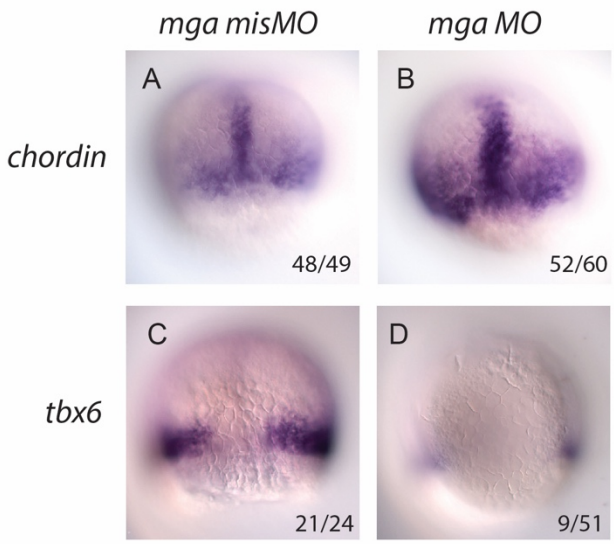
mga misMO
mga MO
chordin
tbx6
A
B
C
D
48/49
52/60
21/24
9/51

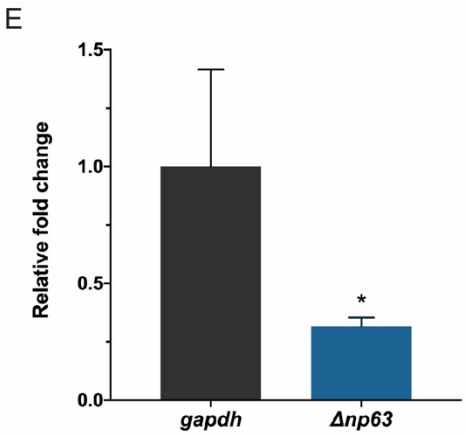
E
Relative fold change
1.5
1.0
0.5
0.0
*
gapdh
Δnp63

Figure 2.8. Suppression of Myc activity in *mga* morphants is not sufficient to rescue neural crest defect. [A-D]: Live images of embryos injected with *misMOs* (A), *mgaMOs* (B), *mgaMOs* + *mxd3* mRNA(C) as well as *mgaMOs* + *β-gal* mRNA at 32hpf. Co-injection of 200pg of *mxd3* mRNA mgaMO (C) shows no significant difference in pigmentation compared to *mgaMOs* injected embryos (B) or to embryos co-injected with *mgaMOs* and 200pg *β-gal* mRNA (D). [E]: qRT-PCR analysis of Myc target genes using total RNA extracted from *mgaMOs* + *mxd3* mRNA and *mgaMOs* + *β-gal* mRNA injected embryos at 24hpf. Overexpression of *mxd3* results in suppression of some of the elevated Myc target genes in *mga* morphants compared to *β-gal* mRNA injected *mga* morphants. Relative fold change is calculated using $2^{-\Delta\Delta Ct}$ method from three biological replicates, with three technical replicates for each experiment. (*: $p < 0.05$. n=3; Error bars: SEM) [F-I]: Analysis of programmed cell death using TUNEL assay. Overexpressing *mxd3* in *mga* morphants (H) is able to decrease cell death compared to control injection (I).

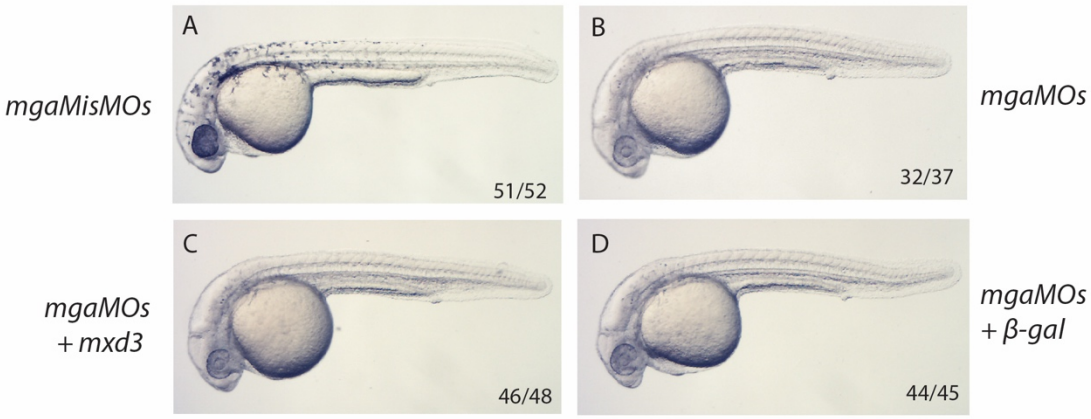
A
B
C
D
mgaMisMOs
mgaMOs
mgaMOs
+ mxd3
mgaMOs
+ β-gal
51/52
32/37
46/48
44/45

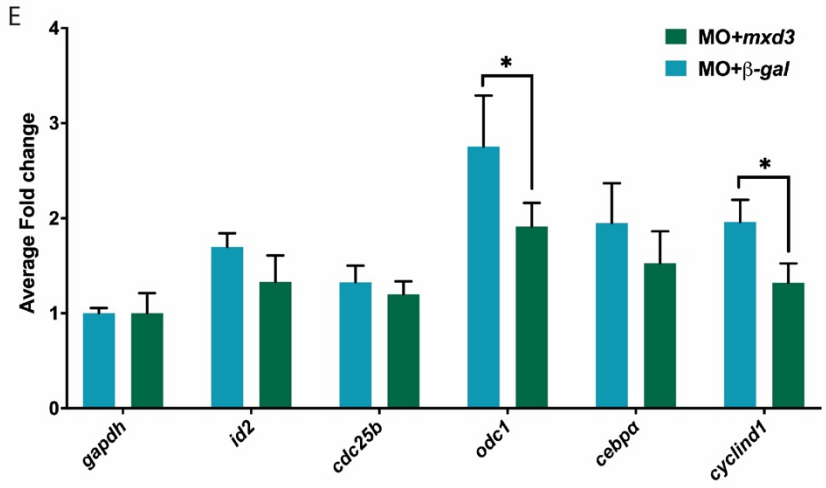
E
MO+mxd3
MO+β-gal
Average Fold change
0
1
2
3
4
*
*
gapdh
id2
cdc25b
odc1
cebpa
cyclind1

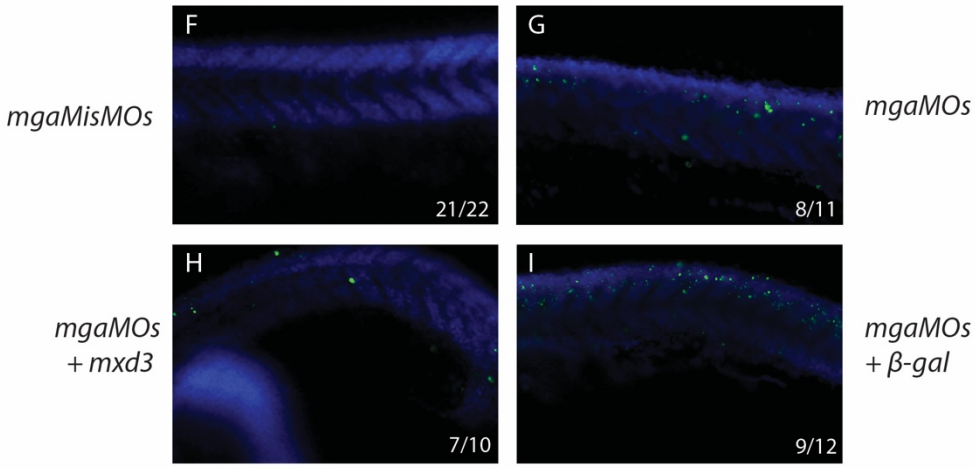
F
G
H
I
mgaMisMOs
mgaMOs
mgaMOs
+ mxd3
mgaMOs
+ β-gal
21/22
8/11
7/10
9/12

SUPPLEMENTAL FIGURES

Figure S2.1. Early melanocyte precursors are decreased in *mga* morphants. [A-B]: L-DOPA staining show decreased tyrosinase positive melanoblast in *mga* morphants (B) compared to the control (B) at 22hpf. [C-D]: Expression of early pigmentation marker *mitfa* is decreased in *mgaMOs* injected embryos (D) compared to the control (C) at 22hpf.

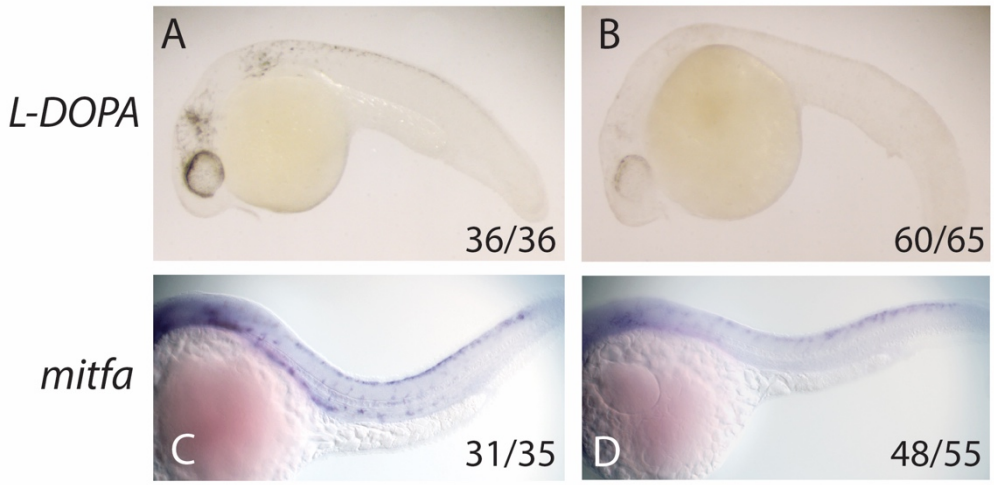
L-DOPA
mitfa
A
36/36
B
60/65
C
31/35
D
48/55

Figure S2.2. Precursors of craniofacial cartilages are affected early in *mga* morphants. Expression of early craniofacial cartilage markers, *hand2* (A, B) and *dlx2a* (C, D) are greatly reduced in *mga* morphants (B, D) compared to control (A, C) at 36hpf.

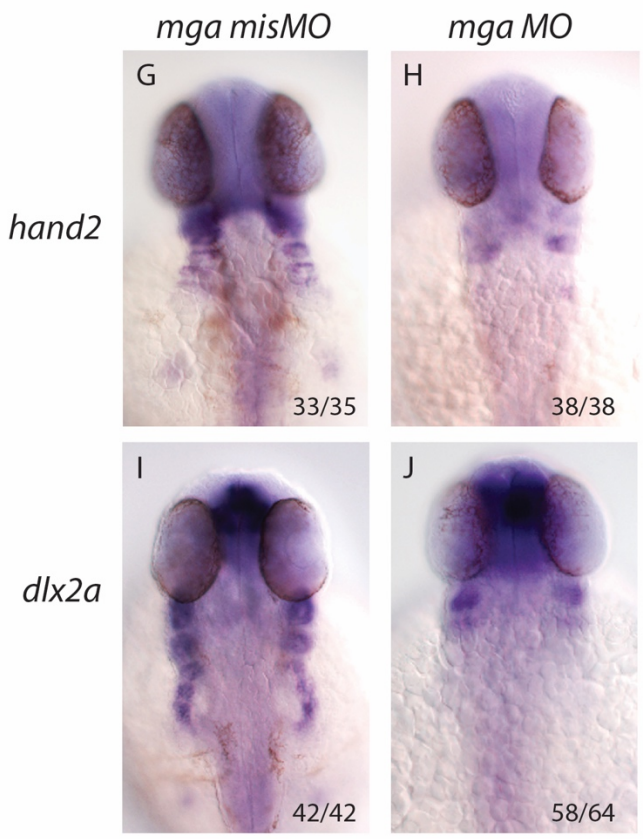
mga misMO
mga MO
hand2
dlx2a
G
H
I
J
33/35
38/38
42/42
58/64

Figure S2.3. Mga acts early during neural crest development. Expression of early neural crest markers *sox10* (A, B) and *snai1b* (C, D) are decreased in *mga* morphants (B, D) compared to control (A, C).

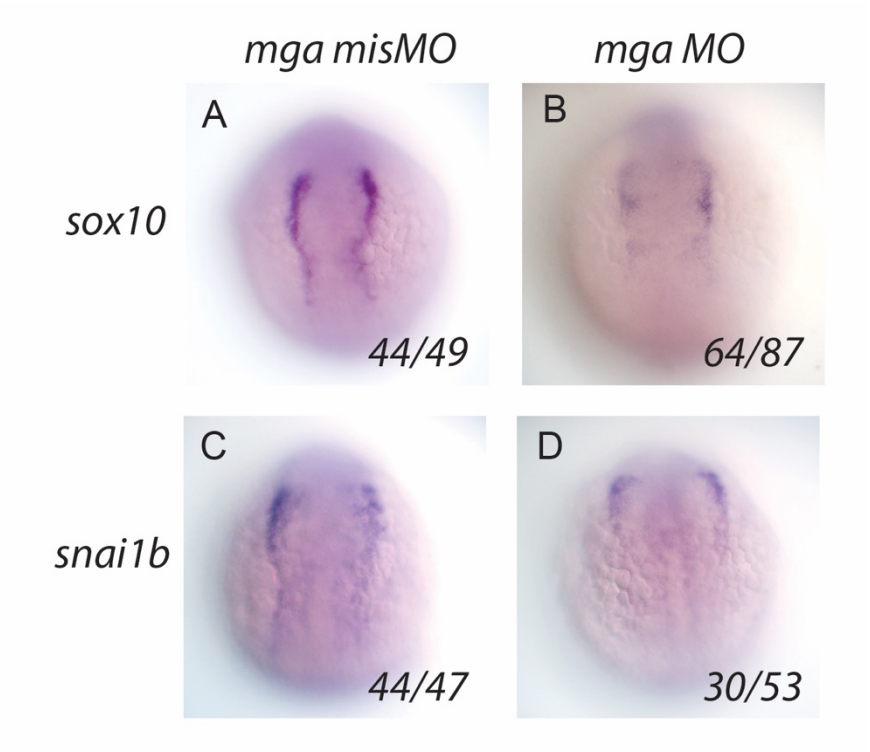
mga misMO
mga MO
sox10
snai1b
A
B
C
D
44/49
64/87
44/47
30/53

Figure S2.4. Suppression of Mga leads to decreased Bmp signaling. [A-B]: Expression of chordin is expanded ventrally in *mga* morphants (B) when compared to control (A). (Animal view) [C-D]: *tbx6* expression is decreased in *mga* morphants (D).

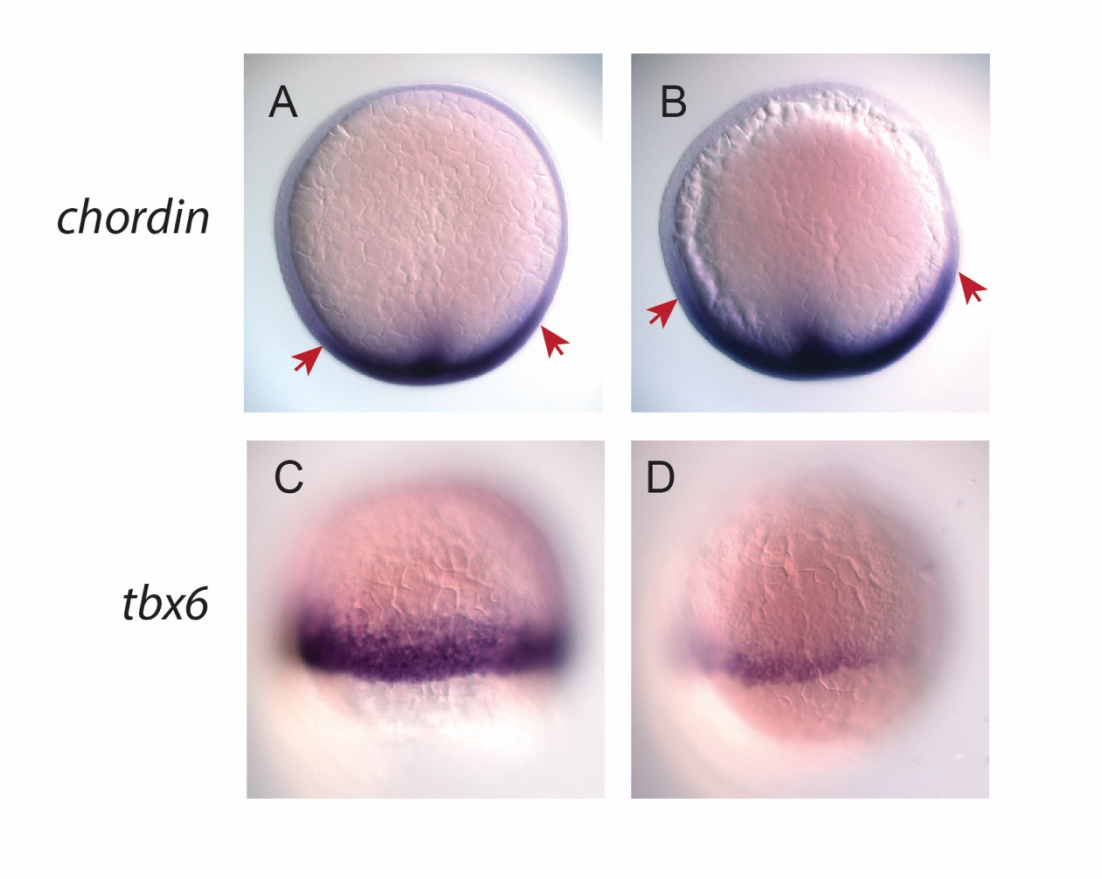
chordin
tbx6
A
B
C
D

Figure S2.5. Decreased expression of neural crest markers persists at 8-somite stage.

Expression of early neural crest markers are analyzed at 8-somite stage using probes specific for *foxd3* (A, B), *tfap2a* (C, D), *sox10* (E, F) and *snai1b* (G, H).

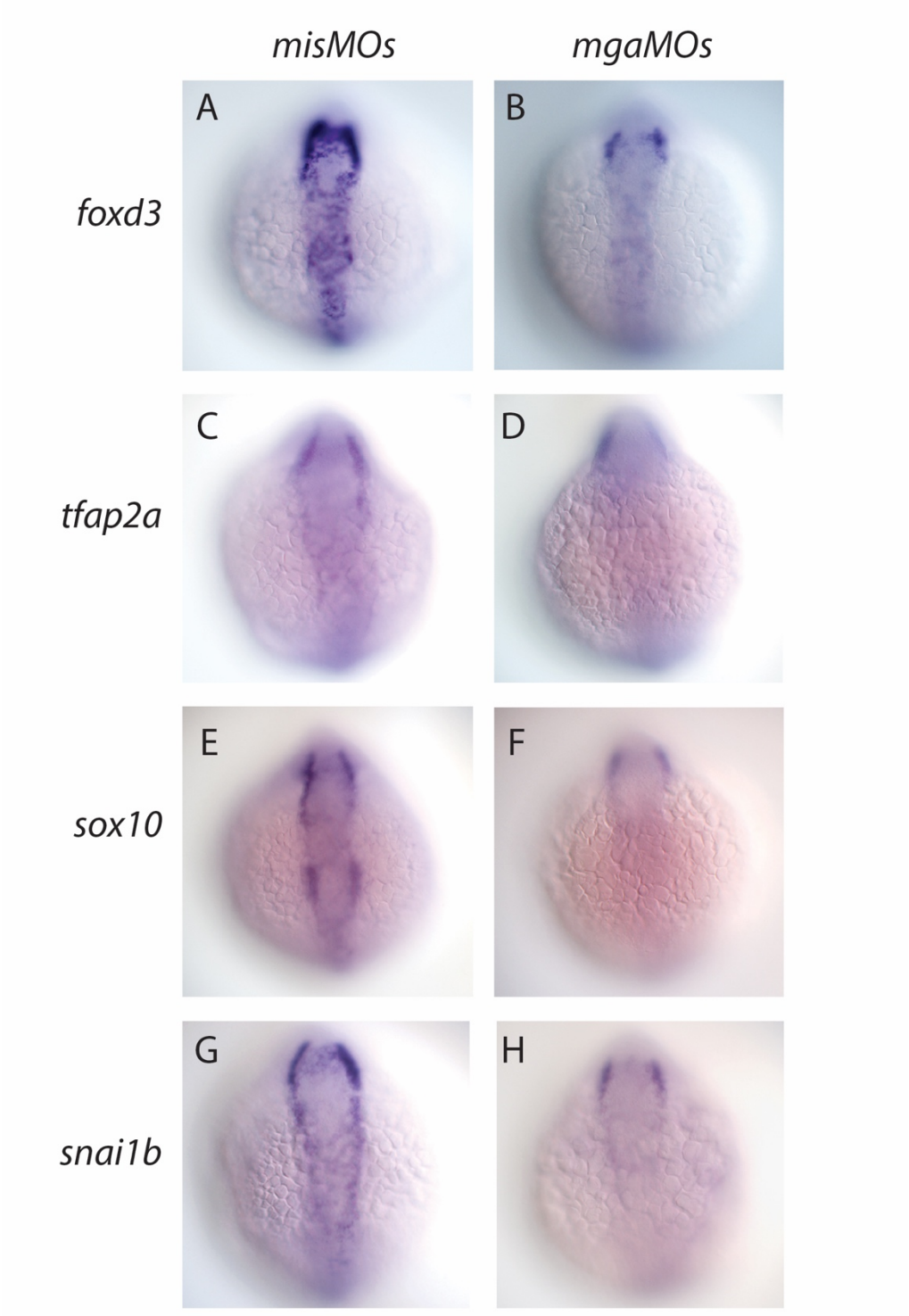
misMOs
mgaMOs
foxd3
tfap2a
sox10
snai1b
A
B
C
D
E
F
G
H

CHAPTER 3

GENERATION OF ZEBRAFISH *mga* MUTANTS USING CRISPR/CAS9 SYSTEM TO STUDY MGA FUCNTION IN EARLY EMBRYONIC DEVELOPMENT

INTRODUCTION

After fertilization, the totipotent zygote gives rise to every single cell type in the body through gradual restriction of cellular potential during embryogenesis. Such process is governed by a complex network of cellular processes including transcriptional regulation, tightly regulated crosstalk among different signaling pathways, cell-cycle control, chromatin remodeling and so on. Disruption of these cellular processes will not only affect normal embryonic development but also contribute to cancer.

One of those proteins whose function is implicated in early embryogenesis as well as in tumorigenesis is MAX Gene Associated protein (MGA). MGA is a member of the MAX interacting transcription factor network family. Proteins of the MAX interacting network include MYC oncoproteins, MAX and putative MYC antagonists including MXD1-4, MNT, and MGA. (Peter J. Hurlin & Huang, 2006) They are involved in regulation of many cellular behaviors including cell proliferation, differentiation, cell-cycle control and chromatin remodeling. (Peter J. Hurlin & Huang, 2006) They exert transcriptional activity via forming heterodimers with MAX through basic Helix-Loop-Helix Zipper (bHLHZip) which also directs sequence specific binding to the upstream E-box element of target genes. (Peter J. Hurlin & Huang, 2006) MGA is a unique member of MAX network family in that it contains another DNA binding motif, T-BOX domain,

in addition to the bHLHZip domain. (P J Hurlin, Steingrimsson, Copeland, Jenkins, & Eisenman, 1999) Despite its involvement in many different cancers in human patients, possibly through mis-regulation of Myc activity, very little is known about its function during embryonic development. Mga has been shown to promote differentiation by antagonizing Myc dependent cell proliferation and exit from cell cycle in cell culture assays. (P J Hurlin et al., 1999) However, more recent work by Washkowitz et al showed that Mga is required for pluripotent cell survival, and that Mouse embryos lacking functional Mga die before implantation due to failure of ICM to maintain pluripotency. (Washkowitz et al., 2015) Although Mga has been found in a network of proteins that interact with core pluripotency factor Oct4 in mouse embryonic stem cells, (van den Berg et al., 2010) the exact mechanism of how Mga regulate pluripotency is unknown. Mga's function to promote and inhibit differentiation maybe context dependent. The presence of another DNA binding domain, the T-box domain, may render complexity to Mga's transcriptional activity through regulating the expression of a wide range of target genes involved in pluripotency maintenance and differentiation. Therefore, characterization of Mga function during early embryonic development will contribute substantially to our understating of the molecular mechanism driving cell fate specification as well as the balance between maintenance of cell identity/potential.

Due to early embryonic lethality in mouse embryos, zebrafish embryos stand out as great model organisms to study Mga function for their availability in large numbers, short generation time and most importantly for accessibility for live imaging during early embryonic development due to *ex utero* development. In the past, study of gene function in Zebrafish has mostly utilized N-ethyl-N-nitrosourea (ENU) based forward genetics screens and the use of antisense oligonucleotides/morpholinos (MOs) to knockdown the expression of gene of interest. Forward

genetic screens in zebrafish have led to the discovery of many important developmental genes involved in early embryogenesis which contributed substantially to our understanding of human development and diseases. (Fuentes, Letelier, Tajer, Valdivia, & Mullins, 2018) On the other hand, due to its cost-effectiveness and faster and easier approach to study the specific gene of interest, MOs has been widely used in zebrafish community. However, limitations do exist for MOs. For example, MOs are known to trigger p53 dependent cell death and other cellular stress responses. (Lai, Gagalova, Kuenne, El-Brolosy, & Stainier, 2019; Robu et al., 2007) In addition, MOs block translation via binding to target mRNAs and have no effect on maternally loaded proteins. This may be crucial in understanding the function of genes such as Mga which is expressed both maternally and zygotically. (Rikin & Evans, 2010; Sun, Tseng, Fan, Ball, & Dougan, 2014) Recent application of clustered regularly interspaced short palindromic repeats (CRISPR) RNA guided/CRISPR-associated (Cas) system in vertebrates has been proved highly effective reverse genetics tool to study gene function *in vivo*. (Hwang et al., 2013; Jao, Wente, & Chen, 2013) By simply injecting CRISPR RNA(crRNA) and transactivating CRISPR RNA (tracrRNA), which directs Cas9 endonuclease to the target locus and create double strand break (DSB) 3-4 nucleotides away from the PAM sequence, together with *cas9* mRNA into zebrafish embryos, one can easily and efficiently generate mutations in any region of the zebrafish genome. (Hwang et al., 2013; Jao et al., 2013)

In this study, by targeting the coding sequence of T-box domain of Mga using CRISPR/Cas9 system, we successfully generated four different *mga* mutant alleles, among which two of them were hypothetically null. We characterized one of the null alleles, mga^{ga121}, through phenotypic and molecular analysis. MZ$mga^{ga121\text{-}/\text{-}}$ lacked more severe phenotype other than developmental delay compared to the phenotype seen in *mga* knockdown studies or mouse

mga mutants. (Rikin & Evans, 2010; Sun et al., 2014; Tseng, 2015; Washkowitz et al., 2015) We found that there is slightly elevated Myc activity in *MZmga*$^{ga121-/-}$ when compare to those wild type. Due to whole genome duplication during the evolution of teleost fish, we hypothesized that the lack of severe phenotype in *MZmga*$^{ga121-/-}$ could be due to functional redundancy or compensation by another *mga* paralog which has not yet been annotated. Through bioinformatics, we identified *mga* paralog, *max-gene associated protein-like* (or *mgab*), that is expressed both maternally and zygotically. We assessed the expression of *mgab* in *mga*$^{ga121-/-}$ and found that its expression is elevated. It's possible that *mgab* act redundantly with *mgaa* to regulate early embryonic development in zebrafish.

MATERIALS AND METHODS

Zebrafish care

Both wild type (WIK) and mutant fish lines are maintained at 28.5°C in the fish facility according to Animal Use Protocol (AUP) approved by the University of Georgia IACUC committee (A2017 08-020-Y3-A0). Embryos were collected using single or multiple pair mating and were kept at 28.5°C in egg water (60mg/ml Instant Ocean Sea Salt Mix, 0.3mg/ml Methylene Blue). Embryos were staged as previously described. (CB, WW, SR, B, & TF, 1995)

CRISPR/Cas9

Single gRNA targeting the T-box domain of Mga was identified using online target finder ZiFiT. (Sander et al., 2010; Sander, Zaback, Joung, Voytas, & Dobbs, 2007) Two DNA oligos (Forward: 5'-TAGGAAGGTGGAGTGGTTGT-3'; Reverse: 5'-

AAACACAACCACTCCACCTT -3') containing the target site (5'-GGAAGGTGGAGTGGTTGT-3') were used to clone into pT7-gRNA plasmid as previously described. (Jao et al., 2013) sgRNAs were transcribed using MEGAshortscript T7 transcription kit (Thermo Fisher Scientific, Cat# AM1354) according to manufacturer's protocol. sgRNA was purified using ethanol precipitation, dissolved in nuclease free water and quantified with NanoDrop 2000 (Thermo Scientific™). pCS2+-nls-zCas9-nls plasmid linearized with NotI was used as a template for making capped *cas9* mRNA which was transcribed with mMessage mMachine SP6 transcription kit (Invitrogen™ Cat#: AM1340) following manufacturer's protocol. *cas9* mRNA was purified with 3M lithium chloride and dissolved in nuclease free water with a final concentration of around 1μg/μl.

Microinjection

Microinjection was carried out as previously described. (Vickaryous & Mclean, 2011) 100pg of sgRNA and 150pg of *cas9* mRNA along with 0.1% phenol red and 0.1M KCl were injected directly into the single cell of the 1-cell stage wild type embryos. Injected embryos were cultured in egg water (60μg/ml Instant Ocean Sea Salt Mix, 0.3μg/ml Methylene Blue) at 28.5°C. Damaged and unfertilized embryos were discarded at around 3-4hpf, the rest were raised to adulthood for further screening for mutations.

Screening for mutations

sgRNA and *cas9* mRNA injected embryos were raised to adulthood and named as F0. T7E1 assay was used to screen for around fifteen F0 adult fish that are carrying possible indel mutations. F1 embryos were obtained from single pair mating of F0 and wild type adult fish.

DNA was extracted from randomly selected 15-20 F1 embryos from each pair mating at 3dpf. PCR was carried using primer pairs mga_tbox_F2 (5'- ATGTGAGAGGGTCAGAAGCTA -3') and mga_tbox_R2 (5'- AGTGCCAATTGAGGATTTCCC -3') under the following PCR condition: 94°C for 2min; 94°C for 30 seconds, 54°C for 30 seconds, 72°C for 15 seconds, 40 cycles; 72°C for 5 minutes. PCR products were boiled initially at 95°C for 5 minutes and cooled down slowly to room temperature in PCR cycler with a gradient of 2.5°C intervals to form heteroduplexes. Once cooled down, PCR products were digested with T7 Endonuclease I (New England BioLabs, Cat#: M0302) at 37°C for two hours. Digested PCR products were then analyzed on 2% agarose gel for possible indel mutations. Once potential mutant founders (F0) were identified, their F1 progeny were raised to adulthood and assessed for mutations individually using DNA extracts from fin-clips. The PCR products from each F1 individual (12 adult fish raised from F0 progenies) carrying indel mutation were cloned into pGEM-T Easy vector (Promega, A1360) for sequencing.

Genotyping mga$^{ga121-/-}$

For genotyping, DNA extracts from either 3dpf larvae or adult fin-clips were used as templates for PCR. Genotyping PCR was carried out using primer pairs mgaT100F (5'- CATTAGATTAGCCTTGTCATT -3') and mgaT100R (5'- CATGAAGAGGGCGTGACTG -3') with the following PCR condition: 94°C for 2 minutes; 94°C for 30 seconds, 55°C for 30 seconds, 72°C for 15 seconds, 40 cycles; 72°C for 30 seconds, PCR products were resolved on 15% PAGE gel on 200V for 2.5 hours.

RT-PCR and qRT-PCR

Total RNA was extracted from 10 embryos randomly selected from either *mga*$^{ga121-/-}$ or wild type single pair mating at 24hpf using TRIzol™ Reagent (Invitrogen™, Cat #: 15596026). Extracted total RNA was dissolved in nuclease free water, quantified with NanoDrop 2000 (Thermo Scientific™) and stored at -80°C until use. 1µg of total RNA was used to make cDNA using RevertAid First Strand cDNA Synthesis Kit (Thermo Scientific™ Cat #: K1622) following manufacturer's protocol. For subsequent PCR analysis, 2µl of 10X diluted cDNA was used as template. *mgaa* and *mgab* transcripts were analyzed using the following primer pairs: MgaEx14F: 5'-CAGCCCGGTCCCCATTGG-3'; MgaEx14R: 5'-CCAGAGGCAGGCTGGGTGAC-3'; mgabEx17F: 5'- CTGAAGCGGAGGAAGACATC -3'; mgabEx17R: 5'- CAAAGCTGAGTCTGGAGAAGG -3'; For endogenous control *gapdh* were used. zGAPDH-Long F1: 5'- CGTCTGGTGACCCGTGCTGC-3'; zGAPDH-Long R1 5'-TGGGGGTGGGGACACGGAAG-3'. PCR conditions for both MgaEx4F/R and zGAPDHF1/R1 primers: 94°C for 2min, 94°C for 30sec, 63°C for 30sec, 72°C for 45sec, 35 cycles, 72°C for 5min. PCR condition for mgabEx17F/R: PCR products were visualized using 1.5% agarose gel. qPCR was carried out using Applied Biosystems™ 7500 Real-Time PCR System using PowerUp™ SYBR™ Green Master Mix (Applied Biosystems™, Cat #: A25742) following manufacturer's protocol. 1µl of 10X diluted cDNA was used as template. qPCR was carried out using the following conditions: 50°C for 2 minutes; 95°C for 2 minutes; 95°C for 30 seconds, 60°C for 1 minutes, 40 cycles. Primers used for qPCR: id2RTF: 5'-CGTGATGAAACCTTGTGAACTCT-3'; id2RTR: 5'-TCTCAGCATACAGCATAACACTTTG-3'; cdc25bRTF: 5'-

AGTGGAGAGGCTGTTTGTTATCG -3'; cdc25bRTR: 5'-GGGCAGTCAGGGAGAATAGGA-3'; odc1RTF: 5'- TACACACTGGCGGTCAACATCA-3'; odc1RTR: 5'- TCGGTCATTGGACACATCCTCT-3'; ccnd1RTF: 5'-CCAGAACCTCACCAACTTCCTC-3'; ccnd1RTR: 5'- GACTCGATCTGTTCCTGACACG-3'; cebpaRTF: 5'- CGAGTTCCTGGCTGACTTATTCC-3'; cebpaRTR: 5'-TTCTTGCTTGGCTGTCGTAGATG-3'.

Luciferase assay

Microinjection of luciferase constructs were carried out as previously described. (Vickaryous & Mclean, 2011) Both pT2-Luci-4xEbox and pRL-TK luciferase vectors were prepared using QIAGEN midi-prep kit prior to injection. 25pg of each of the luciferase constructs were injected into both WIK and *mga*$^{ga121-/-}$ 1-cell stage embryos. Injected embryos were cultured in egg water at 28.5°C until desired stage for subsequent analysis. Luciferase assay was carried out using Dual-Luciferase® Reporter Assay System (Promega, Cat #: E1910) according to manufacturer's protocol with slight adjustments. Briefly, around 30 embryos, from each WIK or *mga*$^{ga121-/-}$ pair mating, were collected at 8hpf, 24hpf and 32hpf, dechorionated and placed in 96-well plate with 10 embryos for one well. Embryos were lysed in 20µl Passive Lysis Buffer (PLB) for 15-20 minutes at room temperature protected from light. Luminescence was measured using Synergy H4 Hybrid Multi-Mode Microplate Reader (BioTek Instruments, Inc.). For measuring firefly luminescence, 100µl of Luciferase Assay Reagent II was added to each well. After the readings, 100µl Stop & Glo® Reagent was added to each well for measuring Renilla luminescence. Luciferase assay was performed in three biological replicates with three technical replicates for each experiment.

Bioinformatics

To identify possible *mgaa* paralog, amino acid sequence of T-box domain of Mgaa was searched on NCBI Basic Local Alignment Search Tool (BLAST) nucleotide collection (nr/nt) using protein to translated nucleotide command. (Altschul et al., 1997) DNA and mRNA accession number for *mgab* are LOC108180286 and XM_021468741 respectively. *mgaa* and *mgab* synteny for zebrafish, mouse, human, and other fish species were analyzed using NCBI Genome Data Viewer. Amino acid sequences for the T-box and bHLHZip domain were retrieved from NCBI as FASTA format and aligned with T-COFFEE (http://tcoffee.crg.cat/apps/tcoffee/do:regular). Alignment results from T-COFFEE were formatted using Boxshade (https://embnet.vital-it.ch/software/BOX_form.html). Sequence identity and similarities were calculated using Iden and Sim (https://www.bioinformatics.org/sms2/ident_sim.html).

Imaging

For fluorescent imaging, embryos were mounted in 80% glycerol on raised coverslip microscope slides. Fluorescent images were taken using Zeiss AXIO Imager D2 compound fluorescence microscope with Colibri.2 LED light source and AxioCam HR CCD camera (Carl Zeiss, Jena, Germany). For live imaging, embryos were mounted in 3% Methyl Cellulose in microscope slides with single concave wells. Pictures were taken using Leica MZ FLIII stereomicroscope (Leica Microsystems, Germany) and Moticam 5 (CMOS) 5.0MP camera (Motic Asia, Hong Kong).

RESULTS

1. Generation of *mga* mutants using CRISPR/Cas9 system

During zebrafish embryonic development, *mga* is broadly expressed throughout the cleavage and blastula stages. (Rikin & Evans, 2010; Sun et al., 2014) To prevent the maternal effect of Mga protein, we set out to generate maternal zygotic *mga* mutants using CRISPR/Cas9 system. We designed sgRNA targeting the coding region of T-box domain of Mga. (Figure 3.1A) We injected 100pg t-box sgRNA along with 150pg of *cas9* mRNA directly into the single of 1-cell stage embryos. At 5dpf, some of the embryos injected showed various degrees of developmental defects such as heart edema and truncated tails. (Figure 3.1D, E) This is likely due to mosaicism of genome targeting during development. We then extracted DNA from ten embryos that showed phenotypes and screened for mutations using T7 endonuclease I which cleaves double strand DNA at positions of mismatches. (Mashal, Koontz, & Sklar, 1995) All ten embryos showed up T7E1 positive indicating successful genome targeting at the t-box locus. (Figure 3.1B) We next raised sgRNA and cas9 mRNA injected wild embryos/founders (F0) to adulthood, outcrossed to wild type fish, and screened their progeny for possible indel mutations again using T7E1 assay. Ten out of twelve F0 adult fish screened carried mutations in the germ line, with a germ line transmission rate ranging from 6.6% to 40%. F1 progenies of these 10 adult F0s were raised to adulthood and screened for mutations using DNA extracts from fin-clips. (Figure 3.1C) Amplicons from T7E1 positive F1 adults were sequenced. We successfully identified four different *mga* alleles, mga^{ga121}, mga^{ga162}, mga^{ga194} and mga^{ga242}. (Figure 3.2A, B) Among these four alleles, two of them, mga^{ga121} and mga^{ga242} were hypothetically null. mga^{ga121} had five base pair deletions immediately next to the PAM site and created a frameshift mutation

in the T-box coding region and multiple stop codons downstream of the mutant position, possibly generating a truncated Mga protein without any functional DNA binding domain. *mga*^{ga242} had five base pair insertion which also created a frameshift mutation. We used *mga*^{ga121} for subsequent phenotypic and molecular analysis. Interestingly, *MZmga*$^{ga121-/-}$ failed to recapitulate *mga* morphant phenotypes except for developmental delay. (See Chapter 2, Figure 2.1C-F) The developmental delay appears to be due to increased cell death rather than reduced cell proliferation. (See Chapter 2, Figure 2.2A-D)

2. *MZmga*$^{ga121-/-}$ have increased Myc activity

It has been shown that overexpression of Myc can trigger apoptosis both in cell culture and *in vivo* in a P53 dependent or independent manner. (McMahon, 2014) Since Mga antagonizes Myc, we hypothesized that increased cell death seen in *MZmga*$^{ga121-/-}$ was due to unopposed Myc activity. To assess whether Myc activity is affected in *MZmga*$^{ga121-/-}$, we injected a reported construct containing four tandem repeats of E-box element driving firefly luciferase gene (Figure 3.3A) along with renilla luciferase vector into both wild type and *MZmga*$^{ga121-/-}$ embryos at 1-cell stage. Firefly and renilla luminescence were measured at 8hpf, 24hpf as well as 31hpf. *MZmga*$^{ga121-/-}$ showed significantly increased firefly to renilla luciferase ratio at all developmental stages tested, suggesting that Myc activity is increased in *MZmga*$^{ga121-/-}$. (Figure 3.3B) To see if increased Myc activity has functional consequence, we analyzed expression of Myc target genes in both wild type and *MZmga*$^{ga121-/-}$. qRT-PCR was performed using total RNA extracts from wild type and *MZmga*$^{ga121-/-}$ embryos at 24hpf. Expression of two of the five Myc target genes tested, *odc1* and *cebpα,* showed significantly increased in *MZmga*$^{ga121-/-}$ compared to the control. (Figure 3.3C) *odc1* encodes an enzyme, Ornithine Decarboxylase, involved in the

polyamine synthesis pathways. (Bachmann & Geerts, 2018) C/EBPα is a key regulator in adipogenesis and lipid metabolism. (Salmerón, 2018) It's possible that delayed development in *mga* mutants is due to abnormalities in various metabolic pathways triggering the cell death.

3. Identification of *mga* paralog

We analyzed the expression level of *mga* transcripts in *MZmga*$^{ga121-/-}$ as well as in wild type. We found that *mga* mRNA expression is decreased in the mutants. (See Chapter 2.2 E-F) This suggests the possibility of non-sense mediated decay (NMD) of the mutant mRNA which may trigger genetic compensation as previously described. (El-Brolosy et al., 2019; El-Brolosy & Stainier, 2017; Ma et al., 2019) Therefore, we asked whether there are any genes that are similar to *mga* that might be upregulated in *MZmga*$^{ga121-/-}$. Currently in zebrafish genome, there's only one *mga* gene has been annotated, that is *mgaa* which encodes for Mgaa protein in zebrafish. Due to whole genome duplication event during the evolution of teleost fish, we highly suspect that there's another *mga* gene in zebrafish genome. To find *mgaa* paralogs, we searched the amino acid sequence of the T-box domain of Mgaa in neucleotide collection database using tblastn with organism limited to zebrafish. Search result returned 111 hits including many genes of the TBX family as well as a predicted protein coding gene *max-gene associated protein-like* (*mgab*) on chromosome 20 (accession number: XM_021468741.1). We analyzed the amino acid sequence of Mgab and found that it contains both DNA binding domains, T-box and bHLHZip domains, present in Mgaa. Protein sequence alignment of Mgab showed a highly conserved T-box domain with 58% similarity to that of zebrafish Mgaa and human MGA and 53% similarity to the mouse Mga T-box domain. (Figure 3.4A) bHLHZip domain of Mgab seems to be less conserved showing 31% similarity to zebrafish Mgaa and 36% similarities to human and mouse

Mga. (Figure 3.4B) We next assessed the degree of conserved synteny in the *mgaa* and *mgab* locus in different species. Genes that are immediately flanking the zebrafish *mgaa* are conserved among human, mouse and other teleost fish species including cave fish, stickleback and fugu fish. (Figure 3.4C) Genes that are upstream of *mgab* are highly conserved among teleosts. Interestingly, *mitogen activated protein kinase binding protein 1*(*mapkbp1*), which is downstream of *mgab* in all teleost species but zebrafish, is downstream of *mgaa* locus in all species including human and mouse. (Figure 3.4C) Taken together, *mga* locus in teleost fish and tetrapods arose from the same common ancestor. However, *mgab* locus in zebrafish seems to be more divergent than other fish species.

4. *mgab* is expressed in zebrafish embryos

To see if *mgab* is expressed during zebrafish early development, we performed RT-PCR using RNA extracts at various developmental time points. *mgab* transcripts were seen as early as 16-cell stage embryos, suggesting that *mgab* is also maternally expressed. (Figure 3.5A) At later stages, *mgab* seems to be expressed at a constant amount. In addition, we observed an increase in *mgab* expression in MZ*mga*$^{ga121-/-}$ as shown by the increased relative fold change of *mgab* compared to the control. (Figure 3.5B) It's possible that increased *mgab* expression is compensating for the loss of Mgaa in MZ*mga*$^{ga121-/-}$. However, further experiments are needed to confirm genetic compensation.

DISCUSSION

In this study, we aim to characterize Mga function during early embryonic development using zebrafish embryos lacking functional Mga. Unlike other members of the Max interacting protein network, Mga is the least studied member of the family. Mga is known as a tumor suppressor for its ability to antagonize Myc dependent cellular transformation. (P J Hurlin et al., 1999) Consistently, mutations or deletions in MGA have been found in many cancers including lung adenocarcinoma, colorectal cancer and malignant transformation of chronic lymphocytic leukemia also known as Ritcher's Syndrome. ("Comprehensive molecular profiling of lung adenocarcinoma.," 2014; de Paoli et al., 2012; Jo, Kim, Yoo, & Lee, 2016; Llabata et al., 2019) Mga also belong to another group of evolutionary conserved transcription factor family, the T-box family, that play important roles during early embryogenesis, ranging from embryonic patterning to many aspects of organogenesis. (Ghosh, Brook, & Wilsdon, 2017) The presence of T-box DNA binding domain suggests that Mga may have more complicated function than solely antagonizing Myc activity in cells. Previous knockdown studies of Mga in zebrafish have shown that Mga is important for dorsoventral patterning, neural crest specification and organogenesis. (Rikin & Evans, 2010; Sun et al., 2014) However, there are limitations of using morpholinos as they don't block maternally deposited proteins such as Mga. Therefore, we generated *mga* mutants using CRISPR/Cas9 system. We successfully identified four different mutant alleles using sgRNA that targets the coding sequence of the T-box domain of Mga. The efficiency of gene targeting was as high as 83% and the germ line transmission ranged from 6-40%. Among these four alleles, mga^{ga121} and mga^{ga242} are hypothetically null.

Embryos that are homozygous for zygotic *mga*^{ga121} are viable and fertile. Interestingly, *MZmga*$^{ga121-/-}$ are also viable and fertile, and have no apparent developmental defects except for developmental delay. We showed that the developmental delay in *MZmga*$^{ga121-/-}$ was most likely due to increased cell death rather than abnormalities in cell proliferation. (See Chapter 2 Figure 2.2A-D) Increased cell death was also observed in the pluripotent epiblast of the mouse embryos that are lacking functional Mga. (Washkowitz et al., 2015) However, the lack of severe phenotype is in stark contrast with the mouse *Mga* mutants who die during peri-implantation. (Washkowitz et al., 2015) In addition, early embryonic lethality in mouse *Mga* mutants was due to decreased expression of *Ornithine decarboxylase 1*(*Odc1*), which encodes a rate-limiting enzyme in the polyamine synthesis pathway, in the epiblast resulting in decreased survival of pluripotent cells. (Washkowitz et al., 2015) Odc1 is positively regulated by c-Myc at the transcriptional level and is also important for cell survival during early mouse embryonic development. (Bello-Fernandez, Packham, & Cleveland, 1993; Pendeville et al., 2001) We found that Myc activity is increased in *MZmga*$^{ga121-/-}$ as shown by the reporter construct containing the Myc response elements. Consistent with elevated Myc activity, expression of *odc1*, as well as another Myc target gene *cebpα*, is increased in *MZmga*$^{ga121-/-}$. *odc1* expression is decreased when zebrafish larvae were treated with a c-Myc inhibitor. (Lee et al., 2016) This is consistent with Mga's function as it compete with Myc for Max to transcriptionally repress Myc target genes. (P J Hurlin et al., 1999) The discrepancy in the regulation of Odc1 expression by Mga and Myc in mammals and fish species could be due to species specific differences in early embryonic development as well as differential requirements for the pluripotency factors. However, one cannot rule out the fact that the *mga*^{ga121} allele is not a true null or that there is alternative translation start site in the coding region of *mga*. The absence of highly specific antibodies for

zebrafish Mga have created difficulties to assess Mga protein level in the mutants. Knocking in polypeptide tags to the endogenous *mga* locus will be helpful in assessing Mga protein level as well as studying Mga function *in vivo*.

We further investigated why *MZmga*$^{ga121-/-}$ fail to show severe phenotype. *mga*^{ga121} allele has five base pair deletion resulting in frameshift mutation and multiple stop codons early in the Mga coding sequence. Premature terminating codons (PTCs) are known to trigger non-sense mediated mRNA decay (NMD), a cellular mechanism for proper protein and mRNA quality control. (Popp & Maquat, 2013) We have shown that *MZmga*$^{ga121-/-}$ embryos have decreased *mga* transcripts compared to wild type. (See Chapter 2 Figure 2.2E, F) suggesting the presence of NMD. Due to the fact that NMDs can trigger increased expression of genes that are ancestrally related to the mutant gene (El-Brolosy et al., 2019; El-Brolosy & Stainier, 2017; Ma et al., 2019), we set out to search for *mga* paralog that has not been annotated in the zebrafish genome. We found a predicted protein coding gene, *max-gene associated protein-like* (*mgab*), located on the chromosome 20 of the zebrafish genome. Mgab protein also contains two DNA binding domains, T-box and bHLHZip domain. T-box domain of Mgab is highly conserved, but the bHLHZip domain show around 30% similarities to the human, mouse and zebrafish bHLHZip domain. *mgab* is also present in other teleost fish species including cave fish, fugu and stickleback. Chromosomal organization around *mgab* is conserved among different teleost fish, indicating that *mgab* arose during the whole genome duplication event happened in the evolution of vertebrates. In addition to conserved protein structure, we found that *mgab* mRNA is also expressed both maternally and zygotically. Furthermore, *mgab* seems to be upregulated in *MZmga*$^{ga121-/-}$ as shown by the increased expression in the qRT-PCR analysis at 24hpf. This data suggests the possibility of genetic compensation in *MZmga*$^{ga121-/-}$. However, additional

experiments are needed to address whether *mgab* has functional redundancy with *mgaa*. A double knockout experiment is necessary to evaluate Mgaa and Mgab function during zebrafish embryonic development. We predict that double knockout embryos will resemble mouse mutants as knocking down Mga using high dose morpholinos also lead to early embryonic lethality. (see Chapter 2.3A) In addition, further evaluation of *mgab* expression pattern in zebrafish embryos may give more insights into whether *mgaa* and *mgab* have overlapping or distinct function during embryogenesis.

REFERENCE:

Altschul, S. F., Madden, T. L., Schäffer, A. A., Zhang, J., Zhang, Z., Miller, W., & Lipman, D. J. (1997). Gapped BLAST and PSI-BLAST: a new generation of protein database search programs. *Nucleic Acids Research*, *25*(17), 3389–3402. https://doi.org/10.1093/nar/25.17.3389

Bachmann, A. S., & Geerts, D. (2018). Polyamine synthesis as a target of MYC oncogenes. *The Journal of Biological Chemistry*, *293*(48), 18757–18769. https://doi.org/10.1074/jbc.TM118.003336

Bello-Fernandez, C., Packham, G., & Cleveland, J. L. (1993). The ornithine decarboxylase gene is a transcriptional target of c-Myc. *Proceedings of the National Academy of Sciences of the United States of America*, *90*(16), 7804–7808. https://doi.org/10.1073/pnas.90.16.7804

CB, K., WW, B., SR, K., B, U., & TF, S. (1995). Stages of embryonic development of the zebrafish. *Developmental Dynamics*, *203*(3), 253–310. Retrieved from https://www.mbl.edu/zebrafish/files/2013/03/Kimmel_stagingseries1.pdf%0Ahttp://www.researchgate.net/profile/Bonnie_Ullmann/publication/227763372_Stages_of_embryonic_development_of_the_zebrafish/links/55352d8b0cf268fd00156437.pdf

Comprehensive molecular profiling of lung adenocarcinoma. (2014). *Nature*, *511*(7511), 543–550. https://doi.org/10.1038/nature13385

de Paoli, L., Cerri, M., Monti, S., Rasi, S., Spina, V., Bruscaggin, A., … Rossi, D. (2012). MGA, a suppressor of MYC, is recurrently inactivated in high risk chronic lymphocytic leukemia. *Leukemia & Lymphoma*, *54*(May 2012), 1087–1090. https://doi.org/10.3109/10428194.2012.723706

El-Brolosy, M. A., Kontarakis, Z., Rossi, A., Kuenne, C., Günther, S., Fukuda, N., … Stainier, D. Y. R. (2019). Genetic compensation triggered by mutant mRNA degradation. *Nature*, *568*(7751), 193–197. https://doi.org/10.1038/s41586-019-1064-z

El-Brolosy, M. A., & Stainier, D. Y. R. (2017). Genetic compensation: A phenomenon in search of mechanisms. *PLOS Genetics*, *13*(7), e1006780. Retrieved from https://doi.org/10.1371/journal.pgen.1006780

Fuentes, R., Letelier, J., Tajer, B., Valdivia, L. E., & Mullins, M. C. (2018). Fishing forward and reverse: Advances in zebrafish phenomics. *Mechanisms of Development*, *154*(August), 296–308. https://doi.org/10.1016/j.mod.2018.08.007

Ghosh, T. K., Brook, J. D., & Wilsdon, A. (2017). T-Box Genes in Human Development and

Disease. *Current Topics in Developmental Biology*, *122*, 383–415. https://doi.org/10.1016/bs.ctdb.2016.08.006

Hurlin, P J, Steingrimsson, E., Copeland, N. G., Jenkins, N. A., & Eisenman, R. N. (1999). Mga, a dual-specificity transcription factor that interacts with Max and contains a T-domain DNA-binding motif. *The EMBO Journal*, *18*(24), 7019–7028. https://doi.org/10.1093/emboj/18.24.7019

Hurlin, Peter J., & Huang, J. (2006). The MAX-interacting transcription factor network. *Seminars in Cancer Biology*, *16*(4), 265–274. https://doi.org/10.1016/j.semcancer.2006.07.009

Hwang, W. Y., Fu, Y., Reyon, D., Maeder, M. L., Tsai, S. Q., Sander, J. D., … Joung, J. K. (2013). Efficient genome editing in zebrafish using a CRISPR-Cas system. *Nature Biotechnology*, *31*(3), 227–229. https://doi.org/10.1038/nbt.2501

Jao, L.-E., Wente, S. R., & Chen, W. (2013). Efficient multiplex biallelic zebrafish genome editing using a CRISPR nuclease system. *Proceedings of the National Academy of Sciences of the United States of America*, *110*(34), 13904–13909. https://doi.org/10.1073/pnas.1308335110

Jo, Y. S., Kim, M. S., Yoo, N. J., & Lee, S. H. (2016, August). Somatic mutation of a candidate tumour suppressor MGA gene and its mutational heterogeneity in colorectal cancers. *Pathology*. England. https://doi.org/10.1016/j.pathol.2016.04.010

Lai, J. K. H., Gagalova, K. K., Kuenne, C., El-Brolosy, M. A., & Stainier, D. Y. R. (2019). Induction of interferon-stimulated genes and cellular stress pathways by morpholinos in

zebrafish. *Developmental Biology*, *454*(1), 21–28. https://doi.org/10.1016/j.ydbio.2019.06.008

Lee, S. G., Huang, M., Obholzer, N. D., Sun, S., Li, W., Petrillo, M., … Chen, Z.-Y. (2016). Myc and Fgf Are Required for Zebrafish Neuromast Hair Cell Regeneration. *PLOS ONE*, *11*(6), e0157768. Retrieved from https://doi.org/10.1371/journal.pone.0157768

Llabata, P., Mitsuishi, Y., Choi, P. S., Cai, D., Francis, J. M., Torres-Diz, M., … Zhang, X. (2019). Multi-Omics Analysis Identifies MGA as a Negative Regulator of the MYC Pathway in Lung Adenocarcinoma. *Molecular Cancer Research : MCR*. https://doi.org/10.1158/1541-7786.MCR-19-0657

Ma, Z., Zhu, P., Shi, H., Guo, L., Zhang, Q., Chen, Y., … Chen, J. (2019). PTC-bearing mRNA elicits a genetic compensation response via Upf3a and COMPASS components. *Nature*, *568*(7751), 259–263. https://doi.org/10.1038/s41586-019-1057-y

Mashal, R. D., Koontz, J., & Sklar, J. (1995). Detection of mutations by cleavage of DNA heteroduplexes with bacteriophage resolvases. *Nature Genetics*, *9*(2), 177–183. https://doi.org/10.1038/ng0295-177

McMahon, S. B. (2014). MYC and the control of apoptosis. *Cold Spring Harbor Perspectives in Medicine*, *4*(7), 1–10. https://doi.org/10.1101/cshperspect.a014407

Pendeville, H., Carpino, N., Marine, J.-C., Takahashi, Y., Muller, M., Martial, J. A., & Cleveland, J. L. (2001). The Ornithine Decarboxylase Gene Is Essential for Cell Survival during Early Murine Development. *Molecular and Cellular Biology*, *21*(19), 6549 LP – 6558. https://doi.org/10.1128/MCB.21.19.6549-6558.2001

Popp, M. W.-L., & Maquat, L. E. (2013). Organizing Principles of Mammalian Nonsense-Mediated mRNA Decay. *Annual Review of Genetics*, *47*(1), 139–165. https://doi.org/10.1146/annurev-genet-111212-133424

Rikin, A., & Evans, T. (2010). The tbx/bHLH transcription factor mga regulates gata4 and organogenesis. *Developmental Dynamics*, *239*(2), 535–547. https://doi.org/10.1002/dvdy.22197

Robu, M. E., Larson, J. D., Nasevicius, A., Beiraghi, S., Brenner, C., Farber, S. A., & Ekker, S. C. (2007). p53 Activation by Knockdown Technologies. *PLOS Genetics*, *3*(5), e78. Retrieved from https://doi.org/10.1371/journal.pgen.0030078

Salmerón, C. (2018). Adipogenesis in fish. *The Journal of Experimental Biology*, *221*(Pt Suppl 1). https://doi.org/10.1242/jeb.161588

Sander, J. D., Maeder, M. L., Reyon, D., Voytas, D. F., Joung, J. K., & Dobbs, D. (2010). ZiFiT (Zinc Finger Targeter): an updated zinc finger engineering tool. *Nucleic Acids Research*, *38*(suppl_2), W462–W468. https://doi.org/10.1093/nar/gkq319

Sander, J. D., Zaback, P., Joung, J. K., Voytas, D. F., & Dobbs, D. (2007). Zinc Finger Targeter (ZiFiT): an engineered zinc finger/target site design tool. *Nucleic Acids Research*, *35*(Web Server issue), W599–W605. https://doi.org/10.1093/nar/gkm349

Sun, Y., Tseng, W. C., Fan, X., Ball, R., & Dougan, S. T. (2014). Extraembryonic Signals under the Control of MGA, Max, and Smad4 Are Required for Dorsoventral Patterning. *Developmental Cell*, *28*(3), 322–334. https://doi.org/10.1016/j.devcel.2014.01.003

Tseng, W.-C. (2015). *NEURAL CREST SPECIFICATION BY MAX'S GIANT ASSOCIATED PROTEIN AND REGULATION OF MICROTUBULE'S FUNCTION BY ALPHA-TUBULIN ACETYLTRANSFERASE 1 IN ZEBRAFISH*. University of Georgia. Retrieved from http://dbs.galib.uga.edu/cgi-bin/write_stats.cgi?stattype=fulltext&dbscode=getd&format=pdf&redirect=http://getd.libs.uga.edu/pdfs/tseng_wei-chia_201505_phd.pdf

van den Berg, D. L. C., Snoek, T., Mullin, N. P., Yates, A., Bezstarosti, K., Demmers, J., … Poot, R. A. (2010). An Oct4-Centered Protein Interaction Network in Embryonic Stem Cells. *Cell Stem Cell*, *6*(4), 369–381. https://doi.org/10.1016/j.stem.2010.02.014

Vickaryous, M. K., & Mclean, K. E. (2011). *Vertebrate Embryogenesis*. *Reptile Embryology* (Vol. 770). https://doi.org/10.1007/978-1-61779-210-6

Washkowitz, A. J., Schall, C., Zhang, K., Wurst, W., Floss, T., Mager, J., & Papaioannou, V. E. (2015). Mga is essential for the survival of pluripotent cells during peri-implantation development. *Development*, *142*(1), 31–40. https://doi.org/10.1242/dev.111104

FIGURES AND FIGURE LEGENDS

Figure 3.1. Generation of *mga* mutants using CRISPR/Cas9 system. A. Schematic representation of *mga* exons, and position of T-box domain and bHLHZip domain coding regions. A sgRNA (shown as black arrow) is designed to target the coding region of the T-box domain of Mga. B, C: representative gel images after screening for possible indel mutations using T7 endonuclease I (T7E1) assay. B: 10 embryos are randomly selected from around 50 wild type embryos injected with sgRNA and cas9 mRNA and screened with T7E1 assay. First lane represented by a dash (-) is the negative control in which DEPC water is used as template for PCR. C: F1 progeny of Fish #11 (T11) was raised to adulthood and screened using T7E1 using DNA extracts from fin-clips. D, E: live images of t-box sgRNA and cas9 mRNA injected embryos at 5dpf.

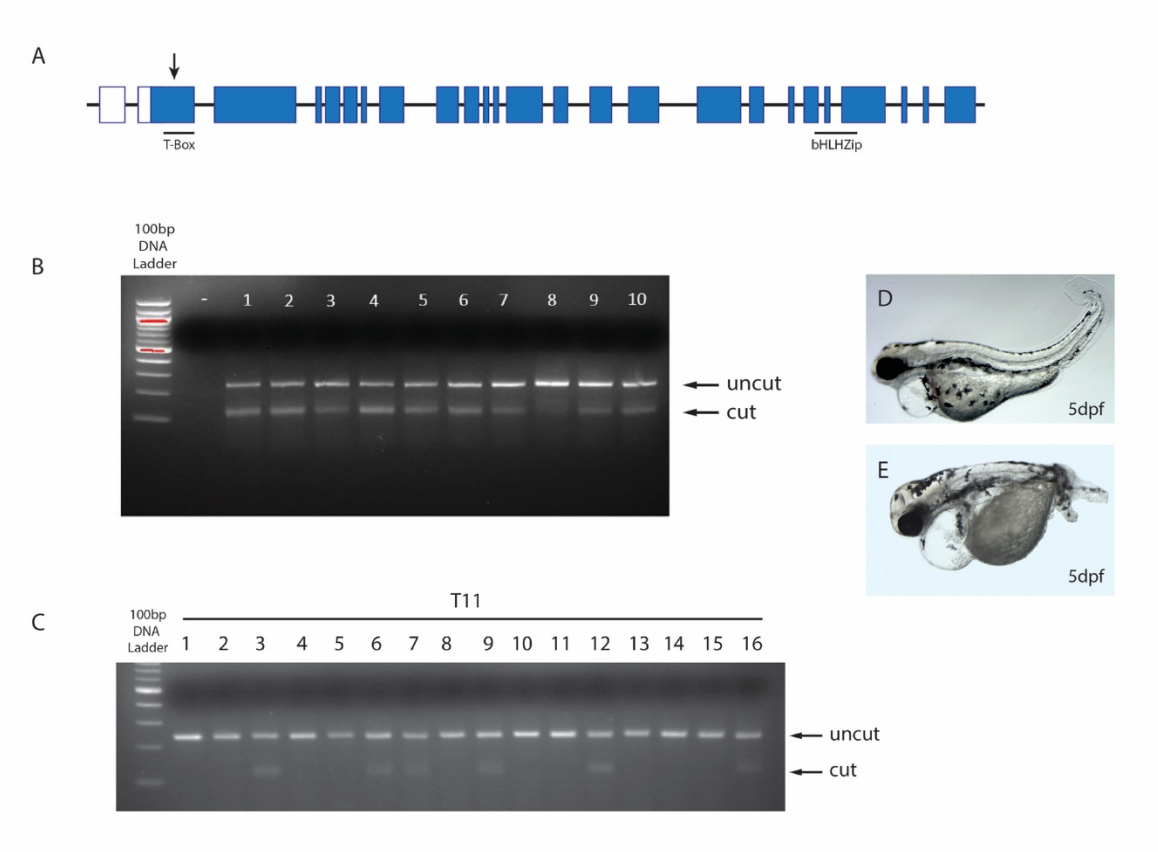
A
T-Box
bHLHZip
B
100bp
DNA
Ladder
- 1 2 3 4 5 6 7 8 9 10
uncut
cut
D
5dpf
E
5dpf
C
T11
100bp
DNA
Ladder
1 2 3 4 5 6 7 8 9 10 11 12 13 14 15 16
uncut
cut

Figure 3.2. *mga* mutant alleles generated from sgRNA targeting the T-box coding region. A: Four different *mga* mutant alleles, mga^{ga121}, mga^{ga162}, mga^{ga194}, mga^{ga242}, were identified in F1 adults. Among these four alleles, mga^{ga121} and mga^{ga242} were hypothetically null. Blue letters represent target sequence; PAM was shown in green; yellow dashed lines represent deletions; Red lowercase letters represent inserted nucleotides. B: Chromatograms of wild type and two of the alleles, mga^{ga121} and mga^{ga162} were shown.

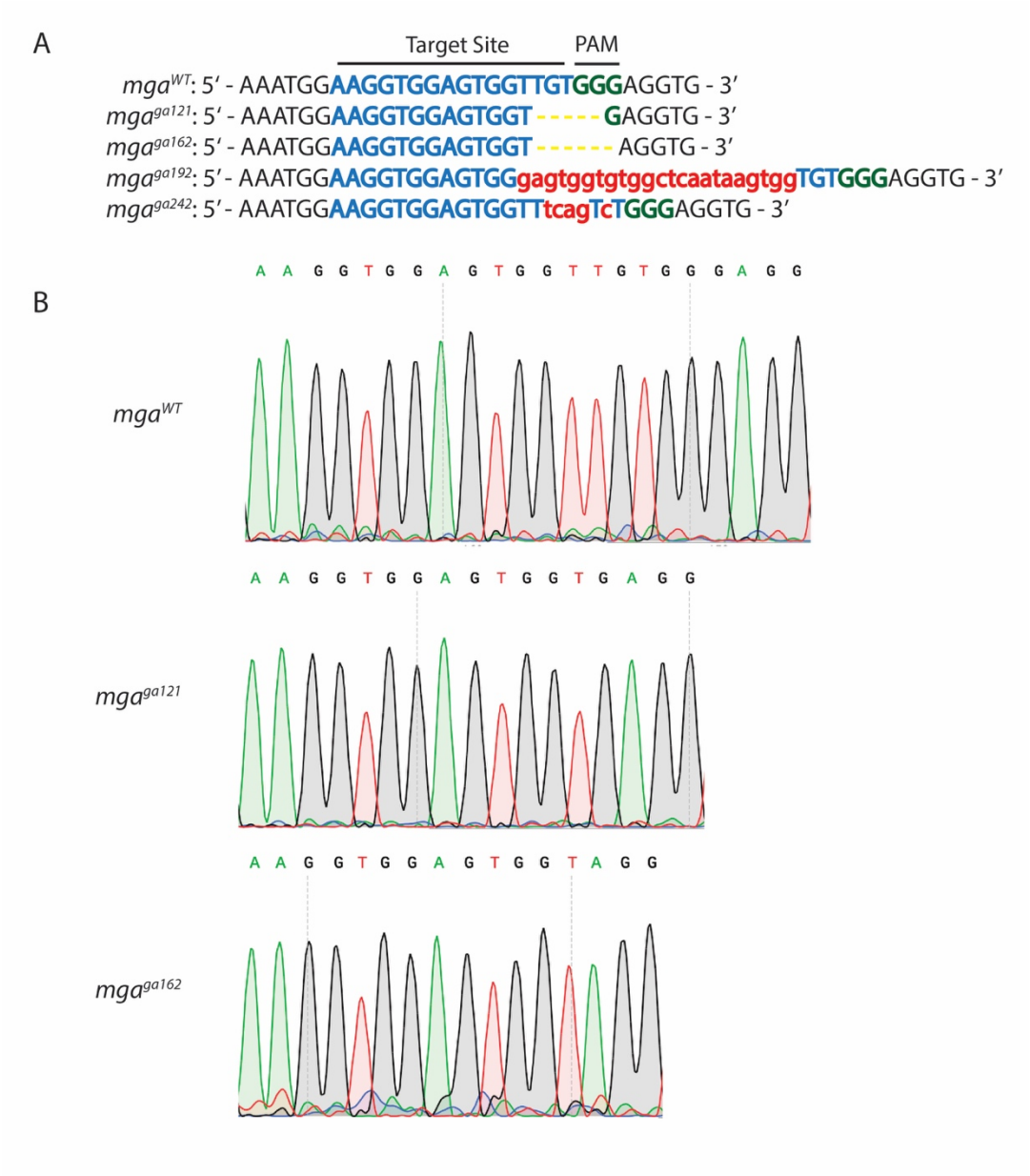
A
Target Site
PAM
mga^WT: 5′ - AAATGGAAGGTGGAGTGGTTGTGGGAGGTG - 3′
mga^ga121: 5′ - AAATGGAAGGTGGAGTGGT-----GAGGTG - 3′
mga^ga162: 5′ - AAATGGAAGGTGGAGTGGT------AGGTG - 3′
mga^ga192: 5′ - AAATGGAAGGTGGAGTGGgagtggtgtggctcaataagtggTGTGGGAGGTG - 3′
mga^ga242: 5′ - AAATGGAAGGTGGAGTGGTTtcagTcTGGGAGGTG - 3′
B
mga^WT
mga^ga121
mga^ga162

Figure 3.3. *mga*$^{ga121-/-}$ have increased Myc activity. A: schematic view of the firefly luciferase construct that is used to assess the Myc activity. Firefly luciferase gene is driven by a minimal promoter and four tandem repeats of E-box binding sites. B: Firefly to renilla ratios were calculated by measuring firefly and renilla luminescence at different developmental time points. *mga*$^{ga121-/-}$ show increased firefly to renilla ratio (green bars) when compared to the wild type (blue bars), suggesting increased Myc activity in *mga*$^{ga121-/}$. Luciferase assay was performed with three biological replicates with three technical replicates for each experiment. *(n = 3. *:P<0.05; **: p<0.005 ***: p<0.001student t-test. Error bar: SEM)* C: Expression of at least two of the Myc target genes, *odc1* and *cebpa,* is significantly increased in *mga*$^{ga121-/-}$. qRT-PCR was performed using total RNA extracts from *mga*$^{ga121-/-}$ and wild-type embryos at 24hpf. Relative gene expression is calculated using $2^{-\Delta\Delta Ct}$ method from three biological replicates, with three technical replicates for each experiment. *(n = 3. P<0.05; student t-test. Error bar: SEM)*

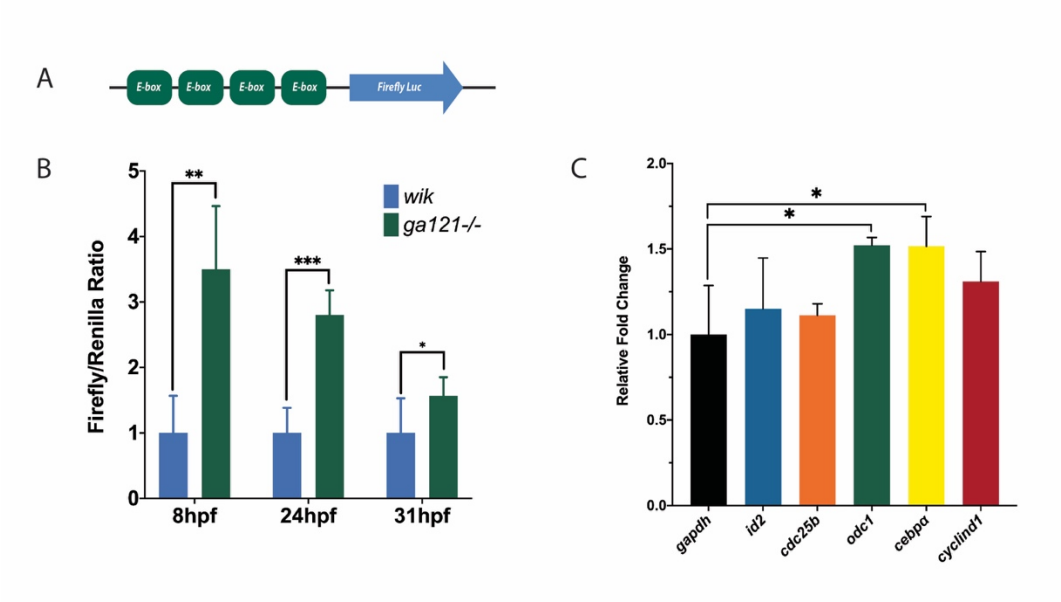
A
E-box
E-box
E-box
E-box
Firefly Luc
B
Firefly/Renilla Ratio
wik
ga121-/-
**
***
*
8hpf
24hpf
31hpf
C
Relative Fold Change
*
*
gapdh
id2
cdc25b
odc1
cebpα
cyclind1

Figure 3.4. Identification of *mgab.* A, B: Comparison of amino acid sequences of zebrafish Mgaa and Mgab (drMgaa and drMgab) with human (hsMGA) and mouse (mmMga). Conserved amino acid sequences were shaded in black. (A) T-box domain of drMgab is 58% similar to that of drMgaa and hsMGA, and 54% similar to that of mmMga. (B) The bHLHZip domain of drMgab is 31% similar to that of drMgaa but is 36% similar to that of mmMga and hsMGA. C: Synteny analysis of human, mouse and teleost fish *mgaa* locus as well as *mgab* locus of zebrafish and other teleost fish species. Genes that are immediately next to mga (mgaa in teleost species) is conserved among humans, mouse and fish.

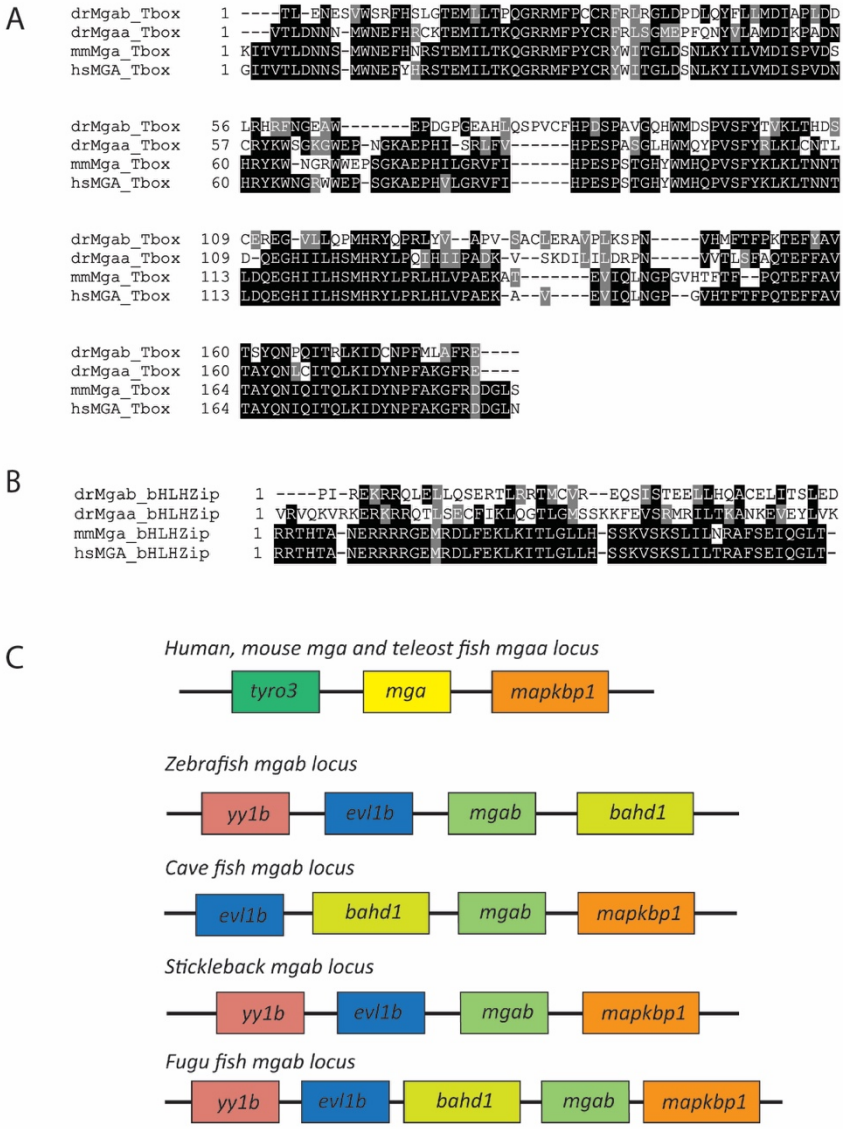
A
drMgab_Tbox
drMgaa_Tbox
mmMga_Tbox
hsMGA_Tbox
B
drMgab_bHLHZip
drMgaa_bHLHZip
mmMga_bHLHZip
hsMGA_bHLHZip
C
Human, mouse mga and teleost fish mgaa locus
tyro3
mga
mapkbp1
Zebrafish mgab locus
yy1b
evl1b
mgab
bahd1
Cave fish mgab locus
Stickleback mgab locus
Fugu fish mgab locus

Figure 3.5. *mgab* is expressed both maternally and zygotically. A: expression of *mgab* mRNA is analyzed using RT-PCR using total RNA extracts from wild-type embryos at different developmental time points. Mgab mRNA is expressed both maternally and zygotically with the earliest expression seen at 18-cell stage. B: expression level of *mgab* mRNA is analyzed using qRT-PCR in wild-type and $mga^{ga121-/-}$ at 8hpf. *mgab* level is elevated in $mga^{ga121-/-}$. Relative gene expression is calculated using $2^{-\Delta\Delta Ct}$ method from three biological replicates with three technical replicates for each experiment.

A

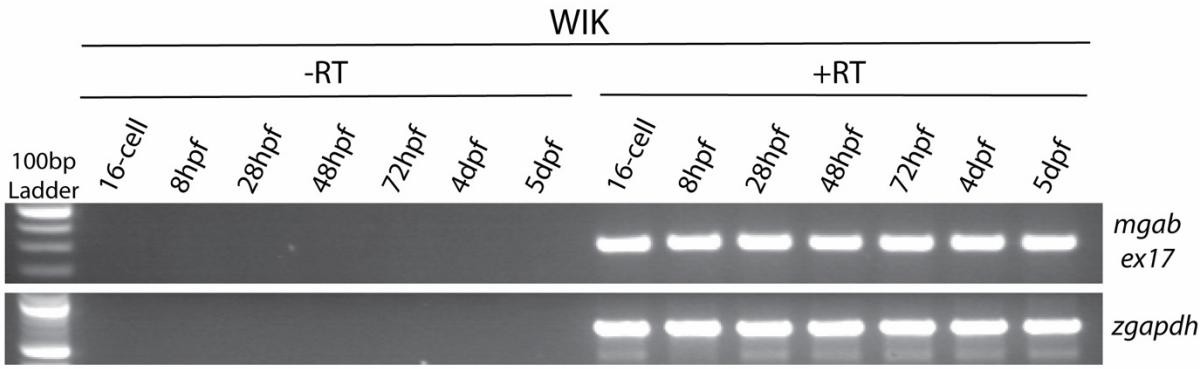
WIK
-RT
+RT
100bp Ladder
16-cell
8hpf
28hpf
48hpf
72hpf
4dpf
5dpf
16-cell
8hpf
28hpf
48hpf
72hpf
4dpf
5dpf
mgab ex17
zgapdh

B

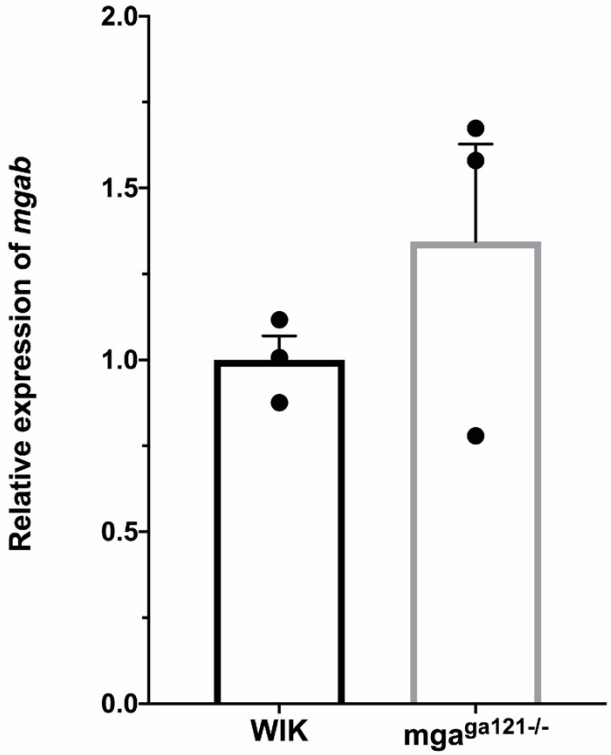
Relative expression of mgab
2.0
1.5
1.0
0.5
0.0
WIK
mga ga121-/-

CHAPTER 4

CONCLUSIONS AND FUTURE DIRECTIONS

DISCUSSION

1. Mga is a novel regulator of zebrafish neural crest development

Mga is the least studied protein in the MAX interacting network of transcription factor family. (Grandori, Cowley, James, & Eisenman, 2000) Due to early embryonic lethality during mouse development, our understating of Mga function during development has been very limited. (Washkowitz et al., 2015) In this study, we identified a novel role of Mga during zebrafish neural crest (NC) development using both knockdown and knockout approaches. Depletion of Mga using antisense morpholinos from 1-cell stage zebrafish embryos resulted in defects in multiple lineages of neural crest derivatives. These defects include abnormalities in skin pigmentation, craniofacial cartilages as well as defects in the development of peripheral and enteric nervous system. These abnormalities were rescued with the injection of mouse *mga* mRNA which contains different sequences at the translation start site that cannot be affected by zebrafish *mga* morpholinos. This suggests that NC defects seen in *mga* morphants are specifically due to loss of Mga function during development.

Expression pattern of Mga also correlate with its role during NC development. Mga is expressed broadly during gastrulation, and its expression is gradually restricted to the head and

tail at later stages. (Rikin & Evans, 2010) This time frame coincide with the patterning of neural plate border which gives rise to presumptive NC cell population. (Pla & Monsoro-Burq, 2018) Once neural plate border is specified, presumptive NC cells start to express transcription factors, such as *foxd3*, *sox10*, *tfap2a*, *snai1b*, that specifies NC cell fate. Expression of these transcription factors were decreased in *mga* morphants at 3-somite stage. Interestingly, although *MZmga*$^{ga121-/-}$ embryos didn't show any neural crest defects, we noticed slightly decreased expression of *foxd3* and *tfap2a*, suggesting reduced specification of neural crest cells. It's possible that these mutants recover at a later time through transcriptional adaptation which is discussed at a later section. Taken together, our data supports Mga's role in neural crest specification in zebrafish embryos.

2. Mga regulates neural crest development independent of Myc

Loss of pigmentation has been reported in a previous study, but the exact mechanism has never been identified. (Rikin & Evans, 2010) In addition to loss of pigmentation, we observed defects in multiple neural crest derivatives in our *mga* morphants. To study the underlying mechanism of how Mga contribute to neural crest development, we analyzed the molecular pathways involved in neural crest specification and are known to be regulated by Mga. Mga was initially identified as a binding partner for Max which is an obligate co-factor for Myc. (Blackwood & Eisenman, 1991; P J Hurlin, Steingrimsson, Copeland, Jenkins, & Eisenman, 1999) In cell culture, Mga competes for Max and sequesters Max from forming transcriptional activating complex with Myc, resulting in the suppression of Myc target genes. (P J Hurlin et al., 1999; Ogawa, Ishiguro, Gaubatz, Livingston, & Nakatani, 2002) Myc family genes are very well known for their involvement in cancer, but it also regulates key developmental events including neural crest specification. (Peter J. Hurlin, 2013) c-Myc was shown to be important for NC

development in frogs and chickens. (Bellmeyer, Krase, Lindgren, & LaBonne, 2003; Kerosuo & Bronner, 2016) In zebrafish, *mych*, a *c-myc* homolog, is expressed at the neural plate border and is required for neural crest survival. (Hong, Tsang, & Dawid, 2008) We found that Myc activity is elevated in *mga* morphants as shown by the increased reporter activity at 24hpf and 31hpf. As a consequence, expression of Myc target genes, including *id2*, *cdc25*, *cyclind1*, *cebpα* and *odc1*, are also elevated at 24hpf. Among these target genes, Id2, a bHLH transcription factor, was shown to be expressed in pre-migratory and migratory NC cells in chicks. (Martinsen, Bronner-fraser, Martinsen, & Bronner-fraser, 2020) Overexpression of chick *id2* in frog embryos leads to expansion of neural crest population due to increased cell proliferation. (Kee & Bronner-Fraser, 2005) On the contrary, *mga* morphants showed reduced neural crest progenitors. In addition, there is an increase in TUNEL positive apoptotic cells in regions correlating to the pre-migratory and migratory NC cells at 22hpf. Increased cell death in *mga* morphants is possibly due to increased Myc activity. Injection of 200pg of *mxd3* mRNA, which encodes another Max interacting protein that antagonizes Myc, in *mga* morphants is able to rescue cell death at 22hpf but is not able to rescue neural crest defects. These data suggest that there's already neural crest specification defect and that Myc elevation is not the attributing factor for neural crest defects in *mga* morphants.

In many species, Bmp signaling has been shown to be important in early steps of NC development. (Betancur, Bronner-Fraser, & Sauka-Spengler, 2010; Pla & Monsoro-Burq, 2018) During gastrulation, high levels of Bmp are expressed in the non-neural ectoderm while low levels are required in the neural ectoderm. Intermediate level of Bmp, on the other hand, is required for proper positioning of the neural plate border. (Reichert, Randall, & Hill, 2013; Schumacher, Hashiguchi, Nguyen, & Mullins, 2011; Tríbulo, Aybar, Nguyen, Mullins, &

Mayor, 2003) When Mga is suppressed from the 1-cell stage, expression of Bmp antagonist *chordin* is slightly expanded ventrally at 75% epiboly. Two of the Bmp target genes, *Δnp63* and *tbx6*, are decreased in *mga* morphants. These results are consistent with the previous finding where Mga positively regulates *bmp2b* expression in the extraembryonic yolk syncytial layer (YSL) together with Max and Smad4. (Sun, Tseng, Fan, Ball, & Dougan, 2014) Knocking down Mga from 1-cell stage embryos may also knockdown Mga from the yolk syncytial layer. Although Bmp level is decreased, we did not observe dorsoventral patterning defects. (Tseng, 2015) Since we used much lower dose of *mgaMOs* than previously used, residual Mga protein level (50% of the control) can the lack of dorsoventral patterning defects. It's possible that neural crest cells are much sensitive to Bmp level than dorsoventral patterning. Taken together, we conclude that Mga plays a role in fine tuning the Bmp level in the neural plate border to promote neural crest specfication.

3. Study of Mga function in zebrafish knockout models

Through targeting the T-box coding region of Mga, we have successfully identified four different alleles carrying indel mutations using CRISPR/Cas9 system. *mga*^{ga121} is a potential null allele with five base-pair deletion creating a frameshift mutation and multiple stop codons downstream. As coding region of the T-box domain is located in the first exon, *mga*^{ga121} should produce a null allele. Zygotic *mga*$^{ga121-/-}$ are viable and fertile. We were able to generate maternal zygotic mutants by in-crossing zygotic *mga*$^{ga121-/-}$ adults. To our surprise, *MZmga*$^{ga121-/-}$ developed normally as their wild type counterparts except for one to two hours of developmental delay. Although *mga* mutants failed to recapitulate morphant phenotypes, we did see similar molecular changes. We found that there's increased apoptosis in MZ*mga*$^{ga121-/-}$ possibly due to

increased Myc activity, although cell proliferation is not affected. Consistent with increased Myc activity, expression of Myc target genes, *odc1* and *cebpa*, are increased in the mutants. These findings are supported by the fact that Myc and Mga compete for Max to occupy E-box sites and control target gene expression. (Blackwood & Eisenman, 1991; P J Hurlin et al., 1999) Both Odc1 and C/EBPα are key regulators in metabolic pathways and cellular homeostasis. (Bachmann & Geerts, 2018; Bello-Fernandez, Packham, & Cleveland, 1993; Salmerón, 2018) It's possible that the dysregulation in cellular metabolism due to increased Myc activity may be the cause of developmental delay in the mutants.

To address the lack of severe phenotype in *mga* mutants, we analyzed the expression of *mga* transcript levels in the MZ*mga*$^{ga121-/-}$. We found that *mga* transcripts are decreased in the mutants compared to the wild type. As stated earlier, the frameshift mutation in *mga*^{ga121} allele creates multiple premature termination codons (PTCs) which can trigger the degradation of mutant mRNA known as non-sense mediated mRNA decay (NMD). Therefore, it's possible that the decreased *mga* expression is due to NMD. It's been proposed that the NMD can activate transcriptional adaptation to protect an organism bearing a non-sense mutations. (El-Brolosy et al., 2019; Ma et al., 2019) Such adaptation mechanism works by upregulating similar or related genes via epigenetic remodeling. (El-Brolosy et al., 2019; Ma et al., 2019) If transcriptional adaptation is responsible for the lack of severity in our mutants, we should see an upregulation of genes that are similar to *mga*. Interestingly, we found another *mga* gene, *mgab*, on chromosome 20 of the zebrafish genome that has not been annotated. *mgab* is expressed both maternally and zygotically. Mgab protein also contains conserved T-box and bHLHZip domain. The chromosomal organization around *mgab* is also conserved among teleost species. In addition, expression of *mgab* mRNA is slightly increased in *mga* mutants. Therefore, it's likely that Mgab

is compensating for the loss of Mgaa in our mutants. We predict that *mgaa* and *mgab* double knockout embryos should display more severe or lethal phenotype and should resemble those seen in mouse embryos lacking functional Mga. (Washkowitz et al., 2015)

Although current evidences in the potentially *mga* null mutants recapitulate the molecular changes that are seen in *mga* knockdown embryos, some caveats need to be taken into consideration. For example, we were not able to analyze the Mga protein level in MZ*mga*$^{ga121-/-}$ embryos. It's possible that Mga protein is made via alternative translation start site downstream of the indel mutation. Currently, there are no commercially available antibodies that can specifically recognize zebrafish Mga. Endogenously knocking in protein tags in *mga* locus using CRISPR/Cas9 system can be helpful to evaluate protein level in the mutants. This can be also helpful in identifying proteins that interacts with Mga and their potential target genes *in vivo*.

4. Mga function in general and future directions

In this study, we identified a novel role of Mga in promoting cell fate specification during neural crest development independent of Myc. This is different from previous reports where they found Mga promoting cell survival and pluripotency maintenance. (Hu et al., 2009; van den Berg et al., 2010; Washkowitz et al., 2015) In fact, Mga and its cofactor Max was found in a transcriptional repressor complex with E2F-6 to occupy and silence Myc target genes and genes with T-box elements in G0 cells. (Ogawa et al., 2002) Mga and Max can also recruit chromatin modifiers, such as Polycomb group proteins to germ cell specific genes and repress their expression preventing premature differentiation of embryonic stem cells. (Endoh et al., 2017) These findings together with ours suggest that Mga can promote both differentiation and pluripotency depending on the cell cycle and the presence of different binding partners. With two

DNA binding domain, Mga may regulate a wide variety of target genes during development and carry out different functions. Indeed, previous reports using knockdown methods in zebrafish have shown Mga's involvement in dorsoventral patterning as well as organogenesis by regulating distinct set of genes. (Rikin & Evans, 2010; Sun et al., 2014)

Mutations in *MGA* have been found in many cancers such as lung adenocarcinoma, colon cancer, malignant transformation of chronic lymphocytic leukemia. (Bachmann & Geerts, 2018; de Paoli et al., 2012; Jo, Kim, Yoo, & Lee, 2016) Understanding how and when Mga promote differentiation or maintain pluripotency will not only contribute substantially to our knowledge in early embryonic development but also will shed more lights on the pathogenesis and therapeutics of cancer. With a mutant in hand and possibly with a double Mga knockouts in the future, we will be able to uncover how Mga function in vertebrate embryonic development.

REFERENCES:

Bachmann, A. S., & Geerts, D. (2018). Polyamine synthesis as a target of MYC oncogenes. *The Journal of Biological Chemistry*, *293*(48), 18757–18769. https://doi.org/10.1074/jbc.TM118.003336

Bellmeyer, A., Krase, J., Lindgren, J., & LaBonne, C. (2003). The protooncogene c-myc is an essential regulator of neural crest formation in xenopus. *Developmental Cell*, *4*(6), 827–839.

Bello-Fernandez, C., Packham, G., & Cleveland, J. L. (1993). The ornithine decarboxylase gene is a transcriptional target of c-Myc. *Proceedings of the National Academy of Sciences of the*

United States of America, *90*(16), 7804–7808. https://doi.org/10.1073/pnas.90.16.7804

Betancur, P., Bronner-Fraser, M., & Sauka-Spengler, T. (2010). Assembling Neural Crest Regulatory Circuits into a Gene Regulatory Network. *Annual Review of Cell and Developmental Biology*, *26*(1), 581–603. https://doi.org/10.1146/annurev.cellbio.042308.113245

Blackwood, E. M., & Eisenman, R. N. (1991). Max: a helix-loop-helix zipper protein that forms a sequence-specific DNA-binding complex with Myc. *Science (New York, N.Y.)*, *251*(4998), 1211–1217. https://doi.org/10.1126/science.2006410

Comprehensive molecular profiling of lung adenocarcinoma. (2014). *Nature*, *511*(7511), 543–550. https://doi.org/10.1038/nature13385

de Paoli, L., Cerri, M., Monti, S., Rasi, S., Spina, V., Bruscaggin, A., … Rossi, D. (2012). MGA, a suppressor of MYC, is recurrently inactivated in high risk chronic lymphocytic leukemia. *Leukemia & Lymphoma*, *54*(May 2012), 1087–1090. https://doi.org/10.3109/10428194.2012.723706

El-Brolosy, M. A., Kontarakis, Z., Rossi, A., Kuenne, C., Günther, S., Fukuda, N., … Stainier, D. Y. R. (2019). Genetic compensation triggered by mutant mRNA degradation. *Nature*, *568*(7751), 193–197. https://doi.org/10.1038/s41586-019-1064-z

Endoh, M., Endo, T. A., Shinga, J., Hayashi, K., Farcas, A., Ma, K. W., … Koseki, H. (2017). PCGF6-PRC1 suppresses premature differentiation of mouse embryonic stem cells by regulating germ cell-related genes. *ELife*, *6*, 1–26. https://doi.org/10.7554/eLife.21064

Grandori, C., Cowley, S. M., James, L. P., & Eisenman, R. N. (2000). T He M Yc / M Ax / M Ad N Etwork and the. *Cancer Research*.

Hong, S.-K., Tsang, M., & Dawid, I. B. (2008). The Mych Gene Is Required for Neural Crest Survival during Zebrafish Development. *PLOS ONE*, *3*(4), e2029. Retrieved from https://doi.org/10.1371/journal.pone.0002029

Hu, G., Kim, J., Xu, Q., Leng, Y., Orkin, S. H., & Elledge, S. J. (2009). A genome-wide RNAi screen identifies a new transcriptional module required for self-renewal. *Genes and Development*, *23*(7), 837–848. https://doi.org/10.1101/gad.1769609

Hurlin, P J, Steingrimsson, E., Copeland, N. G., Jenkins, N. A., & Eisenman, R. N. (1999). Mga, a dual-specificity transcription factor that interacts with Max and contains a T-domain DNA-binding motif. *The EMBO Journal*, *18*(24), 7019–7028. https://doi.org/10.1093/emboj/18.24.7019

Hurlin, Peter J. (2013). Control of vertebrate development by MYC. *Cold Spring Harbor Perspectives in Medicine*, *3*(9). https://doi.org/10.1101/cshperspect.a014332

Jo, Y. S., Kim, M. S., Yoo, N. J., & Lee, S. H. (2016, August). Somatic mutation of a candidate tumour suppressor MGA gene and its mutational heterogeneity in colorectal cancers. *Pathology*. England. https://doi.org/10.1016/j.pathol.2016.04.010

Kee, Y., & Bronner-Fraser, M. (2005). To proliferate or to die: Role of Id3 in cell cycle progression and survival of neural crest progenitors. *Genes and Development*, *19*(6), 744–755. https://doi.org/10.1101/gad.1257405

Kerosuo, L., & Bronner, M. E. (2016). cMyc Regulates the Size of the Premigratory Neural Crest Stem Cell Pool. *Cell Reports*, *17*(10), 2648–2659. https://doi.org/10.1016/j.celrep.2016.11.025

Ma, Z., Zhu, P., Shi, H., Guo, L., Zhang, Q., Chen, Y., … Chen, J. (2019). PTC-bearing mRNA

elicits a genetic compensation response via Upf3a and COMPASS components. *Nature*, *568*(7751), 259–263. https://doi.org/10.1038/s41586-019-1057-y

Martinsen, B. J., Bronner-fraser, M., Martinsen, B. J., & Bronner-fraser, M. (2020). Neural Crest Specification Regulated by the Helix-Loop-Helix Repressor Id2 Published by : American Association for the Advancement of Science Stable URL : https://www.jstor.org/stable/2896124 REFERENCES Linked references are available on JSTOR for this article : digitize , preserve and extend access to Science Neurat Crest Specification Regulated by the Helix-Loop-Helix Repressor 1d2, *281*(5379), 988–991.

Ogawa, H., Ishiguro, K. I., Gaubatz, S., Livingston, D. M., & Nakatani, Y. (2002). A complex with chromatin modifiers that occupies E2f- and Myc-responsive genes in G0 cells. *Science*, *296*(5570), 1132–1136. https://doi.org/10.1126/science.1069861

Pla, P., & Monsoro-Burq, A. H. (2018). The neural border: Induction, specification and maturation of the territory that generates neural crest cells. *Developmental Biology*, *444*(February), S36–S46. https://doi.org/10.1016/j.ydbio.2018.05.018

Reichert, S., Randall, R. A., & Hill, C. S. (2013). A BMP regulatory network controls ectodermal cell fate decisions at the neural plate border. *Development*, *140*(21), 4435 LP – 4444. https://doi.org/10.1242/dev.098707

Rikin, A., & Evans, T. (2010). The tbx/bHLH transcription factor mga regulates gata4 and organogenesis. *Developmental Dynamics*, *239*(2), 535–547. https://doi.org/10.1002/dvdy.22197

Salmerón, C. (2018). Adipogenesis in fish. *The Journal of Experimental Biology*, *221*(Pt Suppl 1). https://doi.org/10.1242/jeb.161588

Schumacher, J. A., Hashiguchi, M., Nguyen, V. H., & Mullins, M. C. (2011). An Intermediate Level of BMP Signaling Directly Specifies Cranial Neural Crest Progenitor Cells in Zebrafish. *PLOS ONE*, *6*(11), e27403. Retrieved from https://doi.org/10.1371/journal.pone.0027403

Sun, Y., Tseng, W. C., Fan, X., Ball, R., & Dougan, S. T. (2014). Extraembryonic Signals under the Control of MGA, Max, and Smad4 Are Required for Dorsoventral Patterning. *Developmental Cell*, *28*(3), 322–334. https://doi.org/10.1016/j.devcel.2014.01.003

Tríbulo, C., Aybar, M. J., Nguyen, V. H., Mullins, M. C., & Mayor, R. (2003). Regulation of Msx genes by a Bmp gradient is essential for neural crest specification. *Development*, *130*(26), 6441 LP – 6452. https://doi.org/10.1242/dev.00878

Tseng, W.-C. (2015). *NEURAL CREST SPECIFICATION BY MAX'S GIANT ASSOCIATED PROTEIN AND REGULATION OF MICROTUBULE'S FUNCTION BY ALPHA-TUBULIN ACETYLTRANSFERASE 1 IN ZEBRAFISH*. University of Georgia. Retrieved from http://dbs.galib.uga.edu/cgi-bin/write_stats.cgi?stattype=fulltext&dbscode=getd&format=pdf&redirect=http://getd.libs.uga.edu/pdfs/tseng_wei-chia_201505_phd.pdf

van den Berg, D. L. C., Snoek, T., Mullin, N. P., Yates, A., Bezstarosti, K., Demmers, J., … Poot, R. A. (2010). An Oct4-Centered Protein Interaction Network in Embryonic Stem Cells. *Cell Stem Cell*, *6*(4), 369–381. https://doi.org/10.1016/j.stem.2010.02.014

Washkowitz, A. J., Schall, C., Zhang, K., Wurst, W., Floss, T., Mager, J., & Papaioannou, V. E. (2015). Mga is essential for the survival of pluripotent cells during peri-implantation development. *Development*, *142*(1), 31–40. https://doi.org/10.1242/dev.111104